DISSERTATION

CHALLENGES OF HYDROLOGICAL ANALYSIS
FOR WATER RESOURCES DEVELOPMENT
IN SEMI-ARID MOUNTAINOUS REGIONS:
A CASE STUDY IN IRAN

SHIRO HISHINUMA

2013

GRIPS

National Graduate Institute for Policy Studies

CHALLENGES OF HYDROLOGICAL ANALYSIS

FOR WATER RESOURCES DEVELOPMENT

IN SEMI-ARID MOUNTAINOUS REGIONS:

A CASE STUDY IN IRAN

A Dissertation

Submitted to the Faculty of the National Graduate Institute for Policy Studies (GRIPS)

in Partial Fulfillment of the Requirements for the Degree of

DOCTOR OF PHILOSOPHY IN DISASTER MANAGEMENT

by

Shiro Hishinuma

September, 2013

Abstract

This study assessed the current state of challenges that water resources engineers and managers face in hydrological analysis for water resources development in semi-arid mountainous regions. These challenges consist of: (1) hydrological model applicability; (2) data availability for efficient hydrological model use; and (3) climate change impact assessment. The Karun River basin that is located in the southwestern semi-arid mountainous area of the Islamic Republic of Iran was selected as a case study. The basin has huge water potential due to the relatively abundant precipitation in the Zagros mountain ranges and suitable topography to storage water by dam construction. Many water resources development projects are planned, including dam construction, irrigation networks and water transfer systems. However, neither water resources development planning from an integrated point of view nor climate change adaptation have been considered in the basin.

First, the applicability of the distributed hydrological model, the Block-wise TOPMODEL with the Muskingum-Cunge routing method (BTOPMC), was confirmed for its use in water resources development in the semi-arid mountainous Karun River basin. The model was set up by using publicly available data sets, and applied to the catchment areas of the existing dams, the Karun1 dam and the Dez dam, which are located in the middle of the basin. The results at Karun1 clearly indicated the potential of the BTOPMC application within semi-arid mountainous regions with necessary modification, which was the introduction of the adjustment coefficient for infiltration capacity of the soil surface to improve the model

i

performance of reproducing flood peaks generated by infiltration excess overland runoff at a daily time scale. BTOPMC was also capable to simulate seasonal discharge with snowpack and snowmelt processes in wet winter and recession of low flows in dry summer, which are indispensable for analyzing multi seasonal dam reservoir use in long-term simulation.

Next, data availability from the point of efficient hydrological analysis use for water resources development in semi-arid mountainous regions was assessed from the application results of BTOPMC in the Karun River basin. The results at Dez clearly indicated that effective model use was significantly affected by the scarcity of ground-gauged precipitation data. In order to avoid inefficient infrastructure investment especially in semi-arid mountainous regions, therefore, considerable efforts to improve ground-based observation of precipitation should well precede water resource development plans.

Finally, potential impacts of climate change on river discharge in the Karun River basin were assessed by coupling BTOPMC with climatic outputs derived from three members of the super-high-resolution Atmospheric General Circulation Models (MRI-AGCMs) under the A1B future emission scenario of green house gases presented in the Special Report on Emission Scenario (SRES). The multi-ensemble results from the hydrological simulations by BTOPMC using bias corrected daily precipitation and daily average surface air temperature derived from MRI-AGCMs indicated that mean monthly discharge at Karun1 and Dez might decrease significantly in the near future climate (2015-2039) and the future climate (2075-2099), particularly from April to July, in comparison with those in the present climate (1979-2003). Despite possible uncertainties in the assessment, low

regrets measures in climate change adaptation of the basin, such as consideration of multi-purpose dams and integrated operation of multiple dams, were recommended to utilize the limited amount of water for satisfying water demands under the projected discharge reduction in the future.

Acknowledgement

iv

Table of Contents

List of Figures

ix

List of Tables

1. Introduction

1.1. Background of the research

1.1.1. Need for water resources development in semi-arid mountainous regions

Water is a precious commodity and supports fundamental human life. One of the most urgent challenges in the world is development of water resources to meet growing water demands due to increasing population, urbanization, irrigation and industrialization. To overcome this challenge, there has been an intensive international emphasis on water resources development and management. For example, the International Conference on Water and the Environment in Dublin in 1992 set out the four Dublin Principles, stating "Fresh water is a finite and vulnerable resource, essential to sustain life, development and the environment" in the Principle No.1 (World Meteorological Organization [WMO], n.d.). In addition, the United Nations Conference on the Environment and Development (UNCED) in 1992 produced the Agenda 21, which recommends on integrated water resources management for sustainable development in Chapter 18 (United Nations Environment Programme [UNEP], n.d.). Furthermore, the United Nations (UN) summit of 2000 set the Millennium Development Goals (MDGs) for poverty reduction. Among the eight goals, the Target 7C in Goal 7 states "Halve, by 2015, the proportion of the population without sustainable access to safe drinking water and basic sanitation" (UN, n.d.)

Since available freshwater is distributed spatially and temporally, supply of water cannot satisfy demands sufficiently. Oki and Kanae (2006) estimate that more than two billion people live in highly water-stressed areas because of the uneven distribution of renewable freshwater resources in time and space although current global water withdrawals of about 3,500 km^3/year are well below the renewable freshwater resources available in all rivers around the world, which is estimated at 45,500 km^3/year.

There is a considerable difference in water resources between arid and humid regions and also between wet and dry seasons. Particularly in arid and semi-arid regions, which occupy about 30% of the Earth's land area (UNEP, 1992), water is severely limited and making the best use of available water is an issue of primary importance. Falkenmark, Lundqvist, and Widstrand (1989) discuss the general vulnerability of the semi-arid regions in terms of water scarcity, and raise a question: "ask *not*: how much water do we need and from where do we get it, but rather: how much water is there and how can we best benefit from it?" That means information on available water in semi-arid regions should be recognized as the basis of water resources development planning.

1.1.2. Difficulty of hydrological analysis in semi-arid mountainous regions

In order to understand how much water is available temporally and spatially at a national or basin scale, hydrological models are suitable tools that can help understand and make decisions on water resources development (Loucks et al., 2005). Hydrological models have been playing an important role in providing critical information in many river basins across the globe, especially in data scarce river basins (Blöschl, Sivapalan, Wagener, Viglione, & Savenije, 2013).

Nevertheless, there are several issues in application of hydrological models to water resources development in semi-arid regions. One of the major issues is a lack of high-quality local data. Since observation stations to collect climatic data, which are primarily used as input for hydrological analysis, are mainly situated in areas of dense population, the availability of such data is relatively limited in most semi-arid regions with sparse population (Nicholson, 2011). The problem of establishing monitoring networks over large areas, where precipitation and runoff are highly variable, is another reason of data scarcity in semi-arid regions. Characteristics of precipitation in semi-arid regions are intense, short and spatially limited (Nicholson, 2011). These characteristics are particularly evident in the mountainous regions due to orographic effects.

Another major issue of hydrological model application to water resources development in semi-arid regions is the difficulty in simulation of complex hydrological processes. For instance, it is extremely difficult to evaluate dominant runoff processes of intense and short precipitation with limited spatial distribution, particularly when high-quality local data are unavailable (Pilgrim, Chapman, & Doran, 1988; Beven, 2002; Wheater, 2008). Hughes (2008) reviews hydrological model application to semi-arid basins in southern Africa and summarizes that the main limitations on the model application are related to the lack of observed precipitation data with spatial and temporal details as well as the lack of adequate quantitative understanding of channel transmission losses. There is thus the urgent need for development and application of hydrological models capable of accurate simulation of runoff processes in semi-arid mountainous regions that are robust in data-poor situations.

Despite these difficulties of hydrological model application in semi-arid mountainous regions, several studies report successful cases in which hydrological

models are effectively used to support decision making for water resources development and management in semi-arid mountainous regions. For example, from the recent study conducted in the Karkheh Basin in Iran, Masih, Maskey, and Uhlenbrook (2012) find that the conversion of rain-fed areas to irrigated areas may cause severe reduction in monthly discharge by using a distributed hydrological model, the Soil and Water Assessment Tool (SWAT) model, and suggest a water development strategy should take into account the high variability of water resources. Güntner and Bronstert (2004) and Güntner, Krol, Araújo, and Bronstert (2004) develop and apply a distributed hydrological model, Model of Water Availability in Semi-Arid Environments (WASA), with a cascade-type reservoir module to a semi-arid basin in northeastern Brazil. They identify the large impact of reservoir storage on downstream flow and stress the need for a coupled simulation of runoff generation, network redistribution and water use in hydrological models. However, these successful examples were supported by quality local data, which were used for model set-up, calibration and validation. Data availability is thus one of the key factors for successful model application in semi-arid mountainous regions.

1.1.3. Need for climate change impact assessment in semi-arid mountainous regions

Projected climate change may adversely affect temporal and spatial availability of freshwater in the world. The Intergovernmental Panel on Climate Change (IPCC) produces comprehensive assessment reports on climate change from the viewpoints of the state of scientific, technical and socio-economic knowledge, its causes, potential impacts, and response strategies by mitigation and adaptation measures. Future climate

conditions under several emission scenarios of green house gases are projected by General Circulation Models (GCMs). Based on the projections by multiple GCMs, the fourth assessment report of IPCC (IPCC AR4) states that arid and semi-arid areas are particularly exposed to the impacts of climate change on freshwater (IPCC, 2007a). The projected higher temperatures might change some amount of snowfall into rainfall and the snowmelt season earlier, and thus the timing and volume of river discharge in spring might change considerably (IPCC, 2007b).

The need for climate change adaptation has been widely recognized and various adaptations have already been instigated, especially since the establishment of the Adaptation Fund put forward by the Bali Action Plan of COP13 (United Nations Framework Convention on Climate Change [UNFCCC], 2007). Subsequent UN statements suggest the need for closer integration of disaster risk management and climate change adaptation in the context of development and development planning (e.g., United Nations Secretariat for International Strategy for Disaster Reduction [UNISDR] 2009, 2011). One of the main massages of the latest special report prepared by IPCC is that "low-regrets" measures that provide benefits under current climate and a range of future climate change scenarios should be taken into account in adaptation to climate change and disaster risk management (IPCC, 2012). It is obvious that formulation of any adaptation policies with low-regrets measures regarding freshwater management under climate change requires as much information as possible on future conditions of water availability at a river basin scale.

A commonly applied method for the basin-scale assessment of climate change impacts on water availability is to run a hydrological model using climatic outputs derived from GCM as input data (e.g. Gosling, Taylor, Arnell, & Todd, 2011; Harding,

Wood, & Prairie, 2012; Chien, Yeh, & Knouft, 2013; Hidalgo, Amador, Alfaro, & Quesada, 2013). The hydrological simulation results, such as river discharge, are then used for assessment of climate change impacts and making decision on climate change adaptation measures.

The most relevant climatic variables used in hydrological analysis for climate change impact assessment are precipitation and surface air temperature (Blöschl & Montanari, 2010). Several studies emphasize the importance of the use of both precipitation and temperature for the impact assessment, particularly in semi-arid mountainous regions. For example, Barnett, Adam, and Lettenmaier (2005) conclude that projected warming temperatures in high altitude basins where spring snowmelt contributes to river discharges are likely to cause a shift in the timing of peak river discharge to earlier in spring, and thus reduce river discharges in summer. In addition, Vivoni, Aragón, Malczynski, & Tidwell (2009) suggest that projected changes in precipitation and temperature should be considered in hydrological analysis over snow-dominated semi-arid basins under climate change conditions through sensitivity analysis on hydrological responses. Therefore, utilizing GCMs outputs of both precipitation and temperature is necessary to assess climate change impact over semi-arid mountainous regions. However, such basin-scale assessment of climate change impacts in semi-arid mountainous regions is underway.

1.2. Objectives of the research

Hydrological analysis plays important roles in making decisions on water

resources development as well as climate change adaptation with low regrets measures by providing information on water availability in time and space. Semi-arid mountainous regions have suffered water shortage, but have potential for water resources development. However, lack of local data and complex hydrological processes prevent successful hydrological model application in semi-arid mountainous regions.

The main objective of this thesis is to assess the current state of challenges that water resources engineers and managers face in hydrological analysis for water resources development in semi-arid mountainous regions. These challenges consist of hydrological model applicability, data availability for efficient hydrological model use, and climate change impact assessment. The main objective is achieved by sub objectives as follows:

(1) Assess hydrological model applicability in semi-arid mountainous regions for the use in water resources development.

(2) Assess data availability from the point of efficient hydrological model use in semi-arid mountainous regions for water resources development.

(3) Assess climate change impacts on basin hydrology in the 21st century in semi-arid mountainous regions to discuss adaptation strategies for water resources development and management.

As a case study for the assessment, the Karun River basin in the Islamic Republic of Iran is selected. The basin has huge water potential and many water resources development projects are planned. However, neither water resources development planning from an integrated point of view nor climate change adaptation

have been considered in the basin.

1.3. Structure of the thesis

The structure of the thesis consists of five chapters. A brief introduction for each chapter is explained below:

Chapter 1 describes the general background and the objectives of this thesis.

Chapter 2 introduces current state and issues of hydrology and water resources in the case study area, the Karun River basin in the Islamic Republic of Iran. First, an overview of water resources development in Iran is presented. Then, an overview of water issues in the Karun River basin, and water resources development plans and related issues are introduced with detailed description.

Chapter 3 assesses hydrological model applicability in semi-arid mountainous regions for water resources development and data availability from the point of efficient hydrological model use. First, general characteristics of hydrological processes in semi-arid mountainous regions are summarized. Next, Indispensable criteria used in the selection of a distributed model appropriate for the Karun River basin are introduced, and a description of the selected hydrological model, the Block-wise TOPMODEL with the Muskingum-Cunge routing method (BTOPMC), is explained. Finally, the model applicability and the data availability are assessed through the application of BTOPMC in the basin.

Chapter 4 assesses climate change impacts on basin hydrology in the Karun River basin by coupling BTOPMC with climatic outputs derived from the super-high-

resolution Atmospheric General Circulation Models (MRI-AGCMs). First, the applicability of a simple statistical bias correction method to MRI-AGCM precipitation for the present climate is examined. Then, the possible impacts of climate change in the basin are assessed by multi-ensemble analysis of hydrological simulations.

Finally, Chapter 5 presents conclusions of this thesis and policy implications of water resources development in semi-arid mountainous regions.

2. Study Area

2.1. Overview of water resources development in Iran

The Islamic Republic of Iran is located in Southwest Asia and covers a total area of about 1.75 million km^2. The country is classified into arid and semi-arid regions based on the Global Humidity Index (UNEP, 1992). The average annual precipitation in the country is about 250 mm; however, it varies greatly in time and space from less than 50 mm in the deserts in central and eastern Iran to more than 2000 mm in the mountain areas; the Zagros mountain ranges in western Iran particularly receives a large amount of precipitation (Food and Agriculture Organization of the United Nations [FAO], 2008). About 50% of the precipitation falls in winter, 23% in spring and autumn, and only 4% in summer (FAO, 2008). This characterizes wet winter and dry summer in Iran. Evapotranspiration is dominant in the country and about 66% of precipitation is estimated to evaporate before reaching the rivers (FAO, 2008).

Water demands have been increasing in the country due to rapid urbanization, expansion of cities and improvement in living standards (Ardakanian, 2005). The total water withdrawal is 93.3 billion m^3 in 2004, which accounts for more than 70% of the total water resources potential, and the percentages of the total water withdrawal by sector are approximately as follows: 92% for agriculture; 6% for domestic use; and 2% for industrial use (FAO, 2008). About 57% of the total water withdrawal is from groundwater and 43% from surface water (International Journal on Hydropower &

Dams [IJHD], 2012). Overexploitation of groundwater is a serious problem in Iran, and most of the overexploitation happens in the central basins where less surface water is available. In order to control the overexploitation, the government plans to increase the percentage of the surface water withdrawal from 43% to 55% (FAO, 2008).

Water resources development has supported sustainable development of the country by supplying energy and water resources to meet growing demands (Ardakanian, 2005). In particular, dams have been playing an important role in harnessing precious water resources for power generation, agricultural, industrial and domestic uses. At the end of the 1980s, the government decided to develop the hydropower potential of the country. The main objectives of the development are as follows (Gharavy, 2005): (1) to provide power; (2) to increase hydropower generation instead of conventional thermal type in order to increase the export of oil; (3) to create new job opportunity in rural areas; (4) to create a new industrial sector achieving self-sufficiency and export potential; (5) to prevent flood damages; and (6) to increase water storage for domestic and industrial use. Currently, there are about 414 large dams in operation and the total water storage of the existing dams is 42.9 billion m^3, which accounts for about 30% of the total water resources potential of the country (IJHD, 2012). Table 2.1 ranks countries for the number of dams under development. Iran has 49 dams under construction and is ranked second behind China, and the rest of the countries are far behind these two. Figure 2.1 shows Iran's electrical installed capacity. The total installed capacity roughly doubled during 2002-2011, and the installed capacity of hydropower increased more than double in the same period. Most of the installed capacities are provided by conventional thermal energy. However, these data clearly indicate that the government of Iran has been enhancing hydropower generation

by dam construction.

Table 2.1 Number of dams under construction by country, from IJHD (2012).

Rank	Country	Number of dams under construction > 60m high
1	China	108
2	Iran	49
3	Turkey	24
4	Japan	16
5	Vietnam	14
6	India	10
7	Morocco	7
7	Myanmar	7
9	Brazil	6
9	Greece	6
9	Laos	6
9	Spain	6
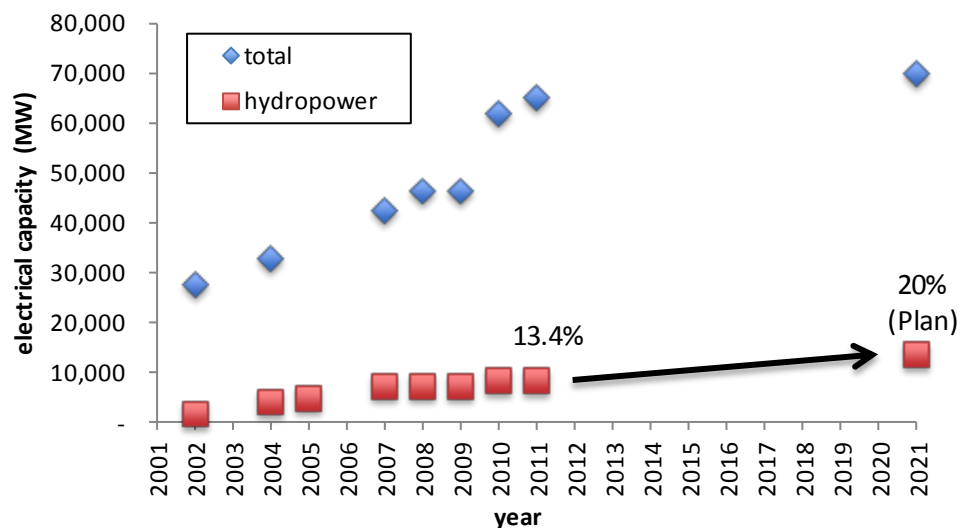
Figure 2.1 Electrical installed capacity in Iran.

(The historical data in 2002-2011 are from Gharavy (2005) and IJHD (2008, 2009, 2010, 2011, 2012).

The data in 2021 are projected values provided by CITC (2012).)

Figure 2.1 also shows future projection of Iran's electrical capacity in 2021. The Center for Innovation and Technology Cooperation (CITC), which is an autonomous government center under the command of the president of Iran, reports that the government plans to generate 14 GW hydroelectric power by 2021, which accounts for 20% of Iran's projected electrical capacity (CITC, 2012). Special attention has been paid to reduce fossil fuel consumption and increase the use of renewable energy, such as hydroelectric, solar, wind, geothermal, tidal, and biomass energies, due to severe environmental pollution caused by growing fossil fuel consumption in the country (CITC, 2012).

Abbaspour, Faramarzi, Ghasemi, & Yang (2009) analyze climate change impacts on water resources in the country, and find that water-related disasters might be more severe in the future, such as more intense and frequent floods in the wet regions and more prolonged droughts in the dry regions. Under projected climate change conditions in the future, role of dams would be more important to support sustainable development of the country by providing power and water resources to meet growing demands as well as preventing water-related disasters.

Three ministries of the government are responsible for water resources in the country. The Ministry of Energy (MOE) is responsible for energy supply and hydropower generation. Under MOE, the Water Affairs Department (WAD) is responsible for overseeing and coordinating the planning, development, management and conservation of water resources. The Water Resources Management Company (IWRMC) is the mother company that manages all water sectors within the MOE except drinking water distribution for rural and urban areas. The Water and Power development Company (IWPC) is another company that is responsible for dam

development. The Ministry of Jihad-e-Agriculture (MOA) and the Ministry of Jihad-e-Sazandagi (MOJ) are other ministries that are responsible for water resources in the country. MOA supervises rain-fed and irrigated crop development and its water use. MOJ deals with watershed management and rural development.

2.2. Overview of water issues in the Karun River basin, Iran

The Karun River basin, which is located in the semi-arid southwestern region of Iran, is one of the largest river basins in the country. Figure 2.2 shows the location of the Karun River basin and its basin map. The catchment area of the basin is about 62,000 km^2 and the length is 720 km. The Karun River flows from the Zagros mountain ranges in the upper catchment to the southwestern part of the country to the Shatt al Arab River, which lies after the confluence of the Euphrates and Tigris Rivers in Iraq. There are several other large rivers in Iran. However, the Karun River is the only navigable river and the others are being too steep and irregular (FAO, 2008). Dominant land cover types in the basin are grassland in the mountainous area and open shrubland in the flat area in the downstream.

Figure 2.3 shows monthly precipitation and dam reservoir inflow at two dam sites, the Karun1 dam and the Dez dam, located in the Zagros mountain ranges. Most precipitation occurs from November to April, in particular from December to January. Winter precipitation accumulates as snowpack in high mountains and snowmelt water contributes to increase river discharge in the spring. Summer is dry with almost no precipitation from June to September. Discharge decreases during summer but perennial

flow is observed.
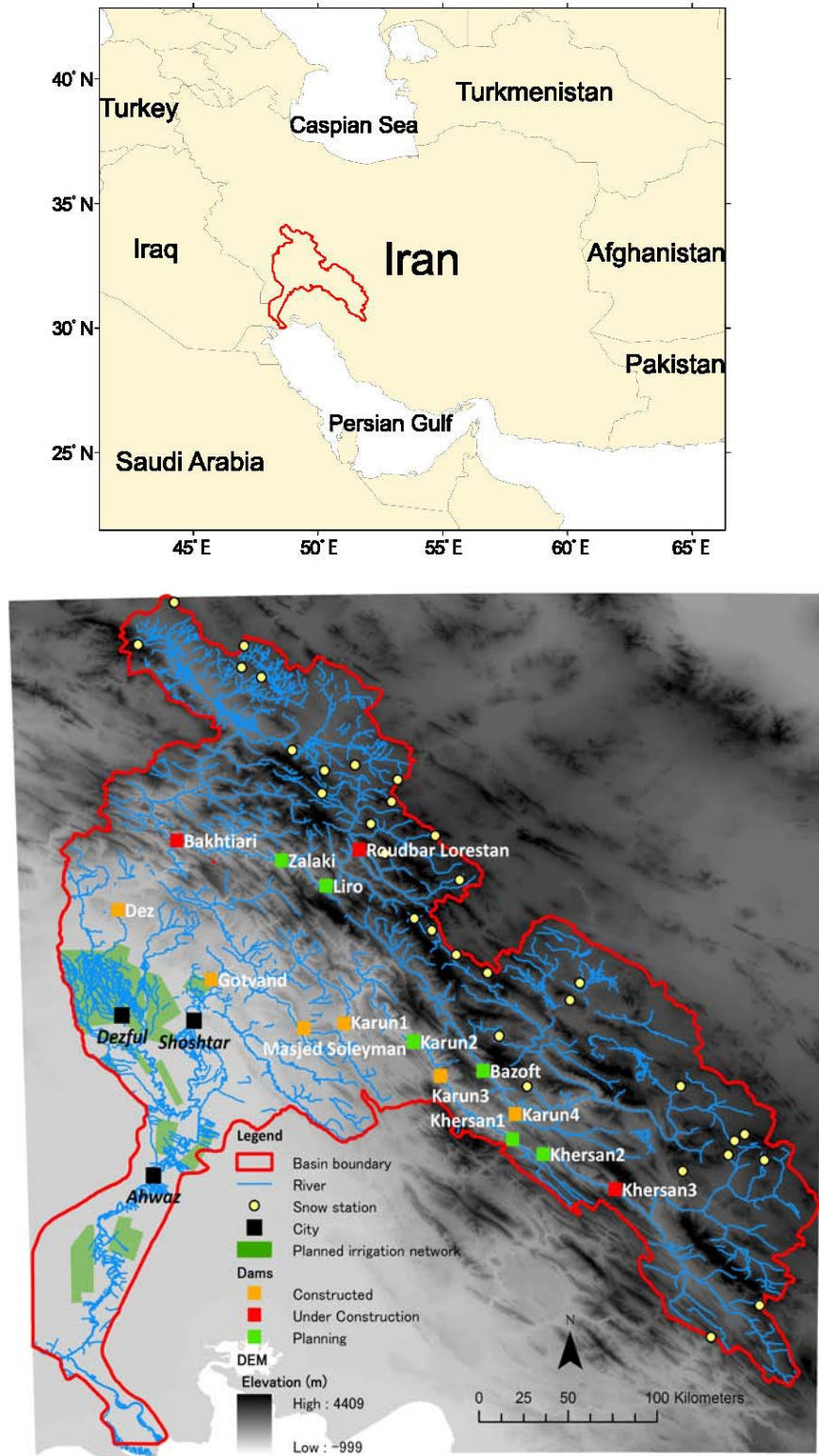
Figure 2.2 Location of the Karun River basin in Iran and its basin map

15
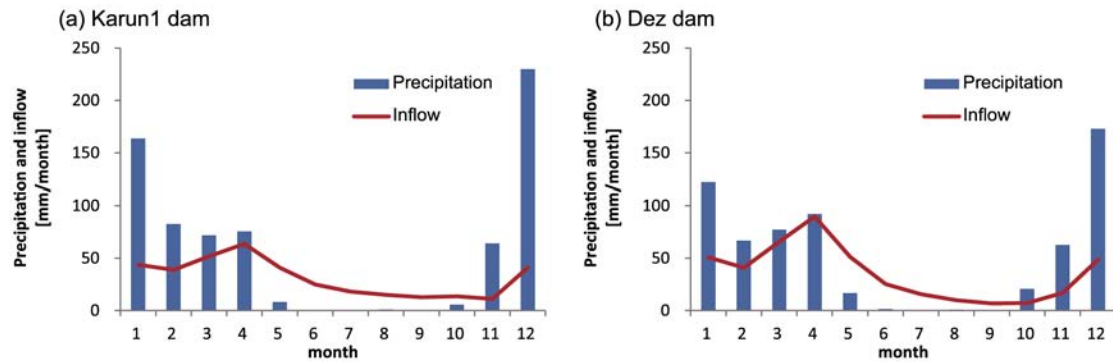
Figure 2.3 Monthly precipitation and dam reservoir inflow at two dam sites, (a) the Karun1 dam and (b) the Dez dam, averaged over 2000-2004.

(Precipitation was spatially averaged in the each dam catchment.)

The Karun River basin has serious water issues in meeting the water demands within the basin. The average annual water discharge in the Karun River is 20.4 billion m^3, which accounts for about one-fifth of the surface water resources of Iran (Sadegh, Mahjouri, & Kerachian, 2010). Meanwhile, the total annual water demand in the basin is around 24.9 billion m^3 (Sadegh et al., 2010). Water use in the basin depends heavily on surface water from the Karun River and its tributaries. In the Khuzestan province, which is located in the middle and downstream part of the basin and demands most of the water use in the basin, about 85% of the freshwater need is met by the rivers and only 15% is taken from groundwater (Afkhami, Shariat, Jaafarzadeh, Ghadiri, & Nabizadeh, 2007). Qanats, a traditional system employed in Iran for using groundwater (Beaumont, 1971), are underdeveloped in the basin as compared with the central region of Iran and are found only around residential areas. Wells have been installed in the past 40 years and are mainly utilized for irrigation and industrial purposes. However,

16

groundwater alkalinity and salinity is high in comparison with surface water (Japan International Cooperation Agency [JICA], 2002).

Floods occur along the main channel of the Karun River and its major tributaries primarily due to intense precipitation and snowmelt in spring. The steepness of the rivers, sedimentation and river bed rise by soil erosion are also among the major causes. Recent floods in 2005 and 2006 resulted in damage to vulnerable flood plain areas and under construction dam sites. The flood in 2005 breached the cofferdam of Karun4 in the upstream of the Karun Basin during the construction of the main dam and cost an estimated damage of more than 7.5 million US dollars (Heidari, 2013). The importance of flood forecasting (Dam inflow forecasting) was recognized, and extensive research on forecasting has been conducted since then (e.g., Ghanbarpour, Abbaspour, & Hipel, 2009; Heidari, 2013; Valipour, Banihabib, & Behbahani, 2013). Periodical droughts also has been a cause of severe disasters in the basin. In 2007-2008, the basin suffered a severe drought similar to the driest year in historical record (A. Heidari, personal communication, May 19, 2012).

Several hydrological models have been developed for the Karun River basin. For instance, Heidari (2013) introduced an early flood forecasting system in the basin, which is linked to the Hydrologic Engineering Center (HEC) series hydrological and hydraulic software developed by the US Army Corps of Engineers (USACE). Additionally, a soil moisture accounting model, which is similar to the Nedbør-Afrstrømnings-Model (NAM) model in Mike11 developed by the Danish Hydraulic Institute (DHI), has been applied for the continuous simulation of basin hydrology (A. Heidari, personal communication, April 2, 2013). These models applied in the Karun River basin are lumped models and have contributed to flood forecasting particularly.

2.3. Water resources development plan in the Karun River basin

In order to reduce water stress in southwestern Iran, a large number of water projects have been implemented in the Karun River basin, including dam construction, irrigation networks and water transfer systems. However, the water resources development in the basin has not been fully implemented yet with merely several dams, hydropower plants and irrigation networks constructed so far. Table 2.2 lists dams in the basin currently in operation, under construction or in the planning phase. Dam development started in the 1950s in the Zagros mountain ranges. Six dams have already been constructed, three dams under construction and six more dams in the planning stage. The major purpose of the dam construction is power generation. The Karun basin contributes 78% of the hydropower generation of the country (Heidari 2013). Additionally, the existing and under-construction dams are expected to supply irrigation water for plains of the downstream areas, whose total cultivation area is 0.8 million hectares including existing and planned networks. Water transfer plans are proposed to supply agricultural water for adjacent plains outside the basin, and optimal operation of the water transfer system is currently being studied (e.g. Sadegh et al. 2010; Nikoo, Nikoo, Kerachian, & Poorsepahy-Samian, 2012).

Although many water resources development projects are being planned, no water resources management has been considered in the Karun River basin from the viewpoint of integration of multiple sectors and also interaction of regulated river discharge between downstream and upstream areas by the development projects.

Table 2.2 List of dams in the Karun River basin

No	Name	Purpose	Storage billion m^3	Height m	Type	status		Catchment area km^2
							since	
1	Gotvand	power, irrigation, flood control	4.53	180	fill	operating	2013	32,480
2	Masjed Soleiman	power	0.23	177	fill	operating	2002	28,681
3	Karun 1	power, irrigation, flood control	2.90	200	arch	operating	1977	26,718
4	Karun 2	power	0.20	130	arch	planning	–	25,000
5	Karun 3	power, irrigation, flood control	2.75	205	arch	operating	2005	24,160
6	Karun 4	power	2.19	230	arch	operating	2010	12,840
7	Khersan 1	power	0.11	181	arch	planning	–	8,873
8	Khersan 2	power	2.30	260	arch	planning	–	8,313
9	Khersan 3	power	0.84	176	arch	under construction	–	7,779
10	Bazoft	power	0.45	207	arch	planning	–	2,191
11	Dez	power, irrigation, flood control	3.34	203	arch	operating	1957	17,350
12	Bakhtiari	power, irrigation	4.80	315	arch	under construction	–	6,412
13	Zalaki	power	1.51	210	arch	planning	–	4,825
14	Liro	power	0.52	210	arch	planning	–	4,085
15	Roudbar Lorestan	power	0.23	158	RCC	under construction	–	2,200

3. Hydrological Model Application in the Karun River Basin

3.1. Background and objectives of this chapter

In arid and semi-arid regions, water is a precious commodity and the management of water resources is a major challenge of the global sustainability, especially when population growth and climate change are considered (Wheater, 2008; Bates, Kundzewicz, Wu, & Palutikof, 2008). Appropriate decision-making processes for water resources development require quantitative prediction of water availability and impact assessment of different management strategies on both water supply and demand sides. The Karun River basin, located in the southwestern semi-arid mountainous area of Iran, would benefit from enhanced hydrological modeling capability for water resources development and planning.

The objectives of this chapter are: (1) to demonstrate the applicability of a distributed hydrological model, with proper modifications wherever necessary, to the semi-arid mountainous Karun River basin in Iran; (2) to assess data availability from the point of efficient hydrological model use; and (3) to outline priorities for enhancing water resources development in semi-arid mountainous regions.

3.2. Hydrological model selection

3.2.1. Hydrological processes in semi-arid mountainous regions

General characteristics of hydrological processes in arid and semi-arid mountainous regions are summarized as follows (Pilgrim et al., 1988; Beven, 2002; Wheater, 2008; Nicholson, 2011) although hydrological processes in such regions are highly variable from region to region: (1) spatial and temporal variability of precipitation, (2) rapid runoff generation dominated by the infiltration excess overland flow, (3) channel transmission loss and (4) snowpack and snowmelt. In general, precipitation in arid and semi-arid regions is spatially and temporally variable, and occurs in local convective storms with high intensity over a short duration in limited areas (Pilgrim et al., 1988). Rapid runoff dominated by infiltration excess overland flow generally occurs in arid and semi-arid regions (Wheater, 2008). Infiltration excess overland flow is generated by intense precipitation that may exceed soil infiltration capacity (Horton, 1940). Infiltration capacity in arid and semi-arid regions has high spatial heterogeneity and temporal variability, which are affected by soil texture, soil structure, vegetation cover, raindrop impact, surface crusting, pattern of rainfall intensity at the soil surface (Beven, 2002). Bare surface soils without vegetation cover are affected by the direct impact of raindrops that rearranges soil particles and forms surface crusts by sealing large pores at the soil surface (Beven, 2002). Surface crusts once formed significantly reduce infiltration capacity of bare surface soils (Morin & Benyamini 1977), and infiltration capacity during an intense precipitation event might increase due to the breakdown or erosion of the surface crust (Beven, 2002).

Furthermore, surface runoff production may also be affected by antecedent soil moisture that controls the infiltration capacity of the soil in the non-linear responses of runoff to precipitation (Beven, 2002).

Channel transmission losses caused by infiltration into river bed and evaporation from the river surface likely occur at streams in arid and semi-arid regions (Pilgrim et al., 1988). The losses dissipate river discharge and might be one of the causes of ephemeral flow. Furthermore, transmission losses are one of the major sources of groundwater recharge, depending on underlying geology (Wheater, 2008).

In addition, snow accumulation in high altitude mountains is significant water resources in semi-arid regions. Snowpack accumulated in wet winter melts with increased temperatures and contributes to river discharge in spring and summer.

3.2.2. Criteria for model selection

A distributed hydrological model may provide more comprehensive information of water availability for decision making concerning water resources development planning in the Karun River basin. For example, distributed models allow for assessment of water availability at any location at various spatial and temporal scales (e.g., Ajami, Gupta, Wagener, & Sorooshian, 2004; Pechlivanidis, Jackson, McIntyre, & Wheater, 2011). This characteristic has advantages for its use in the assessment of upstream to downstream impact of existing and planned water resources development projects (e.g., Lauri et al., 2012; Masih et al., 2012; McCartney & Girma, 2012). Additionally, distributed models allow for more rigorous specification of spatially-

variable intense precipitation events and heterogeneous soil properties (e.g., Smith et al., 2004; Kampf & Burges, 2007). Furthermore, distributed models can take into account impacts of land use change (e.g., Thanapakpawin et al., 2006; Zhang, Shoemaker, Woodbury, Cao, & Zhu, 2013) as well as possible impacts of climate change (e.g., Gosling et al., 2011; Harding et al., 2012; Lauri et al., 2012; Chien et al, 2013; Hidalgo et al., 2013). Therefore, development and application of a distributed hydrological model would further support decision making related to water resources development planning in the Karun River basin.

This study has considered the following five criteria indispensable in the selection of a distributed model appropriate for the Karun River basin. The first criterion is that a model should be based on physical processes. This is essential because especially land surface processes, such as overland flow, evapotranspiration and infiltration, are complicated and important in semi-arid regions. The second criterion is that the model must be capable of long-term simulation. Since water resources development planning requires the consideration of long-term projections of water availability, event-based hydrological models are not suitable for the purpose. The third criterion is that the model needs to be able to simulate snowpack and snowmelt processes. This is because water resources in the semi-arid mountainous regions of Iran are highly dependent on contributions of snowmelt. The fourth criterion is that the chosen model must be capable of using globally-available data efficiently when local observation data are sparse or unavailable. As distributed physical catchment data, such as soil types, land cover types and meteorological data, are often poorly gauged in the basin, hydrological models incorporating remotely-sensed data are highly useful. The last criterion is that the model should be parsimonious and has minimal parameters to be

calibrated, which are preferably robust to new observation data when they are added. In data-poor basins, the calibration of model parameters is highly challenging; thus the parsimonious and robust parameter criterion is vital. The last two criteria are particularly important, not only in arid and semi-arid regions, but for any practical hydrological model to be used anywhere in the world.

3.2.3. Description of BTOPMC

According to the criteria above, this study selected the Block-wise TOPMODEL with the Muskingum-Cunge routing method (BTOPMC; Takeuchi, Ao, & Ishidaira, 1999; Takeuchi, Hapuarachchi, Zhou, Ishidaira, & Magome 2008) that satisfies, as further explained in the subsequent chapters, all the criteria described above and is well suited as a model for the case study in the Karun River basin. The model is based on the TOPMODEL concept (Beven & Kirkby, 1979) with different definitions of topographical index and parameters. BTOPMC is the coupled model of runoff generation and flow routing. The block-wise TOPMODEL concept is used for runoff generation from each grid cell, and the Muskingum-Cunge routing method is used for flow routing. BTOPMC has been used as the core hydrological module of the University of Yamanashi Distributed Hydrological Model (YHyM), which is composed of several modules of hydrological components, such as the core hydrological module, potential evapotranspiration module, snow and soil freezing module, etc.

The structure and parameters of BTOPMC are designed in such a way that leads to its superiority over both lumped and distributed models. The schematic image of

runoff generation in a grid cell in the model is shown in Figure 3.1. The model generates infiltration excess overland runoff, saturation excess runoff and base runoff from each grid cell (q_{ofh}, q_{of} and q_b in Figure 3.1, respectively). The base runoff at grid-cell i at the time step t, $q_{b,i}(t)$, was generated from the following equation:

$$q_{b,i}(t) = D_i \tan \beta_i \exp\left(- SD_i(t) / m\right) \tag{3.1}$$

where D_i is the groundwater discharge ability at grid-cell i in m/day, β_i is the gradient of grid-cell i, $SD_i(t)$ is the saturation deficit in the unsaturated zone at grid-cell i at the time step t in m as shown in Figure 3.1, and m is the runoff decay factor according to the decrease of saturation deficit in m.

The saturation excess runoff at grid-cell i at the time step t, $q_{of,i}(t)$, is generated when drainage to the unsaturated zone exceeds the storage capacity (i.e., the saturation deficit of the unsaturated zone, $SD_i(t)$, is negative), which is described by:

$$q_{of,i}(t) = \begin{array}{ll} -\{SD_i(t) - \min[SD_i(t-1),0]\} & if \quad SD_i(t) < 0 \\ 0 & else \end{array} \tag{3.2}$$

The infiltration excess overland runoff at grid-cell i at time step t, $q_{ofh,i}(t)$, is generated when the intensity of rainfall on the ground exceeds the infiltration capacity of the soil surface, which is described by:

$$q_{ofh,i}(t) = \max\{P_a(t) - Inf_{max}, 0\} \tag{3.3}$$

where $P_a(t)$ is the net precipitation on the land surface at time step t, and Inf_{max} is the infiltration capacity of the soil surface.

The heterogeneity of root zone depth over the basin, which is used to calculate the maximum storage of the root zone, was taken into account by using the distribution of land cover type and rooting depth. The spatial variation of infiltration capacity, hydraulic conductivity and groundwater dischargeability over the basin was considered based on the percentage of sand, silt and clay presented in each soil type.

Generated infiltration excess overland runoff and subsurface runoff drain into a stream segment in each grid cell and then routed to the basin outlet. The flow routing in the model was carried out by the modified Muskingum-Cunge routing method (Masutani & Magome, 2009). The modified method is advantageous in that it can avoid the violation of water conservation when its standard numerical calculation scheme is used. It is particularly effective for routing in a large-scale river basin with a long temporal scale and/or a wide spatial scale (Masutani & Magome, 2009).
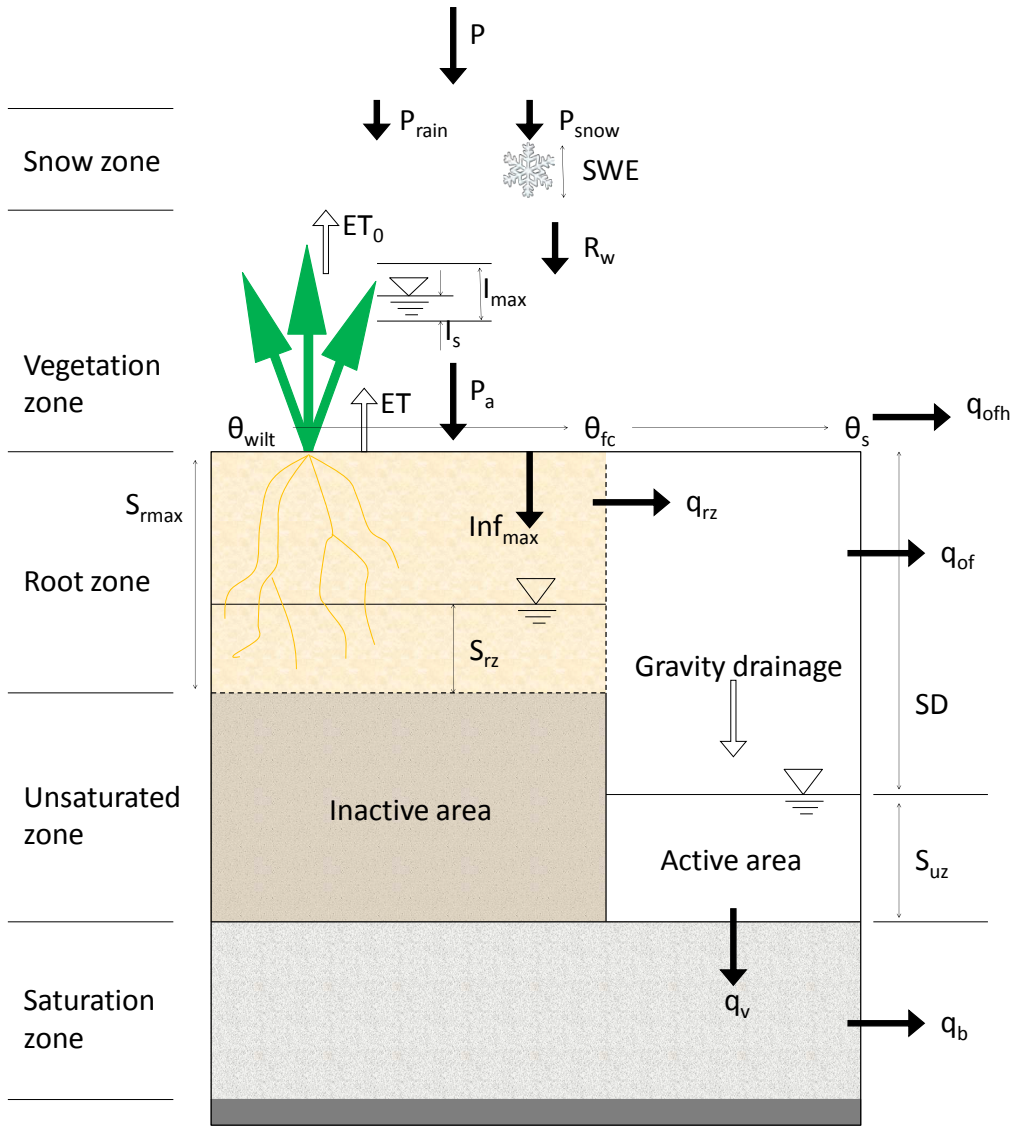
Figure 3.1 Schematic image of runoff generation in a grid cell in BTOPMC (vertical profile).

(P is the gross precipitation, P_{rain} is the rainfall, P_{snow} is the snowfall, SWE is the snow water equivalent, R_w is the meltwater from snowpack, ET_0 is the interception evaporation, I_{max} is the interception storage capacity, I is the interception state, P_a is the net precipitation on the land surface, ET is the actual evapotranspiration, Inf_{max} is the infiltration capacity of soil surface, $S_{r\,max}$ is the storage capacity of the root zone, S_{rz} is the soil moisture state in the root zone, SD is the saturation deficit in the unsaturated zone, S_{uz} is the soil moisture state in the unsaturated zone, q_{ofh} is the infiltration excess overland runoff, q_{of} is the saturation excess runoff, q_{rz} is the storage excess in the root zone that drains into the unsaturated zone under gravity, q_v is the recharge to the saturation zone, and q_b is the base runoff. θ_{wilt}, θ_{fc}, θ_s are the soil water content at the wilting point, field capacity and saturation, respectively.)

An application study of BTOPMC in semi-arid regions was previously conducted by Zhou, Ishidaira, Hapuarachchi, Georgievsky, and Takeuchi (2007). They applied BTOPMC to the Yellow River with snowpack accumulation and snowmelt modules by modifying the land surface processes to incorporate the temperature effects of snowpack and snowmelt. Although their attempts were quite successful to show the applicability of BTOPMC to semi-arid snow-affected regions, the results still need to be improved to better reproduce flood peaks and low flows. It is evident that there is still some room left for improvement especially on the modeling of land surface processes in semi-arid regions, which is a part of the objectives of this study.

It is true that other distributed hydrological models can be also selectable. Widely-used models are, for example, the Soil and Water Assessment Tool (SWAT), developed by the Agricultural Research Service of the United States Department of Agriculture (USDA) (Gassman, Reyes, Green, & Arnold, 2007), and the Variable Infiltration Capacity (VIC) model, which was originally developed by Xu Liang at the University of Washington (Liang, Lettenmaier, Wood, & Burges, 1994). Many application studies of these models in semi-arid regions have been conducted. For example, Masih et al. (2012) apply SWAT to a river basin in Iran and analyze effects on river discharge by conversion of rain-fed areas to irrigated fields. Yong et al. (2013) apply VIC model to the Laohahe Basin, a typical semi-arid zone of northeast China, and investigate historical spatial-temporal changes of water resources. However, this study selected BTOPMC as the most suitable model for the following practical reasons. It well satisfies the criteria described in the previous section and, since it was invented by the author's supervisor, the author's laboratory has a large stock of experiences of successful application of the model to various parts of the world (e.g., Takeuchi et al.

1999, 2008; Ao et al., 2003; Shrestha et al., 2007; Hapuarachchi et al., 2008; Manandhar, Pandey, Ishidaira, & Kazama, 2012).

3.3. Methodology

3.3.1. Modification of infiltration capacity in BTOPMC

Rapid runoff dominated by infiltration excess overland runoff often occurs in arid and semi-arid regions, particularly when precipitation is delivered in intense bursts. Soil infiltration capacity is a key parameter for physical-process models to generate overland runoff. Different types of approaches to model infiltration capacity were developed by, for example, Horton (1940), Philip (1957) and Green and Ampt (1911). These methods require detailed precipitation data, particularly at a minute temporal scale, to model temporally variable infiltration capacity. However, such detailed data is not available in a large area of the target basin in semi-arid regions. Therefore, this study considered modeling infiltration excess overland runoff in a simplified way for a daily simulation with temporally constant infiltration capacities of the soil in the target area.

The original BTOPMC (non-modified version of BTOPMC), which was developed and applied in the Mekong River basin by Takeuchi et al. (2008), assumes that the infiltration capacity at model grid i in m/day, Inf_i, equals to the groundwater dischargeability at model grid i in m/day, D_i. This is considered a function of the texture of the land surface layer and may be considered as a parameter that expresses the potential of groundwater to discharge to the surface of the grid cell (Takeuchi et al.,

29

2008). Dischargeability was calculated by multiplying content percentages of sand, silt and clay and the coefficients of dischargeability in each types, i.e., D_{0_sand}, D_{0_silt} and D_{0_clay}, respectively. The content percentages were obtained from the remotely-sensed data sets listed in Table 3.1. The coefficients of dischargeability must be calibrated to the basin. Nevertheless, this assumption mainly applies to humid regions where infiltration capacity is usually high compared with precipitation intensity, and infiltration excess overland runoff seldom occurs (Takeuchi et al., 2008). Therefore, in this study, the infiltration capacity in each model grid was adjusted by multiplying the adjustment coefficient for arid and semi-arid regions as follows:

$$Inf_{arid,i} = Inf_i \cdot A \tag{3.4}$$

where $Inf_{arid,i}$ is the infiltration capacity in arid and semi-arid regions in m/day. A is the adjustment coefficient for arid and semi-arid regions. The value of the adjustment coefficient is affected by two factors in the target basin: (1) the characteristics of intense precipitation that generate infiltration excess overland runoff; and (2) the effect of soil surface crusts, which significantly decrease the infiltration capacity of the bare soil (Morin & Benyamini 1977). The coefficient represents such unique phenomena in arid and semi-arid regions for hydrological simulations in a daily time scale. The range of the coefficient is 0 – 1, and the coefficient should be calibrated according to the procedure described in the section 3.3.2.

3.3.2. Model verification

This study applied both non-modified and modified versions of BTOPMC to the Karun River basin above the Karun1 dam site (catchment area: 26,718 km^2) and the Dez dam site (catchment area: 17,350 km^2) as depicted in Figure 3.2. These dam sites were selected because model verification data are available. The verification data are dam reservoir daily inflow data at Karun1 and Dez for the period of 2000-2004, which were provided by the Iran Water and Power Resources Development Co. (IWPC). During the time period, the dam inflows were not regulated by dam operations upstream of Karun1 and Dez. The available time-series data were divided into the calibration period of 2000-2002 and the validation period of 2003-2004. Manual calibration through trial and error in consideration with underlying physical processes for runoff generation was applied to obtain an adequate parameter set. The simulation was conducted by daily time step because of the use of daily precipitation data and also due to computational limitations related to long-term simulation. During calibration and validation, the initial state variables were chosen arbitrarily first, then updated at the final time step.

The overall model performances of both non-modified and modified versions of BTOPMC through calibration and validation periods were evaluated by using the Nash-Sutcliffe efficiency coefficient (NSE; Nash & Sutcliffe, 1970) and volume bias (VB) as follows:

$$NSE = 1 - \frac{\sum_{t=1}^{n}(Q_{obs,t} - Q_{sim,t})^2}{\sum_{t=1}^{n}(Q_{obs,t} - \overline{Q}_{obs})^2} \qquad (3.5)$$

$$VB = \frac{\sum\limits_{t=1}^{n}(Q_{sim,t} - Q_{obs,t})}{\sum\limits_{t=1}^{n}Q_{obs,t}} \qquad (3.6)$$

where $Q_{obs,t}$ is the observed discharge at time step t, $Q_{sim,t}$ is the simulated discharge

at time step t, $\overline{Q}_{obs}$ is the average observed discharge and n is the number of time

steps. Periods with missing observed discharge data were excluded from the evaluation.

Model performance regarding snow water equivalent (SWE) estimation was further

evaluated in comparison with observed SWE data at 31 stations. The locations of snow

stations are shown in Figure 2.2. SWE data were not frequently observed, and most of

them were once a year.
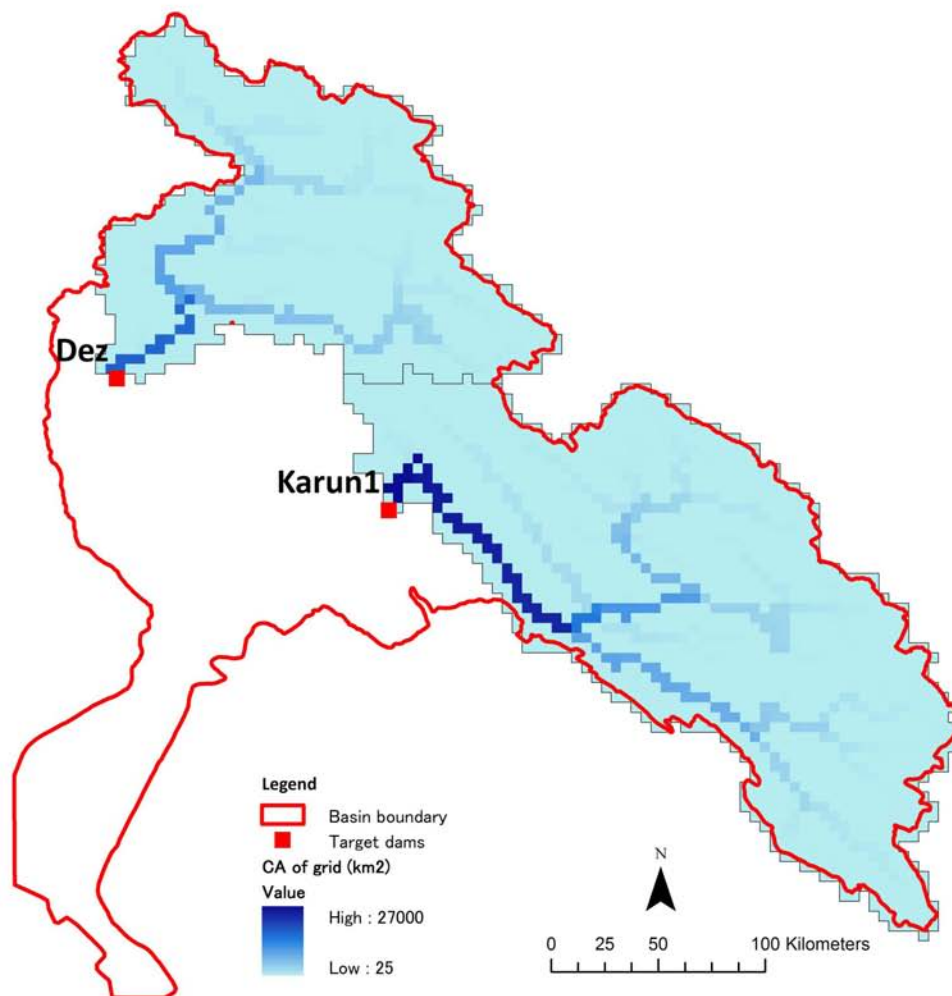
Figure 3.2 Catchments of the Karun1 and Dez dams in the Karun River basin generated by BTOPMC in 5 km spatial resolution.

(The river networks over the catchments in the study area are depicted in blue gradation with each grid showing the size of a catchment area at each location.)

3.4. Data

3.4.1. Data used for model set-up

BTOPMC heavily depends on the Digital Elevation Model (DEM) for topographical index computation and channel network extraction. Data of elevation, flow accumulation and drainage direction were obtained from the Hydrological data and maps based on SHuttle Elevation Derivatives at multiple Scales (HydroSHEDS), based on the NASA Shuttle Radar Topography Mission (SRTM). The novel scaling algorithm developed by Masutani and Magome (2008, 2013) was applied to upscale the original resolution of the HydroSHEDS to 5km resolution, which was selected considering the limitation of computational resources and the original resolution of input data although scale issues in hydrological modeling still remains unsolved. The algorithm reserves the geomorphologic characteristics of the fine-resolution network, such as river length and elevation gradient, into any coarser spatial resolution with sufficient accuracy (Masutani & Magome, 2008).

Modeling snow pack and melt processes is significant to reproduce seasonal discharge in the Karun River basin. Nourani and Mano (2007) applied the TOPMODEL with a kinematic wave model to the Karun river sub-basins. However, they did not consider snow pack and melt processes in the model. In this study, snow pack and melt were represented by the simple degree-day method in BTOPMC (Georgievsky, Ishidaira, & Takeuchi, 2006). Although the amount of snow is controlled by energy balance on the snow surface, it is difficult to obtain necessary data to calculate the energy balance component. Therefore, a simple degree-day method that uses air

temperature to partition precipitation into rainfall and snowfall was adopted.

A soil freezing module was also considered in the model. If the temperature is below the threshold temperature, which has to be calibrated, the top of the soil is considered as frozen and no infiltration occurs, but base flow continues (Hapuarachchi et al., 2008).

The Shuttleworth-Wallace (SW) model was incorporated to estimate long-term seasonal potential evapotranspiration (PET) within BTOPMC. The SW model can estimate evaporation from land and transpiration from plants separately using parameter values from the literature and publicly available data sets (Zhou et al., 2006). The basic data used for the model set-up for the Karun River basin is listed in Table 3.1.

Table 3.1 Basic data used for the model set-up

Type	Description	Source	Original spatial resolution	Additional information
Topography, Land, Soil data	Digital Elevation Map (DEM) Flow direction map Basin boundary	HydroSHEDS	3x3 second (~90x90 m)	Upscaled into 5km using the novel upscaling algorithm (Masutani & Magome, 2008, 2013)
	River width	-	-	Calculated based on the contributing area (Lu, Koike, & Hayakawa, 1989)
	Root depth	Literature values	-	Sellers et al. (1994, 1996)
	Soil map	FAO	-	The Digital Soil Map of the World
	Soil properties	FAO	-	USGS soil triangle (Rawls, Brakensiek, & Saxton,1982; Rawls, & Brakensiek, 1985)
	Land cover type	IGBP Version 2	30x30 second (~1x1 km)	17 types of IGBP land cover classification used to set maximum root zone storage

Notes: HydroSHEDS is hydrological data and maps based on shuttle elevation derivatives at multiple scales, FAO is the Food and Agriculture Organization of the United Nations, USGS is the United States Geological Survey, and IGBP is the International Geosphere-Biosphere Program.

3.4.2. Hydro-meteorological data

The hydro-meteorological data on the Karun River basin are summarized in Table 3.2. As local data are not available, global data sets are used. This study used the Asian Precipitation - Highly-Resolved Observational Data Integration Towards Evaluation (APHRODITE) gridded precipitation data set based on a dense network of daily rain-gauge data throughout Asia, including in the Middle East (Yatagai, Xie, & Alpert, 2008; Yatagai et al., 2012). Climate forcing data from the Climatic Research Unit time-series (CRU-TS) and average climatology (CRU-CL), and the Normalized Difference Vegetation Index (NDVI) data from the Global Inventory Modeling and Mapping Studies (GIMMS) were used for the PET estimation by the SW model. Data were reformatted into the common spatial resolution of the model (5x5 km) before the simulation.

Table 3.2 Hydro-meteorological data used in the Karun river application

Type	Description	Source	Original spatial resolution	Original temporal resolution	Additional information
Hydro-meteorological data	Precipitation	APHRODITE Middle East	0.25x0.25 degree (~25x25km)	Daily	Yatagai et al. (2008, 2012)
	Temperature Cloud cover Daylight duration Radiation Vapor pressure Wind speed	CRU CL1.0, TS3.1	0.50x0.50 degree (~50x50km)	Monthly	Global monthly data for 1901-2009(TS3.1), 1961-1990(CL1.0), used for potential evapotranspiration calculation
	NDVI	NOAA-AVHRR	8x8 km	Half-monthly	
	Observed discharge	Iran Water and Power resources development Co. (IWPC)	Gauged	Daily	Observed daily inflow at the Karun1 dam site and Dez dam site from 2000-2004, used for calibration and validation of BTOPMC.
	Snow Water Equivalent (SWE)			Basically once a year (varying from station to station)	SWE data at 31 stations, used for calibration and validation of BTOPMC.

Notes: APHRODITE is the Asian Precipitation - Highly-Resolved Observational Data Integration Towards Evaluation, CRU-TS and CRU-CL are the Climate Research Unit time series and average climatology, NDVI is the Normalized Difference Vegetation Index, and NOAA-AVHRR is the National Oceanic and Atmospheric Administration (USA)-Advanced Very High Resolution Radiometer.

3.5. Results of model application

Table 3.3 summarizes the overall model performance of both non-modified and modified versions of BTOPMC evaluated by NSE and VB at the Karun1 and Dez dam sites for the calibration and validation periods. Table 3.4 shows the list of parameters in the modified version of BTOPMC and calibrated values. The modified model, which applied the adjustment coefficient to the infiltration capacities of the soil surface in each model grid cell, shows better performance than the non-modified model in all cases, except the validation cases at Dez in which both models show poor performance with NSE reading less than 0.05. The modification improves NSE, for example, from 0.57 to 0.73 at Karun1 during the calibration period, which is the best NSE among all cases. Figure 3.3 shows the best simulation results by the modified model at Karun1 during the calibration period. Figure 3.3(i) compares simulated discharges between the non-modified and modified models. The small figure in Figure 3.3(i) enlarges the results in December 2001. The non-modified model did not generate flood peaks, whereas the modified model generated flood peaks, for example, on 6, 13 and 21 December 2001. These peaks were generated by the infiltration excess overland runoff (Figure 3.3(c)) when the intense rainfall events were observed (Figure 3.3(h)). Despite the simple adjustment for infiltration capacity, the model modification in this study improved the performance a great deal for the flood peak generation.

In addition to the successful flood peak generation by the modified model, the model well simulated seasonal discharge with snowpack and snowmelt processes. Figure 3.4 compares simulated monthly discharges at Karun1 during the calibration period between the models with and without the snow module. The monthly discharge

simulated by the model with the snow module shows the same result of the daily discharge in Figure 3.3(i). The model with the snow module reproduced the seasonal change of the observed discharge better than the model without the snow module, i.e., less discharge in January due to snow pack in the mountainous areas and more discharge in April due to snowmelt. Snowfall (Figure 3.3(g)) accumulated in upstream area as SWE in December and January (Figure 3.3(f)), and snowmelt water contributed to base runoff in February and March (Figure 3.3(c)). Furthermore, the model with the snow module also simulated the recession of low flows in summer dry (Figure 3.3(i)).

However, the modified model after the calibration shows poor performance during the validation period at Karun1 with NSE measured 0.48. Figure 3.5 shows the simulated discharge by the modified model compared with observations at Karun1 during the validation period and at Dez during the calibration and validation periods. As shown in Figure 3.5(a), the model underestimates the discharge from January to March in 2003. Figure 3.6 shows comparison between the observed and simulated SWE. The model also underestimates SWE in 2003 and 2004 as many black filled circles indicate zero for the simulated SWE in Figure 3.6(a).

Furthermore, the model performance at Dez is even far poorer than that at Karun1, as NSE for the calibration and validation periods are 0.27 and 0.04, respectively. Even though parameter calibration was conducted within the range of each parameter shown in Table 3.4, the model mostly underestimates discharge through the years including flood peaks during the calibration and validation periods at the Dez dam site as shown in Figure 3.5(b) and (c), respectively. This underestimation, particularly at the Dez dam site, associates huge negative values of VB, which indicate overall systematic errors in the total simulated discharge volume. The drying function

38

parameter, α, is a key parameter to estimate actual evapotranspiration and affects total water balance. However, the model was not able to reproduce discharge even with the minimum value of the range of α, which decreases actual evapotranspiration and thus increases discharge. Further elaborate investigation of parameters in relation to landscape and composition of geology, such as Zhou et al. (2006, 2007), is necessary to advance model use in semi-arid mountainous regions, but such effort is considered beyond the scope of this study and left it as a priority agenda for the future.

Table 3.3 Overall performance of the non-modified and the modified versions of BTOPMC evaluated by NSE and VB for the calibration (2000-2002) and validation periods (2003-2004) at the Karun1 and Dez dam sites.

Model case	Verification points	Calibration (2000-2002)		Validation (2003-2004)	
		Nash-Sutcliffe Efficiency coefficient[-]	Volume Bias [%]	Nash-Sutcliffe Efficiency coefficient[-]	Volume Bias [%]
Non-modified model	Karun1 dam	0.57	-14.5	0.41	-22.7
Modified model	Karun1 dam	0.73	-12.4	0.48	-19.7
Non-modified model	Dez dam	0.25	-33.6	0.049	-46.4
Modified model	Dez dam	0.27	-33.9	0.042	-46.9

Table 3.4 List of parameters in the modified version of BTOPMC and calibrated values

Categories	Parameters	Unit	Description	Value range	Calibrated value	Sources
Runoff generation	Decay factor (m)	m	It describes how actual subsurface runoff decrease assuming an exponential decay in dischargeability with increasing local saturation deficit.	0.01 – 0.1	0.057	Takeuchi et al. (2008)
	Drying function parameter (α)	-	Empirical constant in the drying function for the estimation of actural evapotranspiration (Vörösmarty et al., 1998).	-10 – 10	-6	Takeuchi et al. (2008)
	Coefficients of groundwater dischargeability (D_{0_sand}, D_{0_silt}, D_{0_clay})	m/day	Potential of groundwater to discharge to the surface which is considered as a function of soil types.	0.01 – 2.0	Sand: 0.09 Silt: 0.04 Clay: 0.01	Takeuchi et al. (2008)
	Adjustment coefficient of infiltration capacity for arid and semi-arid regions (A)	-	Coefficient to adjust the infiltration capacity of the soil in arid and semi-arid regions	0 - 1	0.04	
	Soil freezing threshold temperature (T_{freeze})	℃	Temperature that soil surface is considered as frozen.	-2.0 – 2.0	-1.5	Hapuarachchi et al. (2008)
Snow model parameters	Threshold temperature of snowfall (T_b)	℃	Threshold of temperature below which all precipitation is snowfall	-2.0 – 2.0	-2	Georgievsky et al. (2006); Takeuchi et al. (2008)
	Threshold temperature of rainfall (T_r)	℃	Threshold of temperature above which all precipitation is rainfall	-2.0 – 2.0	2	Georgievsky et al. (2006); Takeuchi et al. (2008)
	Base temperature (T_{base})	℃	Threshold of temperature above which snow melts	0.1 – 1.0	0.1	Georgievsky et al. (2006); Takeuchi et al. (2008)
	Degree-day factor (M_f)	mm/℃/day	Degree day factor for snowmelt calculation	1.0 – 1.9	1	Georgievsky et al. (2006); Takeuchi et al. (2008)
	Maximum liquid water holding capacity of snow (φ)	-	Parameter that characterizes the maximum liquid water holding capacity of snow	0.4 - 0.6	0.5	Georgievsky et al. (2006); Takeuchi et al. (2008)
	Refreezing coefficient (C_{fr})	-	Refreezing coefficient	0.01 – 0.09	0.05	Georgievsky et al. (2006); Takeuchi et al. (2008)
River routing	Block average Manning's roughness coefficient (n_0)	$m^{-1/3}s$	Stream channel roughness which impacts the delay of river flow. The coefficients in each grid were assumed based on local slope of stream segment in each grid.	0.01 – 0.8	0.01	Takeuchi et al. (2008)
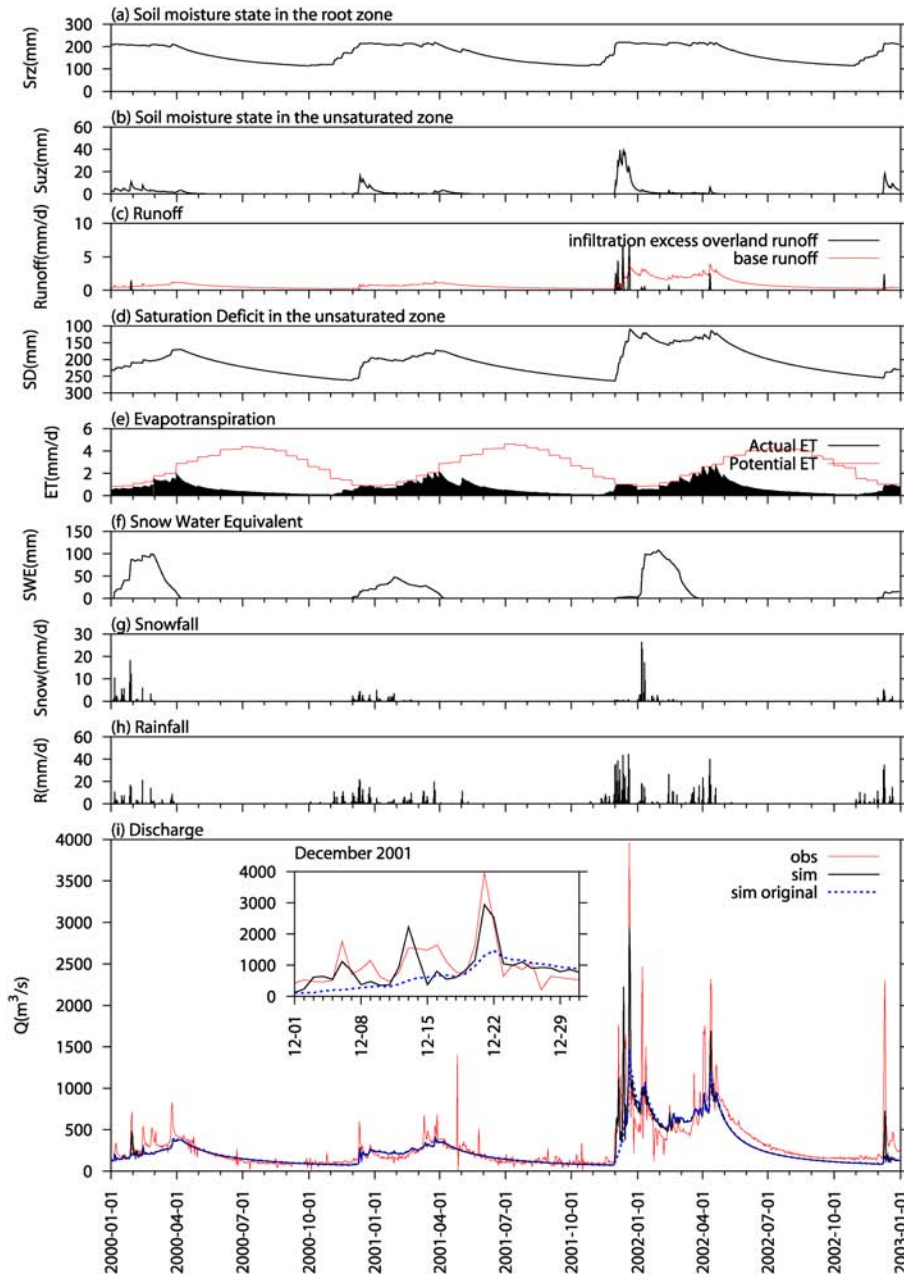
Figure 3.3 Simulation results at the Karun1 dam site during the calibration period of 2000-2002.

((a) Soil moisture state in the root zone, S_{rz}, (b) soil moisture state in the unsaturated zone, S_{uz}, (c) Infiltration excess overland runoff and base runoff, q_{ofh} and q_b, (d) saturation deficit in the unsaturated zone, SD, (e) potential and actual evapotranspiration, PET and ET, (f) snow water equivalent, SWE, (g) snowfall, P_{snow}, (h) rainfall, P_{rain}, and (i) simulated and observed discharge, Q_{sim} and Q_{obs}. For the verification of the modified infiltration capacity in BTOPMC by introducing an adjustment coefficient to the infiltration capacities of the soil surface in each model grid cell as described in section 3.3.1, the simulated discharge by the original BTOPMC without modification, $Q_{sim\_original}$, is also shown in (i). The small figure in (i) shows the enlarged result in December 2001. All variables, except discharge, are spatially averaged in the catchment area of the dam.)

41
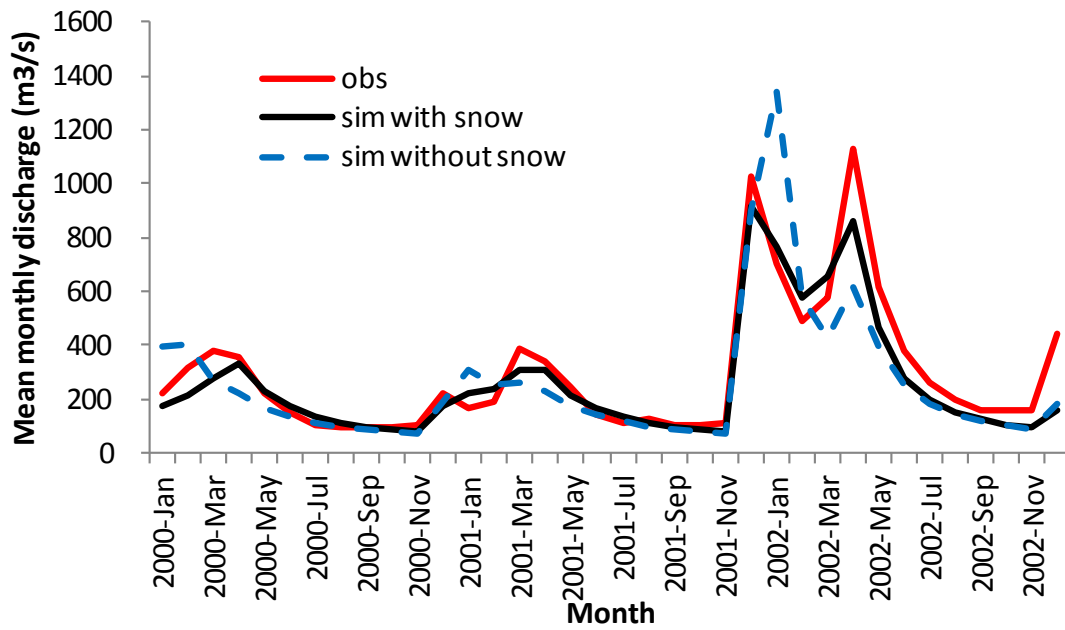
Figure 3.4 Comparison of mean monthly discharge at the Karun1 dam site during the calibration period of 2000-2002.
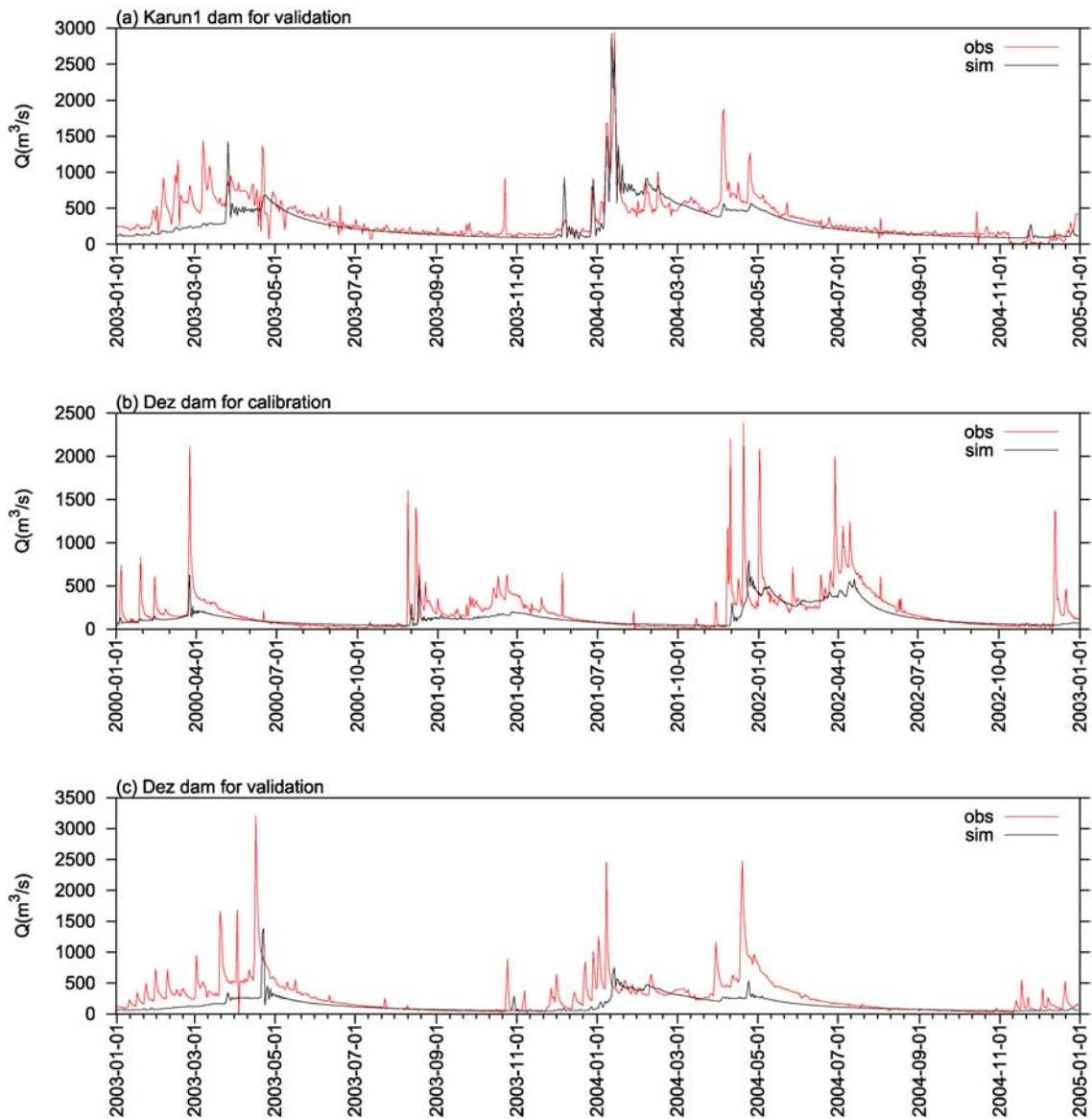
Figure 3.5 Simulated discharges compared with observations (a) at the Karun1 dam site during the validation period of 2003-2004, (b) at the Dez dam site during the calibration period of 2000-2002, and (c) at the Dez dam site during the validation period of 2003-2004.
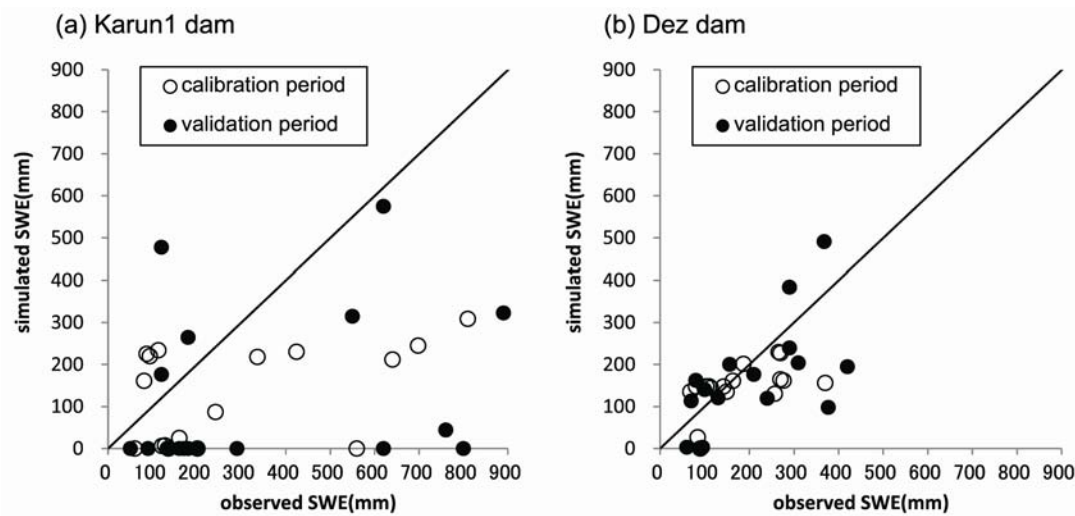
Figure 3.6 Comparison between observed and simulated SWE during the calibration period of 2000-2002 and the validation period of 2003-2004 in the catchment area of (a) the Karun1 dam site and (b) the Dez dam site.

3.6. Discussion

The case study results from the Karun River basin described in the previous section clearly indicate the applicability of BTOPMC with necessary modification for semi-arid mountainous regions. However, serious problems that prevent successful model application, such as the model underestimation particularly at the Dez dam site, were also highlighted. In this section, these results will be examined according to the most important characteristics of hydrological signatures for water resources development in semi-arid mountainous regions. Further, how these results affect water resources development in semi-arid mountainous regions and what should be improved will be discussed.

3.6.1. Important hydrological signatures

Distributed hydrological models are expected to support decision making on integrated water resources development by providing information regarding water availability at any location in a basin at various spatial and temporal scales. For this purpose, hydrological models must be able to provide reliable information about basin hydrology such as annual runoff, seasonal runoff, duration curves, low flows, flood flows and hydrographs, which are collectively called the "signatures" of the basin "organism" (Blöschl et al., 2013).

Annual runoff is a statistic describing water availability on an annual time step, and represents the annual balance between precipitation and evapotranspiration. Seasonal runoff reflects seasonal changes of water storage characteristics of the basin. The flow duration curve represents the frequency characteristics of flow level from the peak to the bottom. The low-flow characteristics represent the minimally available flow, which reflects a precipitation pattern, evapotranspiration and geology, and control water use and environmental flow. The flood-flow characteristics represent the nature of the maximum flows, including its peak, recession and occurrence frequency, which reflects the surface runoff, and the concentration and frequency of heavy precipitation. Finally hydrographs represent all the characteristics mentioned above.

For water resources development in semi-arid mountainous regions, the important hydrological signatures are considered to be annual runoff, seasonal runoff, low flows and flood flows. Annual runoff is the basis of water resources planning and indispensable information for dam storage design and operation. Similarly, seasonal runoff is important for agricultural use and dam storage operation especially of small dams that lack carryover storage. Low-flow and flood-flow characteristics are decisive

in drought and flood management.

3.6.2. Annual runoff

The case study results at the Dez dam site indicate that BTOPMC underestimates discharge. In order to investigate causes of the underestimation, an annual water balance was computed. The annual water balance equation in a river basin can be written as:

$$\frac{dS}{dt} = P - ET - R \tag{3.7}$$

where S is the annual total water storage of the basin in mm, P is the annual precipitation in mm/year, ET is the annual actual evapotranspiration in mm/year and R is the annual total runoff in mm/year. Annual total water storage change, $\frac{dS}{dt}$, may vary between dry and wet years. However, observed data for estimating water storage components in the case study area, such as land surface storage, soil moisture and groundwater, are not available. Thus, this study assumes steady conditions and the remainder of equation (4) becomes:

$$R = P - ET \tag{3.8}$$

Figure 3.7 shows comparison between annual precipitation and observed annual discharge at Karun1 and Dez. Annual variables were calculated from November to October, a period that corresponds to the beginning of the wet season to the end of the

dry season in the basin, respectively. In Figure 3.7, departure from the line, which indicates that discharge is equal to precipitation, is represented as ET. The data of Dez in 2002, 2003 and 2004 show less ET as compared to the others. This discrepancy suggests that there might be underestimation of the precipitation in the basin, which resulted in the underestimation of the model output discharge at Dez.

In order to examine the uncertainty of the precipitation data, first, the spatial coverage of the rain gauges for the APHRODITE data set was checked. Figure 3.8 shows the spatial distribution of the APHRODITE daily precipitation and the reliability of data for each 0.25-degree resolution grid on 15 December 2001. This date was selected as an example because the maximum discharge of 2385 m^3/s during the calibration period was observed on that day at Dez (Figure 3.5(b)), although the upstream average precipitation on the day and the previous day were only 9.4 and 6.5 mm/day, respectively. The reliability in Figure 3.8(b) shows the ratio of valid 0.05-degree grids with the data recorded by rain gauges in each 0.25-degree grid (Yatagai et al., 2012). The reliability can be translated to the spatial coverage of rain gauges in a 0.25-degree grid base, i.e., the red grids of 0% have no rain gauges, the orange grid of 4% have at least one rain gauge, which approximately equals to the spatial coverage of 625 km^2/station, the yellow grid of 8% have at least two rain gauges, or the spatial coverage of 312.5 km^2/station, the light blue grid of 12% have at least three rain gauges, or the spatial coverage of 208.3 km^2/station. Next, the spatial coverage of the rain gauges in APHRODITE was compared with the recommendation by the World Meteorological Organization (WMO). As numerical criteria for the spatial coverage of rain gauges, WMO (1994) recommends minimum densities of precipitation stations for different climatic and geographic zones as shown in Table 3.5. According to the

recommendation, the minimum densities of precipitation stations in a mountainous area should be 250 km^2/station. This means the grids in red, orange and yellow in Figure 3.8(b) does not satisfy the WMO recommendation. The APHRODITE in Iran was developed by using a relatively dense network of observations, which was provided by the Islamic Republic of Iran Meteorological Organization (Yatagai et al., 2008). However, there are still many areas where precipitation is un-gauged (the red grids in Figure 3.8(b)) or poorly-gauged (the orange and yellow grids in Figure 3.8(b)), particularly in the southern part of the Dez dam catchment. It is possible that on 15 December 2001, an intense precipitation might have occurred in the ungauged mountain ranges in the Dez dam catchment and was thus not captured by ground observation. This "mis-captured" precipitation might have caused serious underestimation of discharge simulated by BTOPMC by using the APHRODITE daily precipitation.

A lack of high quality ground-gauged precipitation data is a major issue not only in the Karun River basin but also in most arid and semi-arid regions (Pilgrim et al., 1988; Beven, 2002; Wheater, 2008). This is due to the difficulty of establishing dense monitoring networks that can cover large areas where precipitation is highly variable. If the availability of ground observation is limited, radar observation and gridded data observed at a global or regional scale might be useful for hydrological analysis. In the Karun River basin, a radar network was installed; however, the calibration of the radar data is not complete and still needs revision (Heidari 2013). The available gridded data sets are generated from either mere analysis of ground observations, such as APHRODITE, or combination of ground observation and remotely sensed data, such as NCEP/NCAR Reanalysis data (Kistler et al., 2001), ERA-40 (Uppala et al., 2005) and JRA-25 (Onogi et al., 2007). However, the accuracy of remotely sensed data also

depends heavily on the density and quality of available ground observations. In order to check the accuracy of gridded data sets as well as to calibrate radar data, ground-observed precipitation data is necessary at least from several stations in the target basin to capture a spatial distribution of precipitation in the basin. Such local efforts on improving ground observation should precede water resource development planning.
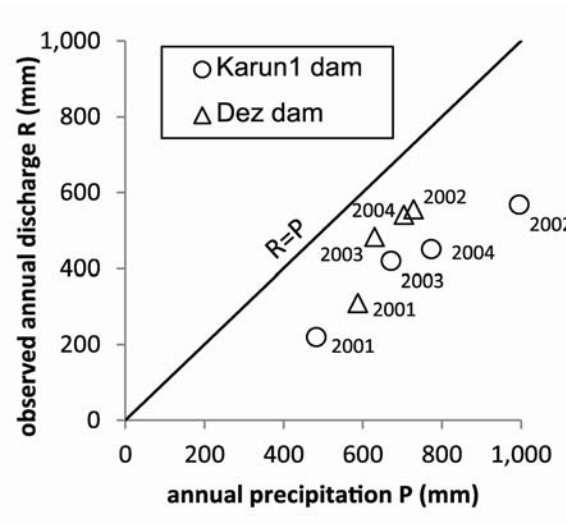
Figure 3.7 Comparison between annual precipitation and observed annual discharge at the Karun1 and the Dez dam sites.

(The line indicates that discharge (R) equals to precipitation (P). Annual variables were calculated from November in the previous year to October in the next year, a period which corresponds to the beginning of the wet season and the end of the dry season. For example, the annual variables of 2001 were calculated for the period of November 2000 to October 2001.)
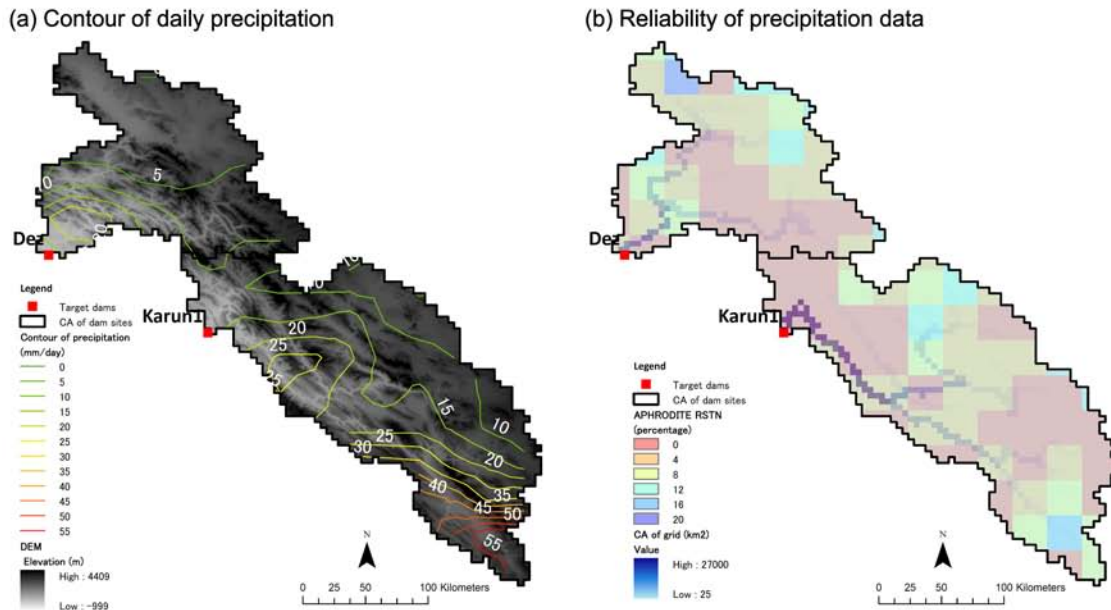
Figure 3.8 Spatial distribution of (a) the APHRODITE daily precipitation and (b) the reliability of precipitation data on 15 December 2001.

(In (a), the contour lines indicate the intensity of daily precipitation in mm/day. The background shows the elevation. In (b), the reliability is shown by RSTN in percentage, which is the ratio of 0.05-degree grids with rain gauge(s) in each 0.25-degree grid. For example, 4% means that there is only one 0.05-degree grid with at least one rain gauge among 25 grids in a 0.25-degree grid. The river networks in the catchments are depicted in the background by model grids in blue gradation.)

Table 3.5 Minimum densities of precipitation stations recommended by WMO (1994).

Physiographic Unit	Minimum densities per station (area in km^2/station)	
	Non-recording	Recording
Coastal	900	9000
Mountainous	250	2500
Interior plains	575	5750
Hilly undulating	575	5750
Small islands	25	250
Urban areas	-	10-20
Polar/arid	10000	100000

3.6.3. Seasonal runoff

The estimation of snow accumulation during the preceding seasons provides the basis of seasonal runoff estimation indispensable for planning multi-seasonal reservoir use. However, modeling snowpack and snowmelt processes without observations of, for example, snowfall and daily diurnal temperature is a difficult challenge in semi-arid mountainous regions. Although there are limitations in this study in comparing the 5x5 km grid averaged SWE with point observations, particularly in mountainous areas with a wide range of elevation, and in applying monthly-averaged temperature from CRU-TS instead of daily diurnal data in the model simulation, the model underestimation of SWE in the Karun River basin is quite likely caused by a lack of ground-gauged precipitation data in the mountainous ranges. Since precipitation is the primary input for snowfall calculation in a hydrological model, lack of precipitation data necessarily causes underestimation of snowfall in the mountainous areas. Enhanced ground-gauged precipitation data in mountainous areas would surely contribute to improve model performance for seasonal runoff generation. In particular, snowfall data are useful in that it can be used to verify the threshold temperature at which precipitation is divided into rainfall and snowfall in the model.

Evapotranspiration is also one of the significant factors affecting seasonal runoff. In the dry season, actual evapotranspiration is limited by the amount of available soil water rather than by PET (Vörösmarty, Federer, & Schloss, 1998). BTOPMC simulates that actual evapotranspiration nearly reaches to PET in the wet season and decreases in the dry season (Figure 3.3(e)), following the soil moisture state in the root zone (Figure 3.3(a)). Therefore, the simulated actual evapotranspiration was found physically reasonable.

3.6.4. Low flows

Base runoff generation is the driving process in BTOPMC for low flow generation during the dry season with no precipitation. On the basis of the simulation results in the Karun River basin, the base runoff (Figure 3.3(c)), which is a function of the saturation deficit in the unsaturated zone (Figure 3.3(d)), contributes to perennial low flows in the dry season from June to September (Figure 3.3(i)). The saturation deficit decreases in the wet season from December to April and generates base runoff even in the subsequent dry season with no precipitation. Figure 3.9 shows the comparison between observed and simulated mean discharges during the dry season from June to September in 2000 to 2004 at Karun1 and Dez. The simulated mean low discharge shows good agreement with the observations in 2000 and 2001, when the observations indicate that the Karun River basin received less precipitation as compared with those in other years. Meanwhile, the model slightly underestimates the low discharges in 2002, 2003 and 2004. The reproducibility of available soil moisture in the catchments at the end of the wet season is critical for runoff generation in the subsequent dry season. However, this is more difficult in wet years when more snowpack and snowmelt occur in mountainous areas than in dry years. Verification of the physical processes for low flow generation in the model is still not possible without high-quality data for precipitation, which is crucial in modeling snowpack and snowmelt processes and base runoff generation processes.
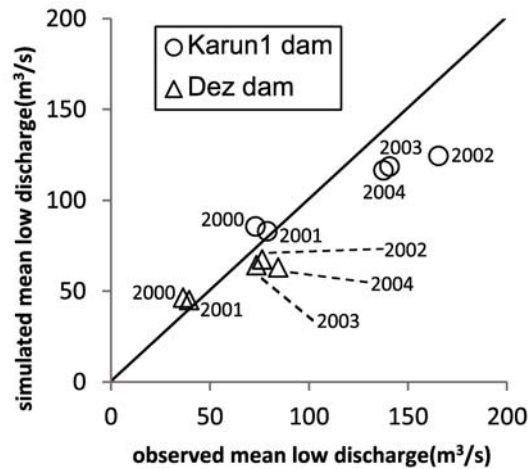
Figure 3.9 Comparison between observed and simulated mean low discharge during the dry season from June to September in 2000 to 2004 at the Karun1 and the Dez dam sites.

3.6.5. Flood flows

The model modification in this study improved flood peak generation, compared with the non-modified model as mentioned previously. However, the reproducibility of flood intensity needs improvement. Primarily, high-quality precipitation data that provide information on intense precipitation events with high spatial variability are necessary. Additionally, modeling infiltration capacity as a function of antecedent precipitation and/or soil moisture might further improve the reproducibility of flood flows since the antecedent moisture plays an important role in flood estimates by continuous simulation (Castillo, Gómez-Plaza, & Martínez-Mena, 2003; Pathiraja, Westra, & Sharma, 2012).

It should be noted that scale issues in hydrological modeling that involve some sort of extrapolation or transfer of information across different temporal and spatial scales remain unsolved (Blöschl & Sivapalan, 1995; Beven, 2002). In particular, hydrological models designed for water resources development require extrapolation at

larger scales; for instance, spatially from a point scale to a model grid or basin scale and temporally from an hourly scale to a daily time scale. This extrapolation raises uncertainty of model applicability and must be considered carefully even where sufficient data are available.

3.7. Conclusions

A distributed hydrological model with modification, BTOPMC, was applied to the Karun River basin in Iran, and the results were analyzed in the light of model applicability and challenges that hydrologists and river basin managers face in assessment and management of water resources development projects in semi-arid mountainous basins. The following are concluded:

(1) Applicability of BTOPMC was confirmed for its use in water resources development in the semi-arid mountainous Karun River basin. This study applied BTOPMC to the catchments of the Karun1 dam site and the Dez dam site located in the middle of the basin. The results at Karun1 clearly indicate the potential of the BTOPMC application in semi-arid mountainous regions, provided that necessary modification is made. The modification introduced was the adjustment coefficient for infiltration capacity of the soil surface in semi-arid regions, which was found useful to improve the model performance of reproducing flood peaks generated by infiltration excess overland runoff at a daily time scale. Seasonal discharge with snowpack and snowmelt processes in the wet winter and spring and recession of low flows in the dry summer were also simulated well. In addition, the simulated actual evapotranspiration was found

physically reasonable. The reproducibility of seasonal runoff patterns is indispensable for analyzing multi seasonal dam reservoir use. The model component that can simulate antecedent moisture state and reproduce soil moisture state at the end of the wet season is important for low flow generation in continuous inter-annual simulation. BTOPMC also fulfills such requirements.

(2) The greatest challenges that hydrologists and river basin managers face in hydrological modeling in semi-arid mountainous basins is to systematically observe and accumulate the ground-based hydrological observation data. This study clearly indicated that effective model use was significantly affected by the scarcity of ground-gauged precipitation data. In the case of the Dez dam site, the simulated discharges were considerably underestimated with data sets used in this study. Data scarcity is a major issue commonly seen in many basins awaiting water resources development in both developed and developing countries. It is especially true in semi-arid mountainous regions, where the spatial and temporal variation of precipitation tends to be greater than in humid regions, and is amplified by orographic effects.

(3) Priorities should be put on data acquisition and further hydrological model improvement in order to enhance water resources development in semi-arid mountainous regions. There is no doubt that BTOPMC needs further improvement to reflect rapid surface runoff processes necessary to model sharp rises of flood peaks, snowpack and snowmelt processes, and low flow generation. For such model improvement and verification, again, high-quality observed data are indispensable. In order to avoid inefficient infrastructure investment especially in semi-arid mountainous regions, therefore, rigorous efforts to improve ground-based observation of precipitation should be made first prior to water resource development planning. Since data scarcity

seriously limits effective use of hydrological simulation models required for design of water resources development, overreliance on hydrological models should carefully be avoided in poorly-gauged basins even with the best available hydrological models. Uncertainties associated with data used for model simulations should be assessed as far as possible, for example, by applying a simple water balance equation to test the reliability of the precipitation data in use, just as this study demonstrated.

4. Climate Change Impact Assessment on Basin Hydrology in the Karun River, Iran

4.1. Background and objectives of this chapter

Coupling hydrological models with General Circulation Models (GCMs) makes the basin-scale assessment of climate change impacts on water resources possible (e.g. Gosling et al., 2011; Harding et al., 2012; Chien et al., 2013; Hidalgo et al., 2013). Projected climate outputs, used as input for hydrological analysis, are derived from GCMs runs under various future emission scenarios of green house gases (IPCC, 2007b), and available in the data sets assembled by the Coupled Modeling Intercomparison Project (CMIP). However, the horizontal resolutions of GCMs, which range from about 100 to 400 km, place considerable limitations on the practical use of GCM outputs in climate change impact assessment, especially on the fringes of semi-arid zones. Such low horizontal resolutions inevitably underestimate extreme phenomena of intense precipitation in semi-arid mountainous regions by spatially averaging, which is a serious limitation on practical application. Therefore, a high horizontal resolution model is much awaited to serve climate change analysis of extreme weather events and adaptation studies. In this respect, it is great scientific strides that the super-high-resolution Atmospheric General Circulation Models (MRI-AGCMs) have been developed by the Japan Meteorological Agency (JMA) and Meteorological Research Institute (MRI). Three members of MRI-AGCMs: MRI-

AGCM3.1S by Kitoh, Ose, Kurihara, Kusunoki, & Sugi (2009); MRI-AGCM3.2S by

Mizuta et al. (2012); and MRI-AGCM3.2H by Endo, Kitoh, Ose, Mizuta, & Kusunoki

(2012), are currently available. The horizontal resolutions of the first two models are

about 20 km and the last model has a resolution of about 60 km. Analysis of the

projected data sets is underway, to which this chapter contributes regarding the use of

the MRI-AGCMs climate output in climate change impact assessment over semi-arid

mountainous regions.

Precipitation and surface air temperature derived from GCMs are the most

relevant climatic variables used in hydrological analysis for climate change impact

assessment (Blöschl & Montanari, 2010), and these variables are particularly crucial in

semi-arid mountainous regions. While surface air temperature derived from GCMs for

the present climate are fairly accurately simulated, precipitation derived from GCMs are

not accurately so (Kundzewicz et al., 2008). In addition, precipitation bias, which is a

difference between observations and GCM outputs, varies from region to region

(Hagemann, Arpe, & Roeckner, 2006). Thus, bias correction for the GCM precipitation

is required for its use in climate change impact assessment. Inomata, Takeuchi, and

Fukami (2011) develop a simple statistical method to correct bias in precipitation

derived from MRI-AGCMs. Their method appropriately corrects the intensity of the

MRI-AGCM precipitation samples of both extreme values and seasonal patterns, and is

easily applicable to any river basins in the world where observed precipitation data are

available. The performance of the correction method for MRI-AGCMs was verified in a

humid river basin in Japan (Inomata et al, 2011). However, no verification of the

method has been conducted in semi-arid mountainous regions.

The main objective of this chapter is to assess the potential impact of climate

change on river discharge in semi-arid mountainous Karun River basin. The main objective will be achieved by implementing the following sub-objectives: (1) examine the applicability of the simple statistical bias correction method to MRI-AGCMs precipitation in the semi-arid mountainous region; and (2) assess climate change impact based on the multi-ensemble results from the simulations using the climatic outputs from the three members of MRI-AGCMs. The Karun River basin was selected as the study area since no study on climate change impact assessment has been conducted in the basin although many development projects, such as dam construction, irrigation networks and water transfer systems, are been planned.

4.2. Data and methodology

4.2.1. Description of MRI-AGCMs

Table 4.1 lists the specifications of the three members of MRI-AGCMs (MRI-AGCM3.1S, MRI-AGCM3.2S and MRI-AGCM3.2H). MRI-AGCM3.1S and MRI-AGCM3.2S conduct global simulations with a horizontal resolution of the TL959 linear Gaussian grid (1920 grids in longitude and 960 grids in latitude), which corresponds to about 20 km, and MRI-AGCM3.2H with the TL319 grid (640 grids in longitude and 320 grids in latitude), corresponding to about 60 km. Among the differences listed in Table 4.1, it should be noted that different types of cumulus convection, which highly affects generation of precipitation, were used in MRI-AGCMs. MRI-AGCM3.1S uses the prognostic Arakawa-Shubert scheme (Arakawa & Schubert, 1974; Randall & Pan, 1993), and MRI-AGCM3.2S and MRI-AGCM3.2H use the Yoshimura scheme

(Yukimoto et al., 2011). According to Mizuta et al. (2012), MRI-AGCM3.2S with the Yoshimura scheme simulates tropical precipitation in the present climate more realistic than MRI-AGCM3.1S with the prognostic Arakawa-Shubert scheme.

For further understanding of characteristics of MRI-AGCM precipitation, low precipitation patterns derived from MRI-AGCM3.1S were compared with a number of Atmospheric Ocean coupled General Circulation Models (AOGCMs) in terms of low precipitation pattern reproducibility in the present climate and its projected future change, and these results were provided in Appendix.

Table 4.1 Major differences in model specifications among the three members of MRI-AGCMs by reference to Mizuta et al. (2012) and Endo et al. (2012).

	MRI-AGCM3.1S	MRI-AGCM3.2S	MRI-AGCM3.2H
Horizontal resolution	TL959 (20km, 1920x960 grids)	TL959 (20km, 1920x960 grids)	TL319 (60km, 640x320 grids)
Vertical layers	60 (top at 0.1 hPa)	64 (top at 0.1 hPa)	64 (top at 0.1 hPa)
Cumulus convection	Prognostic Arakawa-Shubert scheme (Arakawa & Schubert 1974; Randall & Pan 1993)	Yoshimura scheme (Yukimoto et al., 2011)	Yoshimura scheme (Yukimoto et al., 2011)

Climatic outputs from the three members of MRI-AGCMs are currently available in three time-slice 25-year simulations for the present climate (1979-2003), the near future climate (2015-2039) and the future climate (2075-2099). For the present climate simulation, MRI-AGCMs were integrated with the observed historical sea surface temperature (SST) and sea ice data of HadISST1 (Rayner et al., 2003), and run under the 20th Century experiment (20C3M), where experiments were run with increased greenhouse gases as observed through the 20th century. For future simulations, MRI-AGCMs were integrated with future SST and sea ice data, and run under the A1B scenario of future emission of green house gases. This scenario is presented in the Special Report on Emission Scenario as SRES A1B, assuming that a future world of very rapid economic growth, low population growth and rapid introduction of new and more efficient technology (Nakićenović et al., 2000). The boundary SST data for future simulations were prepared by superposing (Kitoh et al., 2009): (1) the trend in the multi-model ensemble of SST within the future period projected by GCMs in phase three of the Coupled Modeling Intercomparison Project (CMIP3); (2) future change in the multi-model ensemble of SST between the present and the future periods; and (3) the detrended observed SST anomalies for the period 1979 to 2003. Future sea-ice distribution was also obtained in the same manner (Kitoh et al., 2009).

4.2.2. Statistical bias-correction method for MRI-AGCMs daily precipitation

The statistical bias-correction method developed by Inomata et al. (2011) was applied to bias correction of daily precipitation simulated by MRI-AGCMs. Their

method processes precipitation data in the following steps:

(a) Daily precipitation samples of observation and those of GCM in the present climate in the entire study period were ranked respectively, and samples with non-exceedence probability (NEP) ≥ 99.5% (i.e., 45 samples = 25 years * 365 days * 0.5%) were extracted from both datasets.

(b) Ratios, i.e., correction coefficients, were calculated between equally ranked observation and GCM extremes extracted in step (a) (Eq. 4.1).

(c) Daily precipitation samples with NEP < 99.5%, which were not extracted in step (a), were sorted and ranked month by month. Correction coefficients were calculated as ratios between equally ranked observation and GCM for each month (Eq. 4.2). If an observed or GCM precipitation value was 0.0 mm/day, the coefficient was regarded as 0.

(d) GCM precipitation in the present climate was corrected by multiplying the coefficients at each rank obtained in steps (b) and (c) (Eq. 4.3 and 4.4).

(e) Assuming that the calculated coefficients in steps (b) and (c) would not change in the future climate, corrected future precipitation was obtained by multiplying the coefficients to GCM precipitation in the future climate (Eq. 4.5 and Eq. 4.6).

$$\alpha(I) = \frac{P_{obs}(I)}{P_{GCM\_present}(I)} \tag{4.1}$$

$$\alpha_m(i) = \frac{P_{obs\_m}(i)}{P_{GCM\_present\_m}(i)} \tag{4.2}$$

$$P'_{GCM\_present}(I) = \alpha(I) \times P_{GCM\_present}(I) \tag{4.3}$$

$$P'_{GCM\_future}(I) = \alpha(I) \times P_{GCM\_future}(I) \tag{4.4}$$

$$P'_{GCM\_present\_m}(i) = \alpha_m(i) \times P_{GCM\_present\_m}(i) \tag{4.5}$$

$$P'_{GCM\_future\_m}(i) = \alpha_m(i) \times P_{GCM\_future\_m}(i) \qquad\qquad (4.6)$$

where I is the rank among all daily precipitation samples in the entire study period, $P_{obs}(I)$ is observation whose rank is I, $P_{GCM\_present}(I)$ is GCM precipitation in the present climate whose rank is I, $\alpha(I)$ is the coefficient between observation and GCM precipitation in the present climate at rank I, i is the rank among daily precipitation samples in the same month in the entire study period, m is month, $P_{obs\_m}(i)$ is observation in month m whose rank is i, $P_{GCM\_present\_m}(i)$ is GCM precipitation in the present climate in month m whose rank is i, $\alpha_m(i)$ is the coefficient between observation and GCM precipitation in the present climate in month m whose rank is i, $P'_{GCM\_present}(I)$ and $P'_{GCM\_future}(I)$ are the corrected GCM precipitation in the present and future climate at rank I, $P'_{GCM\_present\_m}(i)$ and $P'_{GCM\_future\_m}(i)$ are the corrected GCM precipitation in the present and future climate in month m whose rank is i. GCM precipitation in the near future climate was also corrected in the same manner. This study used a prototype of the global gridded daily precipitation data set resulting from the Asian Precipitation - Highly-Resolved Observational Data Integration Towards Evaluation (APHRODITE) project (APHRO_GLB) as observations for bias correction. APHRO_GLB adopts a horizontal resolution of the TL959 grid (about 20 km), which is same as MRI-AGCM3.1S and 3.2S. Since MRI-AGCM3.2H has a lower resolution of TL319 (about 60 km) than MRI-AGCM3.1S and 3.2S, statistical downscaling of precipitation derived from MRI-AGCM3.2H from 60 km to 20 km was also conducted at the same time of the bias correction.

Inomata et al. (2011) suggest that selected extreme samples based on NEP should be physically reasonable for bias correction in the area of interest. In the case of a humid river basin in Japan, they found that a lower NEP selected precipitation in the dry season as an extreme event, which is physically unjustifiable. Therefore, first, this study compared MRI-AGCMs precipitation with observations in terms of intensity and occurrence season of heavy precipitation to determine NEP of extreme precipitation before the bias correction was applied. Next, bias corrected results of the MRI-AGCMs precipitation for the present climate were checked at annual and monthly time scales to verify the applicability of the bias correction method.

4.2.3. Hydrological model set-up and hydro-meteorological data used

The Block-wise TOPMODEL with the Muskingum-Cunge routing method (BTOPMC; Takeuchi et al., 1999, 2008), a distributed hydrological model, was applied to the two catchments of the Karun1 dam and the Dez dam located in the middle of the Karun River basin. This chapter used BTOPMC that was already set up and calibrated in Chapter 3. Hydrological simulations were conducted in a daily time step.

Table 4.2 shows hydro-meteorological data used in climate change impact assessment over the Karun River basin. All hydro-meteorological data was reformatted into the common horizontal resolution of BTOPMC (5x5 km) before simulations. This study used daily precipitation and daily averaged surface air temperature at 2 m above the ground level in the basin, which were derived from the three members of MRI-AGCMs for the present climate, the near future climate and the future climate. The MRI-AGCMs daily precipitation was further corrected by the simple statistical bias-

64

correction method described in the previous section before being fed to BTOPMC for hydrological simulations. The MRI-AGCMs daily average temperature was used in the snow module of BTOPMC. Based on the MRI-AGCM temperature, the total amount of the MRI-AGCM daily precipitation was divided into rainfall and snowfall, and the amounts of snowpack and snowmelt were calculated in an each time step.

In BTOPMC, actual evapotarnspiration (AET) is calculated based on the function of potential evapotranspiration (PET) and available soil moisture in the root zone (Takeuchi et al., 2008). PET might change under warming climate projected for the future period. However, since AET in the Karun River basin is water limited, which means that AET highly depends on the amount of available soil moisture in the root zone, increased PET in the future climate might have little effect on AET estimation. Therefore, this study assumed that PET might not change in the near future climate and future climate. PET for the present climate was estimated by Shutlleworth-Wallace model using climate forcing data from the Climatic Research Unit time-series (CRU-TS) and average climatology (CRU-CL), and Normalized Difference Vegetation Index (NDVI) data from the Global Inventory Modeling and Mapping Studies (GIMMS), and used also for the future simulations.

Table 4.2 Hydro-meteorological data used for climate change impact assessment in the Karun River basin

Type	Description	Source	Original spatial resolution	Original temporal resolution	Additional information
Hydro-meteorological data	Precipitation (bias corrected)	MRI-AGCM3.1S, MRI-AGCM3.2S, MRI-AGCM3.2H	TL959, corresponding to the grid size of 20 km (3.1S and 3.2S). TL319, corresponding to the grid size of 60 km (3.2H).	Daily	Data in the present climate (1979-2003), the near future climate (2015-2039) and the future climate (2075-2099) were used.
	Temperature used for snow module)	MRI-AGCM3.1S, MRI-AGCM3.2S, MRI-AGCM3.2H	TL959, corresponding to the grid size of 20 km (3.1S and 3.2S). TL319, corresponding to the grid size of 60 km (3.2H).	Daily	Daily average surface air tempearture at 2 m from the ground level in the presente, the near future and the future were used..
	Temperature for PET estimation, Cloud cover, Daylight duration, Radiation, Vapor pressure, Wind speed	CRU CL1.0, TS3.1	0.50x0.50 degree (~50x50km)	Monthly	These data are used for Global monthly data for 1901-2009(TS3.1), 1961-1990(CL1.0), used for potential evapotranspiration calculation.
	NDVI	NOAA-AVHRR	8x8 km	Half-monthly	

Notes: CRU-TS and CRU-CL are the Climate research Unit time series and average climatology, NDVI is the Normalized Difference Vegetation Index, and NOAA-AVHRR is the National Oceanic and Atmospheric Administration (USA)-Advanced Very High Resolution Radiometer.

4.2.4. Assessment of climate change impact on river discharge

There are a number of uncertainties associated with climate change projection on river discharge by using a hydrological model coupled with GCMs. Gosling et al. (2011) summarize the four main stages of performing climate change hydrological impact assessment and uncertainties inherent to the assessment: (1) Emissions; (2) Climate projections; (3) Downscaling; and (4) Hydrological projections. A number of studies have investigated these uncertainties in each stage (e.g., Bae, Jung, and Lettenmaier (2011) for (1), (2) and (4); Chen, Brissette, and Leconte (2011) for (3);

Najafi, Moradkhani, & Jung (2011) for (4); Steinschneider, Polebitski, Brown, & Letcher (2012) for (4); Watanabe et al. (2012) for (3); Woldemeskel, Sharma, Sivakumar, & Mehrotra (2012) for (1) and (2)). Since it is difficult to consider all uncertainties from the four stages due to the limited data and resources, this study focused on uncertainty analysis by using multi-GCM projections. The ensemble mean of the three members of MRI-AGCMs was taken into account.

Climate change impacts on basin hydrology were assessed by relative future changes in mean monthly river discharges between the present climate scenario of 20C3M and the future climate scenario of SRES A1B at the karun1 dam site and the Dez dam site. Assessment at a monthly time scale was selected because monthly discharge well interprets the seasonal flow regime of snowpack and snowmelt processes, which are significantly affected by climate change in semi-arid mountainous regions. First, monthly discharge was aggregated from daily discharge simulated by BTOPMC using precipitation and temperature projected by each MRI-AGCM for the three time-slice 25-year periods. Second, mean monthly discharge was calculated based on the result of each MRI-AGCM simulation within each period. Finally, ensemble mean of the mean monthly discharge of the three MRI-ACM simulations for each target period were obtained.

4.3. Results and discussion

4.3.1. Bias correction on the MRI-AGCM precipitation

1) *Selection of non-exceedence probability for extreme events*

First, the intensity of daily heavy precipitation events simulated by the three MRI-AGCMs for the present climate was compared with observations. Figure 4.1 and Figure 4.2 compare the intensity of these heavy precipitation events up to rank 200 at the Karun1 dam catchment and the Dez dam catchment, respectively. All MRI-AGCMs overestimate the intensity of heavy precipitation events compared with observations, except the case of MRI-AGCM3.1S at Dez. As an example of the overestimation, Figure 4.3 shows a spatial distribution of daily precipitation generated by MRI-AGCM3.2S in the domain of the Karun River basin on 24 November 1981, which is the most intense precipitation generated by MRI-AGCMs during the present period. On that day, MRI-AGCM3.2S generated precipitation of more than 300 mm/day, which is an unrealistically intense precipitation event in the domain. This type of overestimation by MRI-AGCMs clearly indicates the need for bias correction for precipitation derived from MRI-AGCMs in the Karun River basin.
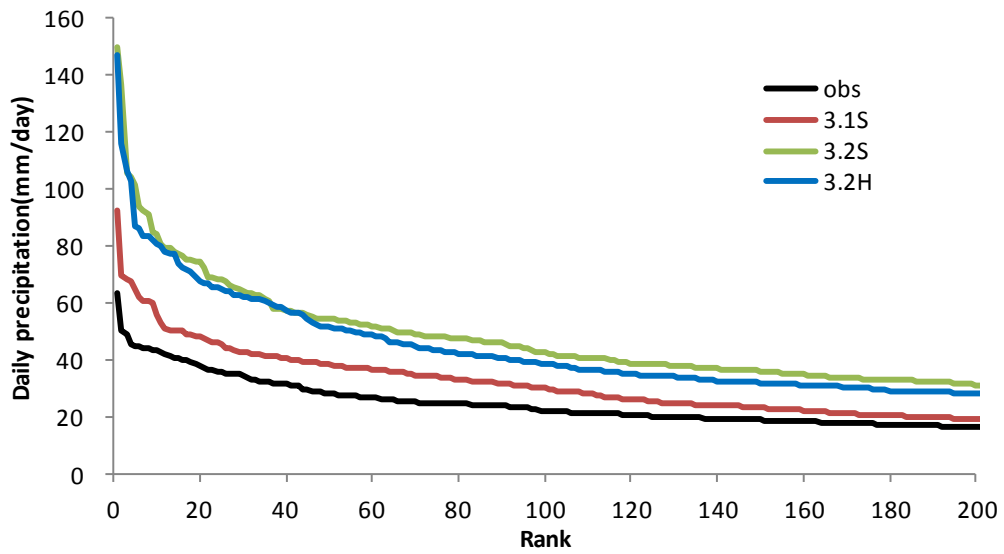
Figure 4.1 Comparison of heavy daily precipitation events in 1979-2003 up to rank 200 at the Karun1 dam catchment between observation and the three MRI-AGCMs.
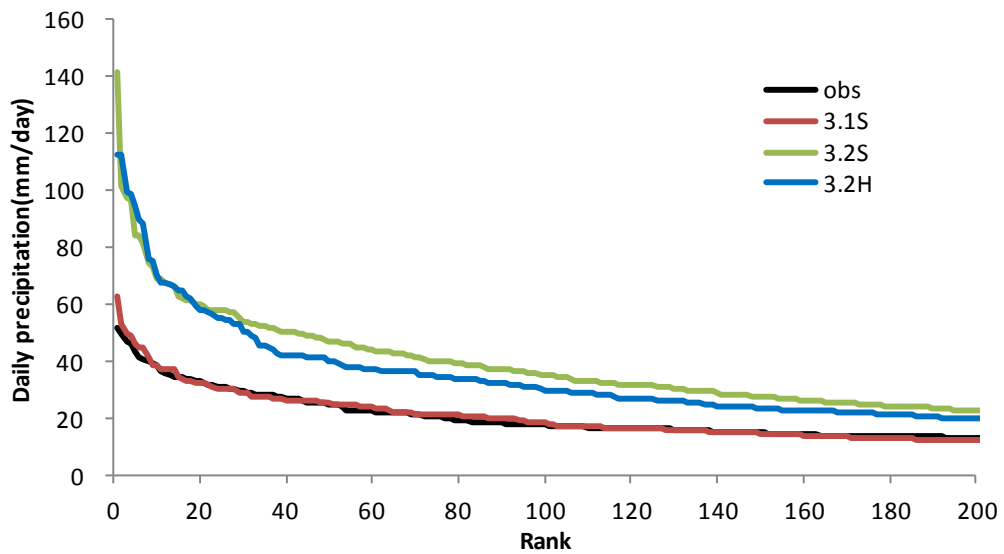
Figure 4.2 Comparison of heavy daily precipitation events in 1979-2003 up to rank 200 at the Dez dam catchment between observation and the three MRI-AGCMs.

69
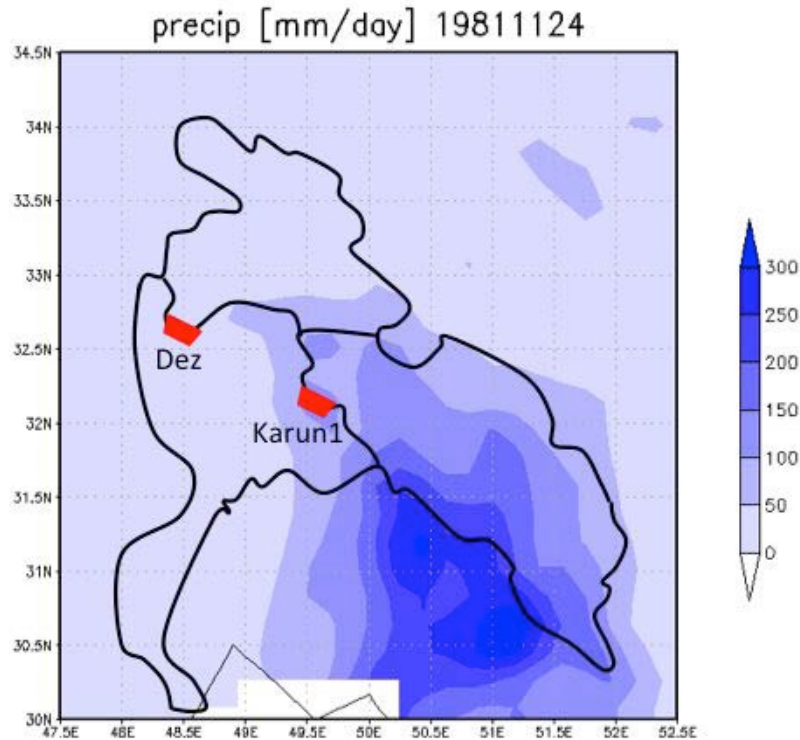
Figure 4.3 Spatial distribution of daily precipitation generated by MRI-AGCM3.2S in the domain of the Karun River basin on 24 November 1981.

(This map shows the most intense precipitation event among the projected events by the three members of MRI-AGCMs as an example of unrealistic intense precipitation events generated by MRI-AGCMs.).

Next, the occurrence season of heavy precipitation events both observed and simulated by the three MRI-AGCMs for the present climate were examined. Table 4.3 lists the intensity and occurrence date of the observed and simulated heavy precipitation events at the Karun1 dam catchment in 1979-2003. Table 4.4 lists same as Table 4.3, but at the Dez dam catchment. All heavy precipitation events, both observed and simulated, up to rank 45, which corresponds to a sample number based on NEP of 99.5% (45 samples = 25 years * 365 days * 0.5%), occurred in the wet season (October to May). This result indicates that selection of heavy precipitation events of MRI-AGCMs for bias correction based on NEP of 99.5% is found physically reasonable. Therefore, this study used NEP of 99.5% as the selection criterion for bias correction of

extreme precipitation events.

Table 4.3 Intensity and occurrence date of heavy precipitation events observed and simulated by the three MRI-AGCMs at the Karun1 dam catchment in 1979-2003.

Rank	Observation		MRI-AGCM3.1S		MRI-AGCM3.2S		MRI-AGCM3.2H	
	prec (mm/day)	date	prec (mm/day)	date	prec (mm/day)	date	prec (mm/day)	date
1	63.7	1998/01/05	92.7	1987/04/14	149.7	1981/11/24	147.2	1986/10/30
2	50.6	1998/03/18	69.5	1982/01/20	136.4	1997/03/03	116.3	1994/02/21
3	48.8	1986/12/20	68.0	2002/01/05	105.9	1997/03/02	106.0	1998/01/21
4	45.6	2001/12/20	67.6	1982/02/04	104.2	2000/03/15	103.1	1985/02/24
5	45.1	2002/01/07	64.8	1979/11/26	101.3	1993/03/11	87.2	1980/01/22
6	45.1	1989/12/04	62.0	2003/11/18	94.0	1981/11/25	86.1	1991/03/01
7	44.2	2001/12/12	60.6	1980/01/27	92.4	1995/02/08	83.6	1990/01/19
8	44.2	2003/12/28	60.4	1979/04/02	90.9	1980/01/24	83.3	1986/02/27
9	43.8	1989/12/03	60.3	2003/12/21	85.0	1980/01/29	82.0	1995/01/16
10	43.3	1998/03/30	55.6	1982/12/01	84.2	1994/12/16	80.9	1994/02/22
11	42.8	1986/11/29	52.8	1995/01/21	80.6	1979/11/30	80.1	1998/01/05
12	42.1	1999/01/09	51.0	1982/11/11	79.5	1979/01/15	78.2	1996/11/18
13	41.2	1999/03/02	50.5	1993/01/21	79.1	1995/02/05	77.5	1991/11/19
14	40.8	1997/03/29	50.5	1980/02/07	77.7	1983/02/23	77.0	2000/01/08
15	40.3	2002/01/08	50.3	1996/12/10	77.5	1998/03/11	73.7	1997/02/23
16	40.2	2002/04/12	50.1	2003/01/15	76.9	2000/01/12	72.2	1986/03/08
17	39.8	2002/12/10	49.3	1987/01/23	75.3	1979/03/27	71.9	1992/12/01
18	39.3	2001/12/05	48.8	2000/01/27	75.1	1990/02/23	70.8	1989/11/24
19	38.5	2003/03/26	48.4	1979/11/27	74.7	1981/11/23	68.8	1991/02/28
20	38.2	1993/01/08	47.9	1986/01/10	74.4	1986/11/13	67.4	1992/02/10
21	37.0	1998/02/10	47.8	1989/12/14	72.3	1996/04/12	67.2	1980/03/30
22	36.8	1995/02/05	46.9	1979/11/16	68.9	1997/02/28	67.1	1989/11/17
23	36.6	1996/01/06	46.4	1985/02/01	68.7	1982/02/10	65.8	1982/03/09
24	35.9	2001/12/02	45.9	2001/12/04	68.6	2001/03/13	65.3	1998/11/28
25	35.8	2002/12/09	45.3	1981/02/26	68.0	1998/01/01	64.9	1993/03/19
26	35.4	1994/11/17	44.4	1994/12/24	67.8	1983/01/25	64.1	1996/11/22
27	35.3	2000/01/28	44.2	1995/11/23	66.1	1998/04/23	64.0	1992/12/03
28	35.2	1998/02/11	43.7	1999/02/23	65.3	1988/11/25	62.6	1988/11/30
29	35.0	2001/12/01	43.0	1996/12/30	64.9	1982/11/19	62.4	1996/04/09
30	34.6	1985/01/02	42.7	1984/04/18	64.4	1991/11/30	62.3	1995/01/21
31	33.7	1998/01/06	42.4	1999/03/22	63.8	1986/12/27	62.1	1995/11/07
32	33.0	1998/02/09	42.1	1991/03/25	63.5	1982/03/21	61.7	1990/01/04
33	32.8	1993/02/03	42.1	1990/11/30	62.7	1991/02/07	61.7	1982/11/20
34	32.5	1980/02/11	41.9	1986/12/29	62.5	1981/12/13	61.2	1984/01/30
35	32.4	1986/11/30	41.7	1988/02/06	61.7	1991/11/05	60.7	1992/05/16
36	32.1	2002/01/11	41.6	1986/12/30	60.4	1981/02/13	60.2	1996/11/21
37	31.7	1997/01/17	41.4	2003/11/19	58.2	1990/01/09	59.5	2003/12/25
38	31.5	1991/03/06	41.1	1996/12/11	57.8	2003/12/18	58.6	1998/12/13
39	31.5	1999/03/13	40.9	1996/02/09	57.7	1986/11/28	58.5	1987/04/01
40	31.4	2001/12/21	40.6	1993/12/26	57.5	1986/11/01	57.3	1995/01/22
41	31.3	1980/02/10	40.2	1992/03/23	57.3	1992/03/12	56.8	1995/02/26
42	31.1	1993/02/21	39.7	1986/03/27	56.7	1994/12/03	56.7	1987/10/20
43	31.1	2001/12/08	39.7	1979/12/09	56.7	1999/01/26	56.5	2001/03/19
44	29.4	2003/12/06	39.5	1992/02/28	56.4	1991/11/23	56.0	1987/02/01
45	29.3	1995/02/06	39.2	1995/12/07	56.0	1991/11/06	54.7	1995/02/03
46	29.0	1991/12/09	39.2	1985/12/15	54.9	1980/02/19	53.3	1989/11/25
47	28.9	1992/02/24	39.0	2003/02/11	54.8	2002/04/15	52.7	1980/02/04
48	28.6	1994/11/06	38.9	1980/12/04	54.7	1988/04/13	52.0	1979/03/25
49	28.5	1999/01/16	38.7	1985/11/07	54.5	1999/12/05	52.0	1992/01/26
50	28.4	1994/11/16	38.7	2003/12/04	54.2	1998/01/25	52.0	1998/12/18

Table 4.4 Intensity and occurrence date of heavy precipitation events observed and simulated by the three MRI-AGCMs at the Dez dam catchment in 1979-2003.

Rank	Observation prec (mm/day)	date	MRI-AGCM3.1S prec (mm/day)	date	MRI-AGCM3.2S prec (mm/day)	date	MRI-AGCM3.2H prec (mm/day)	date
1	51.7	1997/03/29	62.5	1997/03/02	141.3	1997/03/02	112.4	1984/12/19
2	49.3	2003/04/22	53.0	2000/11/03	101.6	2000/11/03	112.3	1988/12/06
3	46.8	1981/03/27	49.4	1998/04/22	97.4	1993/03/11	99.5	1986/02/26
4	46.0	1998/03/29	49.1	1993/03/11	96.6	1998/04/22	99.0	1991/11/19
5	43.3	1990/04/02	46.4	2003/12/18	84.0	2003/12/18	94.7	1989/11/24
6	41.5	1984/03/25	44.8	2002/04/01	83.8	2002/04/01	89.7	1994/11/09
7	40.5	2001/12/01	44.6	1990/02/23	81.8	1990/02/23	88.2	2000/11/30
8	40.2	1994/11/06	41.3	2000/03/28	74.5	2000/03/28	75.9	1998/01/04
9	39.2	1984/03/26	38.6	1992/10/23	73.3	1992/10/23	75.3	1987/03/31
10	38.6	1986/11/29	38.6	1987/03/20	69.3	1981/12/12	70.4	1996/11/21
11	36.7	1985/12/18	37.2	1982/03/21	68.7	1983/02/23	67.6	1990/01/19
12	36.0	1981/03/26	37.2	1985/03/03	67.4	1982/03/21	67.3	1992/11/23
13	34.8	1986/05/03	37.1	1981/12/12	66.7	1987/03/20	66.7	1984/04/03
14	34.7	1999/02/20	36.9	1983/02/23	66.0	1985/03/03	66.3	1996/11/18
15	34.4	1994/11/05	34.3	1996/12/19	62.6	1987/04/06	65.1	1993/03/19
16	34.2	1994/11/25	33.7	1987/03/08	61.8	1998/04/23	64.8	2002/04/16
17	33.7	1987/03/03	32.9	1987/04/06	61.7	1991/04/06	62.8	1996/04/08
18	33.5	2003/03/26	32.9	1994/12/03	61.7	1996/04/11	61.9	1988/12/04
19	33.2	1987/03/02	32.6	1987/05/03	60.0	1996/12/19	59.2	1998/12/18
20	32.8	2001/12/20	32.4	1997/02/27	59.8	1987/03/08	58.3	1986/03/07
21	32.4	1999/01/09	32.1	1981/12/20	59.3	1994/12/03	57.8	1988/11/29
22	31.9	1981/01/11	31.8	1998/04/23	58.2	1997/04/30	57.4	1995/11/06
23	31.7	2000/03/24	30.8	1991/04/06	58.2	1981/12/20	56.9	1985/02/24
24	31.0	2000/12/01	30.5	1982/11/19	58.0	1980/11/30	55.3	1981/11/21
25	30.9	2001/12/02	30.3	1995/02/05	57.7	1991/10/28	54.9	1986/03/08
26	30.7	2000/12/10	30.0	1996/04/11	57.6	1982/11/19	54.5	1986/10/30
27	30.4	1994/11/07	30.0	2000/01/11	57.5	1997/02/27	54.3	1998/01/05
28	30.0	1993/02/02	30.0	1980/11/30	57.3	1995/02/05	53.3	1984/03/28
29	29.6	1988/03/04	29.1	2003/12/17	54.9	1980/04/11	53.1	1999/02/24
30	29.4	1996/02/02	29.0	1991/10/28	54.0	1999/04/21	50.4	1982/11/20
31	29.2	1994/03/11	28.6	1979/12/05	53.6	1995/11/25	50.0	1995/03/20
32	28.9	1998/03/30	27.8	1997/02/28	53.4	1987/05/03	49.0	1987/03/16
33	28.5	1997/03/28	27.5	1979/03/27	53.3	1990/11/17	48.0	1995/12/24
34	28.5	2000/12/11	27.2	1998/01/25	52.4	1982/11/16	45.4	2002/11/13
35	28.2	1988/03/08	27.2	1990/02/06	52.4	2000/01/11	45.3	2003/03/13
36	28.2	2001/12/04	27.2	1987/12/10	52.0	1979/11/07	44.6	2002/02/08
37	28.1	1984/11/11	27.0	1990/11/17	51.7	1979/12/05	43.8	1988/11/30
38	27.6	1987/12/23	26.9	1980/04/11	50.7	1998/01/25	43.0	1998/12/13
39	27.4	1991/03/05	26.6	1995/11/25	50.6	1997/02/28	42.4	1984/11/28
40	27.1	2001/12/05	26.5	1997/04/30	50.5	1994/11/09	42.3	1991/04/26
41	27.1	1997/11/03	26.4	1994/11/09	50.1	1981/11/14	42.1	1992/12/01
42	27.0	1993/11/25	26.4	1994/12/16	50.1	1990/02/06	42.0	1980/03/30
43	26.7	1994/11/24	26.4	1982/11/16	49.7	2003/12/17	42.0	1994/10/29
44	25.8	1996/02/19	26.1	1981/11/14	49.7	1979/03/27	41.8	1999/01/15
45	25.7	1992/12/14	26.1	1981/12/02	49.2	1986/11/12	41.2	1987/05/15
46	25.5	1993/04/26	25.9	1991/03/25	48.8	1994/12/16	41.2	1986/10/14
47	25.4	1988/03/09	25.8	1986/12/27	48.4	1992/11/12	41.2	1979/03/25
48	25.3	1993/04/25	25.7	1979/11/07	48.3	1996/04/12	41.1	1994/11/04
49	25.1	1993/03/08	25.7	1992/03/12	47.6	1992/11/10	41.1	1995/05/09
50	25.0	1999/03/04	25.3	1984/03/08	47.0	1992/03/12	39.9	1984/07/10

2) *Reproducibility of MRI-AGCM precipitation for the present climate and bias correction results*

First of all, the reproducibility of MRI-AGCMs precipitation at annual and monthly time scales without bias correction was examined. Figure 4.4 and Figure 4.5 respectively show mean annual precipitation and mean monthly precipitation both observed and simulated by MRI-AGCMs without and with bias correction for the present climate at the Karun1 dam catchment. Same results at the Dez dam catchment are shown in Figure 4.6 and Figure 4.7. Each error bar in the figures indicates the standard deviation of the interannual variability. The results without bias correction show that MRI-AGCM3.1S well reproduces mean and interannual variability of annual and monthly precipitation, whereas MRI-AGCM3.2S and 3.2H show an overestimation tendency. For example, despite slight overestimation in dry summer, MRI-AGCM3.1S well reproduces monthly precipitation characteristics in wet winter as shown in Figure 4.5(a) and Figure 4.7(a). On the other hand, MRI-AGCM3.2S and 3.2H overestimate monthly precipitation to a large degree in wet winter, although reproducing dry summer fairly well by simulating almost no precipitation. This difference among the results of MRI-AGCMs might originate from different schemes of cumulous convection adopted by each GCM models. The Yoshimura scheme applied to MRI-AGCM3.2S and MRI-AGCM3.2H might have a tendency to generate more intense daily precipitation and might be more likely to overestimate precipitation in wet winter in the basin than MRI-AGCM3.1S. Although further improvement is necessary to reproduce the intensity of precipitation, it should be pointed out that MRI-AGCMs are highly capable of reproducing the seasonal variability of precipitation in the basin during wet winter and dry summer.

73

Next, the bias corrected results of the MRI-AGCMs daily precipitation for the present climate were examined from the viewpoint of the reproducibility of annual and monthly precipitation to verify the applicability of the bias correction method to the semi-arid mountainous Karun River basin. Although MRI-AGCMs show a strong overestimation tendency for the present daily precipitation, the bias correction method worked well with NEP of 99.5% for selection of heavy precipitation event samples and well corrected the characteristics of annual and monthly precipitation, as shown in Figure 4.4(b) and Figure 4.5(b) for Karun1, and Figure 4.6(b) and Figure 4.7(b) for Dez. These results verify the applicability of the statistical bias-correction method developed by Inomata et al. (2011) in the semi-arid mountainous regions.
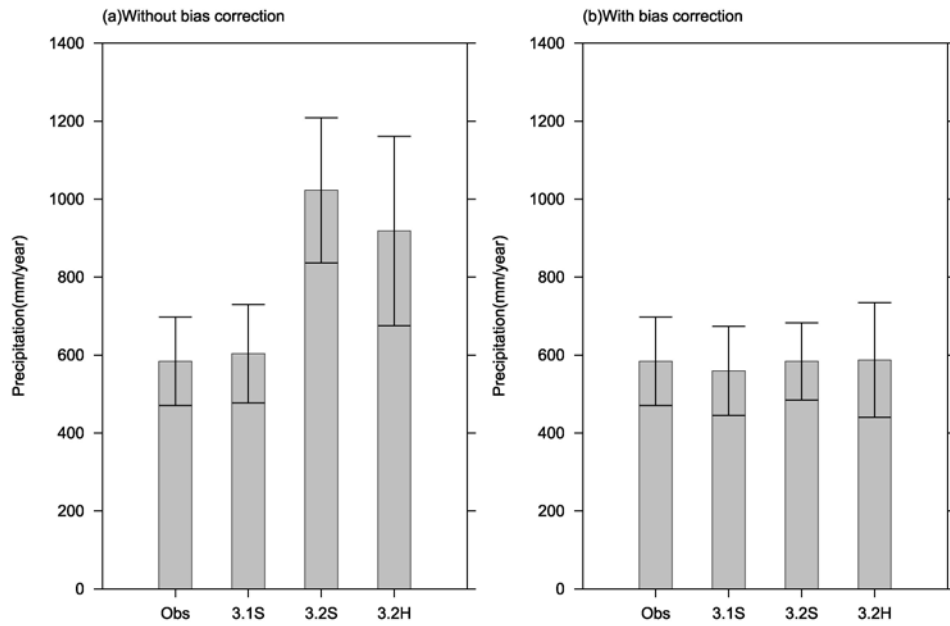
Figure 4.4 Mean annual precipitation in the Karun1 dam catchment for 1979-2003 from observation and MRI-AGCMs (a) without bias correction and (b) with bias correction.

(Each error bar indicates the standard deviation of the interannual variability.)
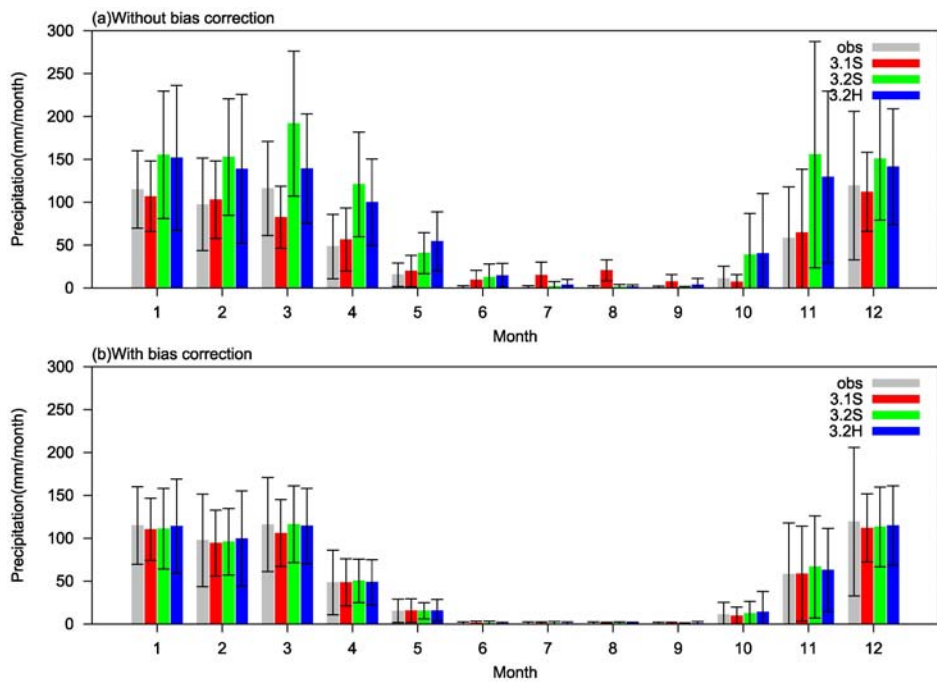
Figure 4.5 Mean monthly precipitation in the Karun1 dam catchment for 1979-2003 from observation and MRI-AGCMs (a) without bias correction and (b) with bias correction.

(Each error bar indicates the standard deviation of the inter-annual variability.)
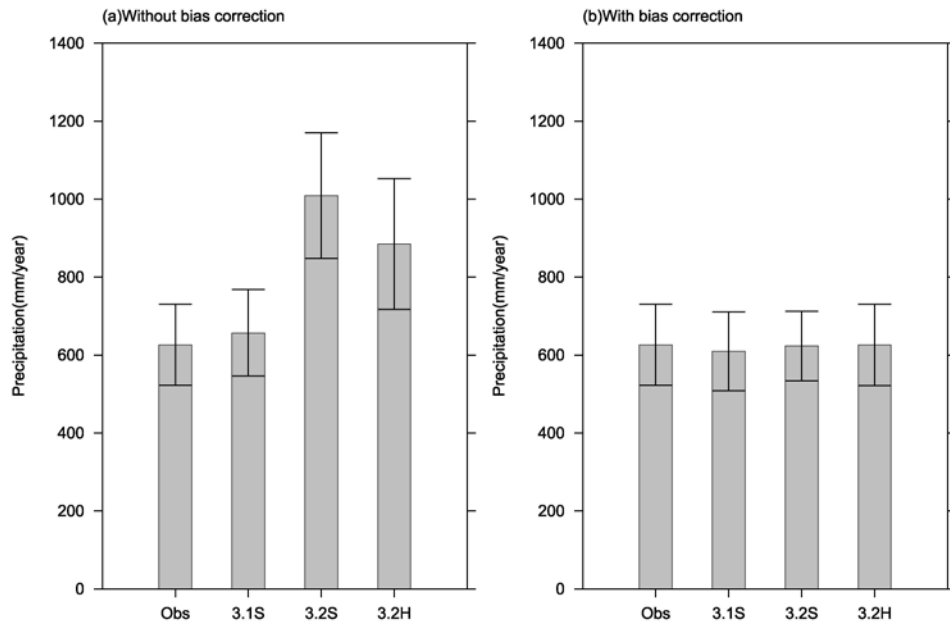
Figure 4.6 Mean annual precipitation in the Dez dam catchment for 1979-2003 from observation and three MRI-AGCMs (a) without bias correction and (b) with bias correction.

(Each error bar indicates the standard deviation of the interannual variability.)
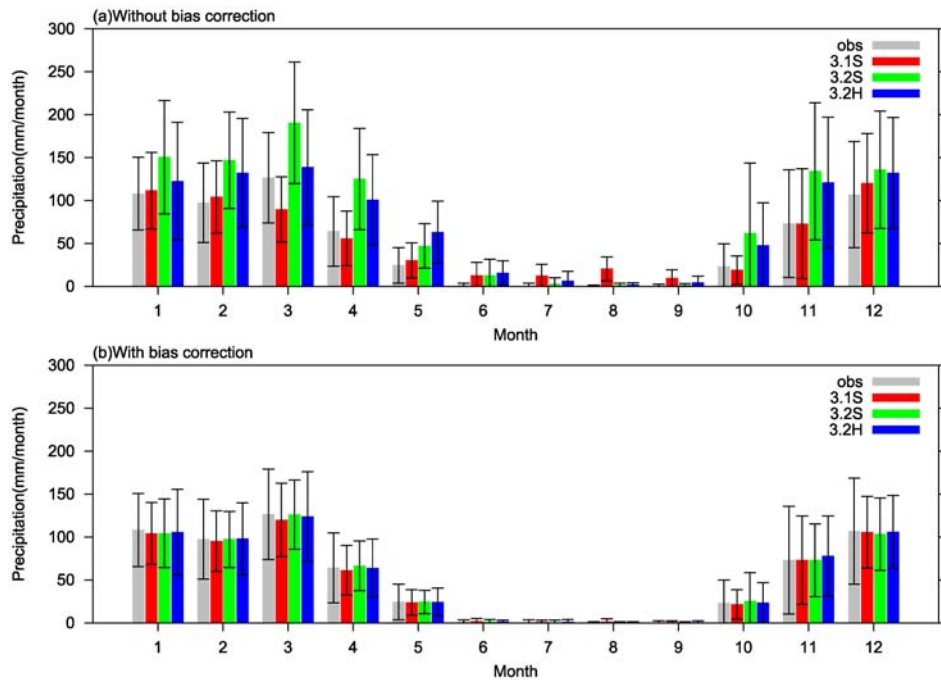
Figure 4.7 Mean monthly precipitation in the Dez dam catchment for 1979-2003 from observation and three MRI-AGCMs (a) without bias correction and (b) with bias correction.

(Each error bar indicates the standard deviation of the inter-annual variability.)

Finally, the bias corrected results of the MRI-AGCMs precipitation for the three target periods were examined. Figure 4.8 shows mean monthly precipitation projected by MRI-AGCMs over the Karun1 dam catchment for the present climate, the near future climate and the future climate, without and with bias correction. Same results at the Dez dam catchment are shown in Figure 4.9. The results of without bias correction indicate that three MRI-AGCMs project less precipitation during wet winter in the near future and the future climate, particularly from January to March, compared with the simulated precipitation in the present climate, as shown in (a), (c) and (e) of Figure 4.8 and Figure 4.9. The bias correction method applied here assumes that the estimated correction coefficients for the present climate are invariant for the future climate periods. Thus, the future precipitation during wet winter also remains at a lower level than the present precipitation even after the bias correction was applied, as shown in (b), (d) and (f) of Figure 4.8 and Figure 4.9. The assumption of the invariant coefficient might work as an advantage to keep the characteristics of precipitation in the future climates, which reflect the different characteristics of MRI-AGCMs; however, this assumption might also be a source of an uncertainty that affects climate change impact assessment.
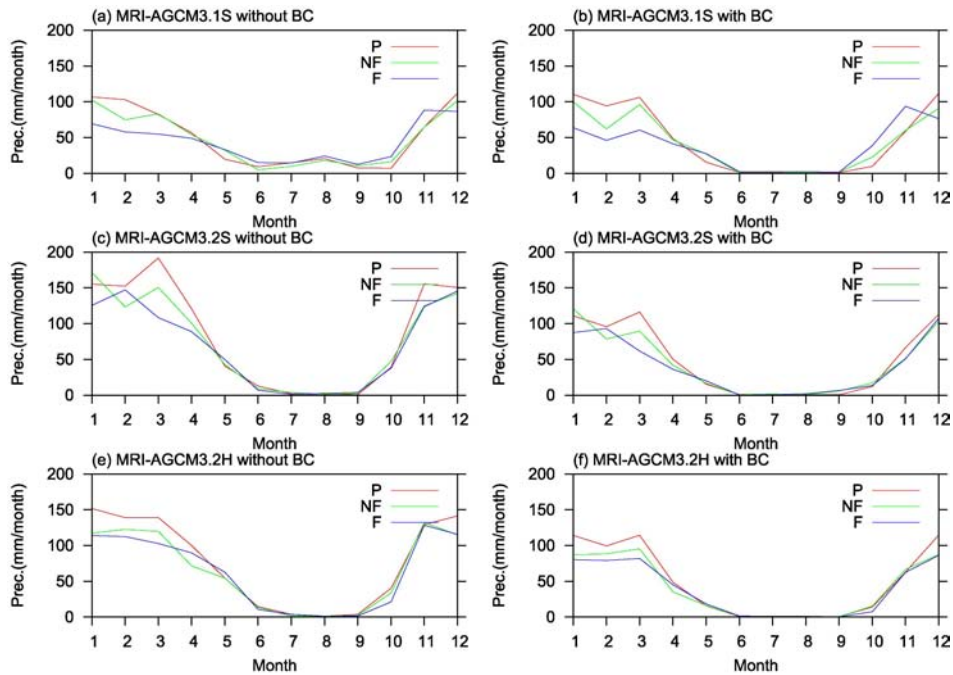
Figure 4.8 Mean monthly precipitation at the Karun1 dam catchment for the present climate (P, 1979-2003), the near future climate (NF, 2035-2059) and the future climate (F, 2075-2099) derived from three MRI-AGCMs (3.1S, 3.2S and 3.2H) without and with bias correction (BC).
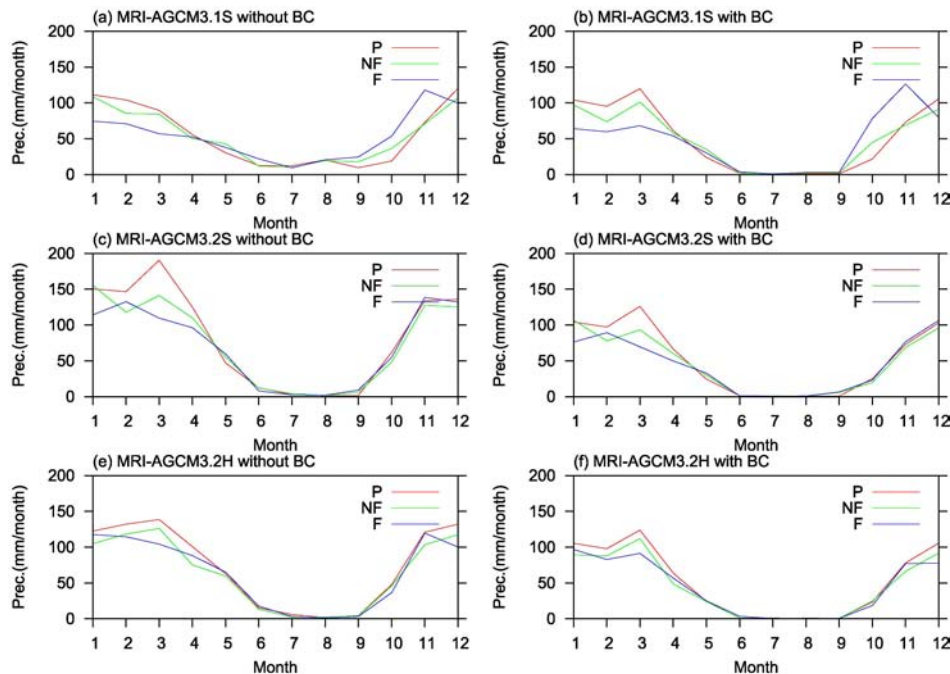
Figure 4.9 Mean monthly precipitation at the Dez dam catchment for the present climate (P, 1979-2003), the near future climate (NF, 2035-2059) and the future climate (F, 2075-2099) derived from three MRI-AGCMs (3.1S, 3.2S and 3.2H) without and with bias correction (BC).

4.3.2. Future changes in basin climatology and hydrology

Figure 4.10 shows mean monthly climatology and hydrology at the Karun1 dam site for the present climate, the near future climate and the future climate simulated by BTOPMC using bias-corrected daily precipitation and daily averaged surface air temperature derived from the three members of MRI-AGCMs. Figure 4.11 shows mean monthly climatology and hydrology at the Dez dam site for the three target periods.. The thick solid lines indicate the ensemble mean of the mean monthly variables from the three MRI-AGCMs. The ensemble results show that the mean monthly discharge might decrease significantly in the near future climate and the future climate, particularly from April to July (Figure 4.10(g) and Figure 4.11(g)). The largest reductions in mean monthly discharge at Karun1 and Dez were projected in May at -35% and -33% in the near future climate and at -61% and -60% in the future climate compared to the present climate, respectively, in comparison with those in the present climate. These reductions in spring and summer might be primarily caused by the decline in precipitation projected in winter. Although rainfall, which was divided from precipitation based on temperature, may not change significantly in winter (Figure 4.10(c) and Figure 4.11(c)), snowfall might decrease (Figure 4.10(d) and Figure 4.11(d)) and SWE might also decrease in the near future climate and the future climate (Figure 4.10(e) and Figure 4.11(e)). The projected increase in temperature (Figure 4.10(b) and Figure 4.11(b)) might further affect division of precipitation into rainfall and snowfall, which is likely to result in more rainfall and less snowfall in winter. Thus, snowmelt in spring might decrease, eventually leading to less discharge in spring and summer.
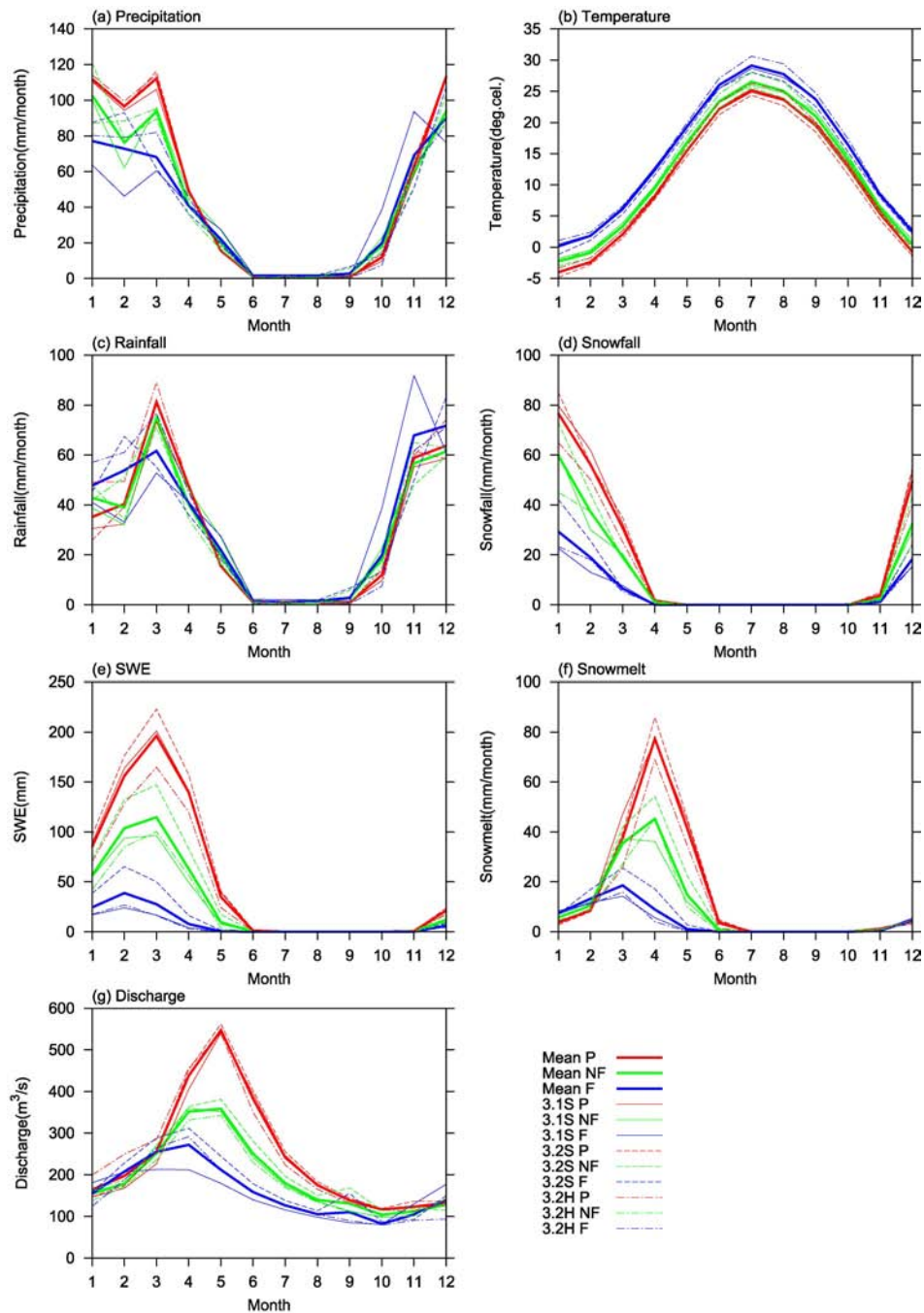
Figure 4.10 Hydrological simulation results of mean monthly climatology and hydrology at the Karun1 dam site for the present climate, the near future climate and the future climate.

(The thin solid, dotted and dashed lines indicate simulation results by BTOPMC using bias-corrected precipitation and temperature derived from MRI-AGCM3.1S, 3.2S and 3.2H, respectively. The thick solid lines indicate multi-ensemble mean of these three results. The red, green and blue lines indicate the results for the present climate (P, 1979-2003), the near future climate (NF, 2015-2039) and the future climate (P, 2075-2099), respectively. The mean monthly variables are the catchment average values, except for discharge.)

Figure 4.11 Hydrological simulation results of mean monthly climatology and hydrology at the Dez dam site for the present climate, the near future climate and the future climate.

(The thin solid, dotted and dashed lines indicate simulation results by BTOPMC using bias-corrected precipitation and temperature derived from MRI-AGCM3.1S, 3.2S and 3.2H, respectively. The thick solid lines indicate multi-ensemble mean of these three results. The red, green and blue lines indicate the results for the present climate (P, 1979-2003), the near future climate (NF, 2015-2039) and the future climate (P, 2075-2099), respectively. The mean monthly variables are the catchment average values, except for discharge.)

81

4.4. Conclusions

This chapter assessed the potential impact of climate change on river discharge in the semi-arid mountainous Karun River basin by coupling a distributed hydrological model (BTOPMC) with climatic outputs derived from the three members of MRI-AGCMs (MRI-AGCM3.1S, MRI-AGCM3.2S and MRI-AGCM3.2H) under a future emission scenario of SRES A1B. The Karun River basin in Iran was selected as case study because no impact assessment study of climate change has been conducted in the basin although many development projects are being planned.

First, the study examined the applicability of the simple statistical bias correction method developed by Inomata et al. (2011) to daily precipitation derived from MRI-AGCMs for the present climate. Generally, the three MRI-AGCMs have a good reproducibility in terms of seasonal variability of precipitation in wet winter and dry summer. More specifically, however, MRI-AGCM3.2S and 3.2H show an overestimation tendency in precipitation during wet winter. This overestimation clearly indicates the need for application of bias correction to precipitation derived from MRI-AGCMs in the study basin. The bias correction method with NEP of 99.5% as the criterion for extreme precipitation well corrected mean annual and monthly precipitation for the present climate in both mean values and interannual variability. Thus, the applicability of the statistical bias-correction method to the semi-arid mountainous basin was verified.

Second, potential impacts of climate change on river discharge at the Karun1 dam site and the Dez dam site were assessed by BTOPMC using bias-corrected daily precipitation and daily average surface air temperature derived from the three members

of MRI-AGCMs. Each MRI-AGCM result shows that the combination of decreased precipitation and increased temperature in winter might reduce snow accumulation in the near future climate and the future climate. The multi-ensemble results from the simulations indicate that mean monthly discharge might decrease significantly in the near future climate and the future climate, particularly from April to July. The largest reductions in mean monthly discharge at Karun1 and Dez were projected in May at -35% and -33% in the near future climate and at -61% and -60% in the future climate, respectively, in comparison with those in the present climate. These projected impacts on river discharge suggest the urgent need for climate change adaptation to secure water to meet future water demands in the basin during spring and summer.

In terms of uncertainties associated with making climate change projections on river discharge by using a hydrological model coupled with GCMs, further studies are needed on uncertainty analysis. One of the limitations in this study is the use of a single future emission scenario. This study used climatic outputs derived from MRI-AGCMs under a future emission scenario from IPCC, i.e., SRES A1B, because they are only such data currently available. Other limitations are that the study only employed a same type of GCMs from one developer group, a single bias correction method with assumption that the correction coefficients obtained in the present climate were invariant for the future climate, and a single hydrological model. Despite these uncertainties, this study demonstrated one possible procedure utilizing the outputs of the super-high-resolution AGCMs with bias correction in climate change impact assessments over semi-arid mountainous regions.

5. Conclusions of the Thesis and Policy Implications

5.1. Conclusions of the thesis

Hydrological models have been playing an important role in providing critical information on water availability at a national or basin scale that can help understand and make decisions on water resources development. Nevertheless, in semi-arid mountainous regions, lack of high-quality local data and complex hydrological processes are serious issues in application of hydrological models to water resources development. In addition, projected climate change may adversely affect temporal and spatial availability of water in the regions. It is obvious that formulation of any adaptation policies with low-regrets measures regarding freshwater management under climate change requires as much information as possible on future climate conditions of water availability at a river basin scale.

Based on the background, this thesis aimed to assess the current state of challenges that water resources engineers and managers face in hydrological analysis for water resources development in semi-arid mountainous regions. These challenges consist of hydrological model applicability, data availability for efficient hydrological model use, and climate change impact assessment. As a case study for hydrological analysis, the Karun River basin, located in the southwestern semi-arid mountainous area of the Islamic Republic of Iran, was selected.

5.1.1. Hydrological model applicability

A distributed hydrological model, BTOPMC, was selected that satisfies following five indispensable criteria appropriate for the Karun River basin application: (1) the model should be based on physical processes; (2) the model must be capable of long-term simulation; (3) the model needs to be able to simulate snowpack and snowmelt processes; (4) the model must be capable of using globally-available data efficiently when local observation data are sparse or unavailable; and (5) the model should be parsimonious and has minimal parameters to be calibrated.

BTOPMC with modification was applied to the catchments of the existing dams, the Karun1 dam and the Dez dam, which are located in the middle of the basin. The modification introduced was the adjustment coefficient for infiltration capacity of the soil surface in the land surface process of BTOPMC to improve the model performance of reproducing flood peaks generated by infiltration excess overland runoff at a daily time scale. The results at Karun1 clearly indicated that BTOPMC was capable to simulate flood peaks as well as seasonal discharge with snowpack and snowmelt processes in wet winter and recession of low flows in dry summer, which are indispensable for analyzing multi seasonal dam reservoir use in long-term simulation.

5.1.2. Data availability in hydrological analysis for water resources development

Data availability from the point of efficient hydrological analysis use for water resources development in semi-arid mountainous regions was assessed in the Karun River basin through an application of BTOPMC using publicly available data sets. The

application results clearly indicated that effective model use was significantly affected by the scarcity of ground gauged precipitation data. In the case of Dez dam site, the simulated discharges were considerably underestimated with the data sets used in this study. Data scarcity is a major issue commonly seen in many basins awaiting water resources development in both developed and developing countries. It is especially true in semi-arid mountainous regions, where the spatial and temporal variation of precipitation tends to be greater than in humid regions, and is amplified by orographic effects.

5.1.3.   Climate change impact assessment

Potential impacts of climate change on river discharge in the semi-arid mountainous Karun River basin were assessed by coupling BTOPMC and daily precipitation and daily averaged surface air temperature derived from three members of MRI-AGCMs (MRI-AGCM3.1S, MRI-AGCM3.2S and MRI-AGCM3.2H) under a future emission scenario of SRES A1B. MRI-AGCMs daily precipitation were corrected by a simple statistical bias correction method with NEP of 99.5% as the criterion for extreme precipitation before being fed to BTOPMC. The multi-ensemble results from the simulations indicate that mean monthly discharge might decrease significantly in the near future climate and the future climate, particularly from April to July. The largest reductions in mean monthly discharge at Karun1 and Dez were projected in May at -35% and -33% in the near future climate and at -61% and -60% in the future climate, respectively, in comparison with those in the present climate. These projected impacts on river discharge suggest the urgent need for climate change

86

adaptation to secure water to meet future water demands in the basin during spring and summer.

In terms of uncertainties associated with making climate change projections on river discharge by using a hydrological model coupled with GCMs, further studies are needed on uncertainty analysis considering multiple future emission scenarios, different type of GCMs, multiple bias correction methods and hydrological models. Despite these uncertainties, this study demonstrated one possible procedure utilizing the outputs of the super-high-resolution AGCMs with bias correction in climate change impact assessments over semi-arid mountainous regions.

5.2. Policy implications

5.2.1. Data acquisition to enhance hydrological analysis for water resources development planning

The greatest challenge that hydrologists and river basin managers face in hydrological modeling in semi-arid mountainous basin is to systematically observe and accumulate ground-based hydrological observation data. There is no doubt that in order to further improve BTOPMC to more accurately simulate rapid surface runoff processes necessary to model sharp rises of flood peaks, snowpack and snowmelt processes and low flow generation. Higher-quality observed data are indispensable for such model improvements and verification. Efforts to improve ground-based observation of precipitation should well precede water resource development plans. Therefore, priorities should be put on data collection and further hydrological model improvement in order to enhance water resources development in semi-arid mountainous regions.

However, as data scarcity largely limits an effective use of hydrological simulation models required for design of water resources development, overreliance on hydrological models should carefully be avoided in poorly-gauged basins even with the best available hydrological models.

5.2.2. Climate change adaptation

The projected huge reduction in river discharge at the Karun1 dam and the Dez dam from April to July may cause severe water stress in the basin not only for power generation to meet peak demands in summer but also for water supply for irrigation. Despite possible uncertainties in the assessment, climate change adaptation should take the projected discharge reduction into consideration as one possible future state of water availability. These projected results clearly indicate that how to utilize the limited amount of available water will become an increasingly more important issue in the future. In that sense, water storage by dams in winter may play a more significant role in satisfying water demand in subsequent spring and summer. From the supply side of water resources, enhancement of water use efficiency is the key for climate change adaptation. Possible low regrets measures in climate change adaptation in the Karun River basin can be summarized as follows:

(1) Consideration of multi-purpose dams should be recommended. Most of the dams in the basin have a single purpose of hydropower generation. In order to utilize the limited amount of water for satisfying water demands, multi-purpose dams, i.e., for hydropower generation, irrigation, domestic and industrial supply, flood control, and environmental flow, should be considered for the dam development in the basin.

88

(2) Integrated operation of multiple dams should be proposed. Although multiple dams are constructed and planned, interaction of dam operation between downstream and upstream areas has not been analyzed yet in the basin. Thus, integrated operation of multiple dams, which aims to optimize the total dam reservoir capacity among all dams in the basin, should be considered by analyzing the interaction of dam operation.

In order to assess the performance of the proposed measures above, a hydrological model incorporating anthropogenic impacts, such as dam reservoir operation, water withdrawal from a river and water diversion, is required. For example, Lauri et al. (2012) examine future impacts on river discharge caused by both climate change and reservoir operation in the Mekong River basin. However, hydrological analysis involving reservoir operation primarily requires accurate simulation of reservoir inflow. This kind of simulation is difficult particularly in semi-arid mountainous regions, and again, high-quality local data is indispensable to improve the performance of hydrological models.

Reference

Abbaspour, K.C., Faramarzi, M., Ghasemi, S.S., & Yang, H. (2009). Assessing the impact of climate change on water resources in Iran. *Water Resources Research, 45*, W10434. doi:10.1029/2008WR007615

Afkhami, M., Shariat, M., Jaafarzadeh, M., Ghadiri, H., & Nabizadeh, R. (2007). Developing a water quality management model for Karun and Dez rivers. *Iranian Journal of Environmental Health Science & Engineering, 4*(2), 99–106.

Ajami, N.K., Gupta, H., Wagener, T., & Sorooshian, S. (2004). Calibration of a semi-distributed hydrologic model for streamflow estimation along a river system, *Journal of Hydrology*, *298*(1-4), 112-135.

Ao, T.Q., Yoshitani, J., Takeuchi, K., Fukami, K., Mutsura, T., & Ishidaira, H. (2003). Effects of sub-basin scale on runoff simulation in distributed hydrological model: BTOPMC. In: Tachikawa, Y., Vieux, B.E., Georgakakos, K.P., Nakakita, E., (Eds), *Weather Radar Information and Distributed Hydrological Modelling*. *IAHS Publication 282* (pp. 227–234). Oxfordshire: International Association of Hydrological Sciences.

Arakawa, A., & Schubert, W. H., 1974. Interaction of a cumulus cloud ensemble with the large-scale environment, Part I, *Journal of the Atmospheric Sciences*, *31*(3), 674–701. doi:10.1175/1520-0469(1974)031<0674:IOACCE>2.0.CO;2

Ardakanian, R. (2005). Overview of water management in Iran. In: *Water conservation, reuse, and recycling, Proceeding of an Iranian American workshop* (pp. 153-172). Washington, DC: The National Academies Press.

Ashraf Vaghefi, S., Mousavi, S. J., Abbaspour, K. C., Srinivasan, R., & Yang, H. (2013). Analyses of the impact of climate change on water resources components, drought and wheat yield in semiarid regions: Karkheh River Basin in Iran. *Hydrological Processes*. doi: 10.1002/hyp.9747

Bae, D-H., Jung, I-W., & Lettenmaier, D.P. (2011). Hydrologic Uncertainties in Climate Change from IPCC AR4 GCM Simulations of the Chungju Basin, Korea. *Journal of Hydrology*, *401*, 90-105. doi: 10.1016/j.jhydrol.2011.02.012

Barnett, T.P., Adam, J.C., & Lettenmaier, D.P. (2005). Potential impacts of a warming climate on water availability in snow-dominated regions. *Nature, 438*, 303–309.

Bates, B., Kundzewicz, Z.W., Wu, S., & Palutikof, J.P. (Eds.). (2008). *Climate change and water, technical paper of the intergovernmental panel on climate change* (IPCC Technical Paper VI). Retrieved April 8, 2013, from http://www.ipcc.ch/pdf/technical-papers/climate-change-water-en.pdf

Beaumont, P. (1971). Qanat systems in Iran. *International Association of Scientific Hydrology. Bulletin*, *16*(1), 39-50.

Beven, K.J. (2002). Runoff generation in semi-arid areas. In L. J. Bull , & M. J. Kirkby (Eds.), *Dryland rivers: hydrology and geomorphology of semi-arid channels* (pp. 57-106). West Sussex: John Wiley & Sons Ltd.

Beven, K.J., & Kirkby, M.J. (1979). A physically based, variable contributing area model of hydrology. *Hydrological Science Bulletin, 24*(1), 43–69.

Blöschl, G., & Montanari, A. (2010). Climate change impacts—throwing the dice?. *Hydrological Processes*, *24*, 374–381. doi: 10.1002/hyp.7574

Blöschl, G., & Sivapalan, M. (1995). Scale issues in hydrological modelling: A review. *Hydrological Processes*, *9*, 251–290. doi: 10.1002/hyp.3360090305

Blöschl, G., Sivapalan, M., Wagener, T., Viglione, A., & Savenije, H. (Eds.). (2013). *Run-off Prediction in Ungauged Basins. Synthesis across Processes, Places and Scales.* Cambridge: Cambridge University Press.

Castillo, V.M., Gómez-Plaza, A., & Martínez-Mena, M. (2003). The role of antecedent soil water content in the runoff response of semiarid catchments: a simulation approach. *Journal of Hydrology*, *284*(1-4), 114-130.

Chen, J., Brissette, F.P., & Leconte, R. (2011). Uncertainty of downscaling method in quantifying the impact of climate change on hydrology. *Journal of Hydrology*, *401*, 190-202.

Chien, H., Yeh, P. J.-F., & Knouft, J. H. (2013). Modeling the potential impacts of climate change on streamflow in agricultural watersheds of the Midwestern United States. *Journal of Hydrology*, *491*, 73-88.

CITC. (2012). *A summary of selected technology achievements in The Islamic Republic of Iran*. Retrieved June 11, 2013, from http://www.infocyt.gob.bo/files/iran_ciencia_y_tecnologia.pdf

Endo, H., Kitoh, A., Ose, T., Mizuta, R., & Kusunoki, S. (2012). Future changes and uncertainties in Asian precipitation simulated by multi-physics and multi-sea surface temperature ensemble experiments with high-resolution Meteorological Research Institute atmospheric general circulation models (MRI-AGCMs). *Journal of Geophysical Research*, doi:10.1029/2012JD017874

Falkenmark, M., Lundqvist, J., & Widstrand, C. (1989). Macro-scale water scarcity requires micro-scale approaches. *Natural Resources Forum*, *13,* 258–267. doi: 10.1111/j.1477-8947.1989.tb00348.x

FAO. (2008). *AQUASTAT: FAO's information system on water and agriculture.* Retrieved February 13, 2013, from

http://www.fao.org/nr/water/aquastat/countries_regions/IRN/index.stm

FAO. (2011). *Climate change, water and food security. FAO WATER REPORTS 36*. Retrieved June 14, 2011, from http://www.fao.org/docrep/014/i2096e/i2096e00.htm

Hagemann, S., Arpe, K., & Roeckner, E. (2006). Evaluation of the hydrological cycle in the ECHAM5 model. *Journal of Climate, 19*, 3810–3827.

Gassman, P.W., Reyes, M.R., Green, C.H., & Arnold, J.G. (2007). The soil water assessment tool: Historical development, applications, and future research directions. *Transactions of the ASABE, 50*(4), 1211-1250.

Georgievsky, M.V., Ishidaira, H., & Takeuchi, K. (2006). Development of a distributed snow model coupled with a new method of degree-day factors estimation. *Annual Journal of Hydraulic Engineering*, *JSCE, 50*, ROMBUNNO.009.

Ghanbarpour, M.R., Abbaspour, K.C., & Hipel, K.W. (2009). A comparative study in long-term river flow forecasting models. *International Journal of River Basin Management, 7*(4), 403-413.

Gharavy, M. (2005). Hydropower development in Iran: achievements and plans. *International Journal of Hydropower & Dams*, *2*, 43-46.

Gosling, S. N., Taylor, R. G., Arnell, N. W., & Todd, M. C. (2011). A comparative analysis of projected impacts of climate change on river runoff from global and catchment-scale hydrological models. *Hydrology and Earth System Sciences*, *15*, 279-294. doi:10.5194/hess-15-279-2011

Green, W.H., & Ampt, G. (1911). Studies of soil physics, part I – the flow of air and water through soils. *Journal of Agricultural Science, 4*, 1-24.

Güntner, A., & Bronstert, A. (2004). Representation of Landscape Variability and Lateral Redistribution Processes for Large-Scale Hydrological Modelling in Semi-Arid Areas. *Journal of Hydrology*, *297*(1-4), 136-161.

Güntner, A., Krol, M. S., de Araújo, J. C., & Bronstert, A. (2004). Simple water balance modelling of surface reservoir systems in a large data-scarce semiarid region. *Hydrological Sciences Journal*, *49*(5), 901-918.

Hapuarachchi, H.A.P., Takeuchi, K., Zhou, M., Kiem, A. S., Georgievski, M., Magome, J., & Ishidaira, H. (2008). Investigation of the Mekong River basin hydrology for 1980–2000 using the YHyM. *Hydrological Processes, 22*(9), 1246–1256.

Harding, B. L., Wood, A. W., & Prairie, J. R. (2012). The implications of climate change scenario selection for future streamflow projection in the Upper Colorado River Basin. *Hydrology and Earth System Sciences*, *16*, 3989-4007. doi:10.5194/hess-16-3989-2012

Heidari, A. (2013). Flood vulnerability of the Karun River System and short-term mitigation measures. *Journal of Flood Risk Management*. doi: 10.1111/jfr3.12032

Hidalgo, H.G., Amador, J.A., Alfaro, E.J., & Quesada, B. (2013). Hydrological Climate Change Projections for Central America. *Journal of Hydrology*, *495*, 94-112. doi: 10.1016/j.jhydrol.2013.05.004

Horton, R.E. (1940). An approach towards a physical interpretation of infiltration capacity. *Soil Science Society of America Proceedings, 5*, 399-417.

Hughes, D.A. (2008). Modelling semi-arid and arid hydrology and water resources: The southern Africa experience. In H. S. Wheater, S. Sorooshian, & K. D. Sharma (Eds.), *Hydrological modelling in arid and semi-arid areas* (pp. 29-40). Cambridge: Cambridge University Press.

IJHD. (2009). *The International Journal of Hydropower & Dams 2009 World Atlas & Industry Guide.* Surrey: Aqua Media International.

IJHD. (2010). *The International Journal of Hydropower & Dams 2010 World Atlas & Industry Guide.* Surrey: Aqua Media International.

IJHD. (2011). *The International Journal of Hydropower & Dams 2011 World Atlas & Industry Guide.* Surrey: Aqua Media International.

IJHD. (2012). *The International Journal of Hydropower & Dams 2012 World Atlas & Industry Guide.* Surrey: Aqua Media International.

Inomata, H., Takeuchi, K., & Fukami, K. (2011). Development of a statistical bias correction method for daily precipitation data of GCM20. *Annual Journal of Hydraulic Engineering, JSCE, 55*, S_247-S_252.

IPCC. (2007a). *Climate Change 2007: Impacts, Adaptation and Vulnerability. Contribution of Working Group II to the Fourth Assessment Report of the Intergovernmental Panel on Climate Change*. Cambridge: Cambridge University Press.

IPCC. (2007b). *Climate Change 2007: The Physical Science Basis. Contribution of Working Group I to the Fourth Assessment Report of the Intergovernmental Panel on Climate Change.* Cambridge: Cambridge University Press.

IPCC. (2012). *Managing the Risks of Extreme Events and Disasters to Advance Climate Change Adaptation. A Special Report of Working Groups I and II of the Intergovernmental Panel on Climate Change.* Cambridge: Cambridge University Press.

JICA. (2002). *The study on watershed management plan for Karoon river in the Islamic republic of Iran.* Tokyo: Japan International Cooperation Agency

Kampf, S. K., & Burges, S. J. (2007). A framework for classifying and comparing distributed hillslope and catchment hydrologic models. *Water Resources Research*, *43*, W05423, doi:10.1029/2006WR005370

Kistler, R., Kalnay, E., Collins, W., Saha, S., White, G., Woollen, J., Chelliah, M., Ebisuzaki, W., Kanamitsu, M., Kousky, V., van den Dool, H., Jenne, R., & Fiorino, M. (2001). The NCEP-NCAR 50-Year Reanalysis: Monthly Means CD-ROM and Documentation. *Bulletin of the American Meteorological Society*, *82*, 247-268.

Kitoh, A., Ose, T., Kurihara, K., Kusunoki, S., & Sugi, M. (2009). Projection of changes in future weather extremes using super-high-resolution global and regional atmospheric models in the KAKUSHIN Program: Results of preliminary experiments. *Hydrological Research Letters*, *3*, 49–53. doi: 10.3178/HRL.3.49

Kundzewicz, Z. W., Mata, L. J., Arnell, N. W., Doll, P., Jimenez, B., Miller, K., Oki, T., Sen, Z., & Shiklomanov, I. (2008). The implications of projected climate change for freshwater resources and their management. *Hydrological Sciences Journal*, *53*(1), 3–10.

Lauri, H., de Moel, H., Ward, P. J., Räsänen, T. A., Keskinen, M., & Kummu, M. (2012). Future changes in Mekong River hydrology: impact of climate change and reservoir operation on discharge. *Hydrology and Earth System Sciences*, *16*, 4603-4619. doi:10.5194/hess-16-4603-2012

Lee, S.-Y., Hamlet, A.F., Fitzgerald, C.J., & Burges, S.J. (2009). Optimized flood control in the Columbia River basin for a global warming. *Journal of Water Resources Planning and Management*, *135*(6), 440–450.

Liang, X., Lettenmaier, D. P. , Wood, E. F., & Burges, S. J. (1994). A Simple hydrologically Based Model of Land Surface Water and Energy Fluxes for GSMs. *Journal of Geophysical Research*, *99*(D7), 14415-14428.

Loucks, D. P., van Beek, E., Stedinger, J. R., Dijkman, J. P.M., & Villars, M. T. (2005). *Water Resources Systems Planning and Management: An Introduction to Methods, Models and Applications*. Paris: UNESCO

Lu, M., Koike, T., & Hayakawa, N. (1989). A rainfall-runoff model using distributed data of radar and altitude (in Japanese). *Proceedings of JSCE,* No.411/II- 12, 135–142.

Manandhar, S., Pandey, V. P., Ishidaira, H., & Kazama, F. (2012). Perturbation study of climate change impacts in a snow-fed river basin. *Hydrological Processes.* doi: 10.1002/hyp.9446

Masih, I., Maskey, S., & Uhlenbrook, S. (2012). Supporting well-informed decision and policy making through hydrological data analysis and modelling: the case of the Karkheh Basin, Iran. *Water International*, *37*(4), 427–441.

Masutani, K., & Magome, J. (2008). Effects of the Novel Scaling Algorithm of River Networks on Discharge Simulations (in Japanese). *Journal of Japan Society of Hydrology and Water Resources, 21*(3), 242-247.

Masutani, K., & Magome, J. (2009). An application of modified Muskingum-Cunge routing method with water conservation condition to a distributed runoff model (in Japanese). *Journal of Japan Society of Hydrology and Water Resources,* 22(4), 294-300. doi: 10.3178/jjshwr.22.294

Masutani, K., & Magome, J. (2013). Runoff analysis with DEM scale independent TOPMODEL (in Japanese). *Journal of Japan Society of Hydrology and Water Resources,* 26(1), 26-37.

McCartney, M.P., & Girma, M.M. (2012). Evaluating the downstream implications of planned water resource development in the Ethiopian portion of the Blue Nile River. *Water International*, *37*(4), 362–379.

Mizuta, R., Yoshimura, H., Murakami, H., Matsueda, M., Endo, H., Ose, T., Kamiguchi, K., Hosaka, M., Sugi, M., Yukimoto, S., Kusunoki, S., & Kitoh, A. (2012). Climate simulations using MRI-AGCM3.2 with 20-km grid. *Journal of the Meteorological Society of Japan, 90*A, 233–258. doi:10.2151/jmsj.2012-A12

Morin, J., & Benyamini, Y. (1977). Rainfall infiltration into bare soils. *Water Resources Research*, *13*(5), 813-817.

Najafi, M. R., Moradkhani, H., & Jung, I. W. (2011). Assessing the uncertainties of hydrologic model selection in climate change impact studies. *Hydrological Processes*, *25*, 2814–2826. doi: 10.1002/hyp.8043

Nakićenović, N., Davidson, O., Davis, G., Grübler, A., Kram, T., Rovere, E. L. L., Metz, B., Morita, T., Pepper, W., Pitcher, H., Sankovski, A., Shukla, P., Swart, R., Watson, R., & Dadi, Z. (2000). *Emissions scenarios—summary for policymakers. Intergovernmental Panel on Climate Change.* Retrieved October 29, 2010, from http://www.ipcc.ch/ipccreports/sres/emission/index.php?idp=1

Nash, J. E., & Sutcliffe, J. V. (1970). River flow forecasting through conceptual models part I — A discussion of principles, *Journal of Hydrology*, *10*(3), 282–290.

Nicholson, S.E., (2011). *Dryland Climatology*. Cambridge: Cambridge University Press.

Nikoo, M.R., Kerachian, R., & Poorsepahy-Samian, H. (2012). An Interval Parameter Model for Cooperative Inter-Basin Water Resources Allocation Considering the Water Quality Issues. *Water Resources Management, 26*(11), 3329-3343.

Nourani, V., & Mano, A. (2007). Semi-distributed flood runoff model at the subcontinental scale for southwestern Iran. *Hydrological Processes*, *21*, 3173–3180. doi: 10.1002/hyp.6549

Oki, T., & Kanae, S. (2006). Global Hydrological Cycles and World Water Resources, *Science*, *313*(5790), 1068-1072. DOI: 10.1126/science.1128845

Onogi, K., Tsutsui, J., Koide, H., Sakamoto, M., Kobayashi, S., Hatsushika, H., Matsumoto, T., Yamazaki, N., Kamahori, H., Takahashi, K., Kadokura, S., Wada, K., Kato, K., Oyama, R., Ose, T., Mannoji N., & Taira, R. (2007). The JRA-25 Reanalysis. *Journal of the Meteorological Society of Japan*, *85*, 369-432.

Pathiraja, S., Westra, S., & Sharma, A. (2012). Why continuous simulation? The role of antecedent moisture in design flood estimation, *Water Resources Research*, *48*, W06534, doi:10.1029/2011WR010997

Pechlivanidis I.G., Jackson B.M., McIntyre N.R., & Wheater H.S. (2011). Catchment scale hydrological modelling: a review of model types, calibration approaches and uncertainty analysis methods in the context of recent developments in technology and applications. *Global NEST Journal*, *13*(3), 193-214.

Philip, J. R. (1957). The theory of infiltration: 4. Sorptivity and algebraic infiltration equations. *Soil Science, 84*, 257–264.

Pilgrim, D.H., Chapman, T.G., & Doran, D.G. (1988). Problems of rainfall-runoff modelling in arid and semi-arid regions, *Hydrological Sciences Journal*, *33*(4), 379-400.

Randall, D. A., & Pan, D.-M. (1993). Implementation of the Arakawa-Schubert cumulus parameterization with a prognostic closure. In K. A. Emanuel, & D. J. Raymond (Eds.), *The Representation of Cumulus Convection in Numerical Models* (pp. 137-144). Boston: American Meteorological Society.

Rawls, W.J., Brakensiek, D.L., & Saxton, K.E. (1982). Estimation of soil water properties. *Transactions of ASAE, 25*(5), 1316–1320.

Rawls, W.J., & Brakensiek, D.L. (1985). Prediction of soil water properties for hydrologic modeling. In: E. B. Jones, (Ed.), *Watershed Management in the Eighties* (pp. 293–299). New York: American Society of Civil Engineers.

Rayner, N. A., Parker, D. E., Horton, E. B., Folland, C. K., Alexander, L. V., Rowell, D. P., Kent, E. C., & Kaplan, A. (2003). Global analyses of sea surface temperature, sea ice, and night marine air temperature since the late nineteenth century, *Journal of Geophysical Research*, *108*(D14), 4407. doi: 10.1029/2002JD002670

Sadegh, M., Mahjouri, N., & Kerachian, R. (2010). Optimal inter-basin water allocation using crisp and fuzzy shapley games. *Water Resoureces Management, 24*(10),

2291–2310.

Sellers, P.J., Los, S.O., Tucker, C.J., Justice, C.O., Dazlich, D.A., Collatz, G.J., & Randall D.A. *(*1994). A global 1 degree by 1 degree NDVI data set for climate studies. Part 2: the generation of global fields of terrestrial biophysical parameters from NDVI. *International Journal of Remote Sensing, 15*(17), 3519–3545.

Sellers, P.J., Tucker, C.J., Collatz, G.J., Los, S.O., Justice, C.O., Dazlich, D.A., & Randall D.A. *(*1996). A revised land surface parameterization (SiB2) for atmospheric GCMs. Part II: the generation of global fields of terrestrial biophysical parameters from satellite data. *Journal of Climate, 9*, 706–737.

Shrestha, S., Bastola, S., Babel, M. S., Dulal, K. N., Magome, J., Hapuarachchi, H. A. P., Kazama, F., Ishidaira, H., & Takeuchi, K. *(*2007). The assessment of spatial and temporal transferability of a physically based distributed hydrological model parameters in different physiographic regions of Nepal. *Journal of Hydrology, 347*, 153–172.

Smakhtin, V. U. (2001). Low flow hydrology: a review. *Journal of Hydrology*, *240*, 147–186. doi: 10.1016/S0022-1694(00)00340-1

Smith, M.B., Koren, V.I., Zhang, Z., Reed, S.M., Pan, J-J., & Moreda, F. (2004). Runoff response to spatial variability in precipitation: an analysis of observed data. *Journal of Hydrology, 298*(1-4), 267-286.

Steinschneider, S., Polebitski, A., Brown, C., & Letcher, B. H. (2012). Toward a statistical framework to quantify the uncertainties of hydrologic response under climate change, *Water Resources Research*, *48*, W11525, doi: 10.1029/2011WR011318

Takeuchi, K., Ao, T., & Ishidaira, H. (1999). Introduction of block-wise use of TOPMODEL and Muskingum-Cunge method for the hydroenvironmental simulation of a large ungauged basin. *Hydrological Sciences Journal*, *44*(4), 633–646.

Takeuchi, K., Hapuarachchi, H. A. P., Kiem, A. S., Ishidaira, H., Ao, T., Magome, J., Zhou, M., Georgievski, M., Wang, G., & Yoshimura, C. (2013). Distributed runoff predictions in the Mekong River basin. In G. Blöschl, M. Sivapalan, T Wagener, A. Viglione, & H. Savenije (Eds.), *Run-off Prediction in Ungauged Basins. Synthesis across Processes, Places and Scales* (pp. 349-353). Cambridge: Cambridge University Press.

Takeuchi, K., Hapuarachchi, H. A. P., Zhou, M., Ishidaira, H., & Magome, J. (2008). A BTOP model to extend TOPMODEL for distributed hydrological simulation of

large basins. *Hydrological Processes, 22*, 3236–3251.

Thanapakpawin, P., Richey, J., Thomas, D., Rodda, S., Campbell, B., & Logsdon, M. (2006). Effects of landuse change on the hydrologic regime of the Mae Chaem river basin, NW Thailand. *Journal of Hydrology, 334*, 215–230. doi: 10.1016/j.jhydrol.2006.10.012

UN. (n.d.). Millennium Development Goals. Retrieved October 6, 2011, from http://www.un.org/millenniumgoals/

UNEP. (n.d.). Agenda 21. Retrieved October 6, 2011, from http://www.unep.org/Documents.Multilingual/Default.asp?DocumentID=52&ArticleID=66&l=en

UNEP. (1992). *World Atlas of Desertification*. London: UNEP/Edward Arnold.

UNFCCC. (2007). *Report of the Conference of the Parties on its thirteenth session, held in Bali from 3 to 15 December 2007*. Retrieved October 6, 2011, from http://unfccc.int/resource/docs/2007/cop13/eng/06a01.pdf

UNISDR. (2009). *Global Assessment Report on Disaster Risk Reduction – Risk and Poverty in a Changing Climate. Invest Today for a Safer Tomorrow.* Retrieved October 6, 2011, from http://www.preventionweb.net/english/hyogo/gar/report/documents/GAR_Chapter_2_2009_eng.pdf

UNISDR. (2011). *Global Assessment Report on Disaster Risk Reduction*. Retrieved October 6, 2011, from http://www.preventionweb.net/english/hyogo/gar/2011/en/home/index.html

Uppala, S. M., Kållberg, P.W., Simmons, A.J., Andrae, U., da Costa Bechtold, V., Fiorino, M., Gibson, J.K., Haseler, J., Hernandez, A., Kelly, G.A., Li, X., Onogi, K., Saarinen, S., Sokka, N., Allan, R.P., Andersson, E., Arpe, K., Balmaseda, M.A., Beljaars, A.C.M., van de Berg, L., Bidlot, J., Bormann, N., Caires, S., Chevallier, F., Dethof, A., Dragosavac, M., Fisher, M., Fuentes, M., Hagemann, S., Hólm, E., Hoskins, B.J., Isaksen, L., Janssen, P.A.E.M., Jenne, R., McNally, A.P., Mahfouf, J.-F., Morcrette, J.-J., Rayner, N.A., Saunders, R.W., Simon, P., Sterl, A., Trenberth, K.E., Untch, A., Vasiljevic, D., Viterbo, P., & Woollen, J. (2005). The ERA-40 re-analysis. *Quarterly Journal of the Royal Meteorological Society*, *131*, 2961–3012. doi: 10.1256/qj.04.176

Valipour, M., Banihabib, M.E., & Behbahani, S.M.R. (2013). Comparison of the ARMA, ARIMA, and the autoregressive artificial neural network models in forecasting the monthly inflow of Dez dam reservoir. *Journal of Hydrology, 476*, 433‑441.

Vivoni, E. R., Aragón, C. A., Malczynski, L., & Tidwell, V. C. (2009). Semiarid watershed response in central New Mexico and its sensitivity to climate variability and change. *Hydrology and Earth System Sciences, 13*, 715-733. doi: 10.5194/hess-13-715-2009

Vörösmarty, C.J., Federer, C.A., & Schloss, A.L. (1998). Potential evaporation functions compared on US watersheds: possible implications for global-scale water balance and terrestrial ecosystem modeling. *Journal of Hydrology, 207*, 147–169.

Watanabe, S., Kanae, S., Seto, S., Yeh, P. J.-F., Hirabayashi, Y., & Oki, T. (2012). Intercomparison of bias-correction methods for monthly temperature and precipitation simulated by multiple climate models, *Journal of Geophysical Research, 117*, D23114. doi:10.1029/2012JD018192

Wheater, H.S. (2008). Modelling Hydrological Processes in Arid and Semi Arid Areas – an Introduction to the Workshop. In H. S. Wheater, S. Sorooshian, & K. D. Sharma (Eds.), *Hydrological modelling in arid and semi-arid areas* (pp. 1-20). Cambridge: Cambridge University Press.

WMO. (n.d.). The Dublin statement on water and sustainable development. Retrieved October 6, 2011, from http://www.wmo.int/pages/prog/hwrp/documents/english/icwedece.html

WMO. (1994). *Guide to hydrological practices: data acquisition and processing, analysis, forecasting and other applications.* Retrieved March 12, 2012, from http://library.wmo.int/pmb_ged/wmo_168-1994_en.pdf

Woldemeskel, F. M., Sharma, A., Sivakumar, B., & Mehrotra, R. (2012). An error estimation method for precipitation and temperature projections for future climates, *Journal of Geophysical Research*, *117*, D22104. doi:10.1029/2012JD018062

Yatagai, A., Xie, P., & Alpert, P. (2008). Development of a daily gridded precipitation data set for the Middle East. *Advances in Geosciences*, *12*, 165-170. doi:10.5194/adgeo-12-165-2008

Yatagai, A., Kamiguchi, K., Arakawa, O., Hamada, A., Yasutomi, N., & Kitoh, A. (2012). APHRODITE: Constructing a Long-Term Daily Gridded Precipitation Dataset for Asia Based on a Dense Network of Rain Gauges. *Bulletin of the American Meteorological Society*, *93*, 1401‑1415. doi: 10.1175/BAMS-D-11-00122.1

Yong, B., Ren, L. L., Hong, Y., Gourley, J. J., Chen, X., Dong, J., Shen, Y., & Wang, W. (2013). Spatial-temporal changes of water resources in a typical semi-arid

basin of North China over the past 50years and assessment of possible natural and socioeconomic causes. *Journal ofHydrometeorology*. in press. doi: 10.1175/JHM-D-12-0116.1

Yukimoto, S., Yoshimura, H., Hosaka, M., Sakami, T., Tsujino, H., Hirabara, M., Tanaka, T.Y., Deushi, M., Obata, A., Nakano, H., Adachi, Y., Shindo, E., Yabu, S., Ose, T., & Kitoh, A. (2011). Meteorological Research Institute-Earth System Model version 1 (MRI-ESM1), Model description (Technical reports of the Meteorological Research Institute, Number 64). Retrieved October 28, 2011, from http://www.mri-jma.go.jp/Publish/Technical/DATA/VOL_64/tec_rep_mri_64.pdf

Zhang, C., Shoemaker, C. A., Woodbury, J. D., Cao, M. & Zhu, X. (2013). Impact of human activities on stream flow in the Biliu River basin, China. *Hydrological Processes*, *27*, 2509–2523. doi: 10.1002/hyp.9389

Zhou, M.C., Ishidaira, H., Hapuarachchi, H. A. P., Magome, J., Kiem, A. S., & Takeuchi, K. (2006). Estimating potential evapotranspiration using the Shuttleworth-Wallace model and NOAA-AVHRR NDVI to feed the hydrological modeling over the Mekong River Basin. *Journal of Hydrology, 327*, 151–173.

Zhou, M.C., Ishidaira, H., Hapuarachchi, H. A. P., Georgievsky, M., & Takeuchi, K. (2007). Roles of snow, infiltration and saturation excess processes in runoff generation of Yellow River basin. In *Methodology in Hydrology (Proceedings of the Second International Symposium on Methodology in Hydrology 32 held in Nanjing, China, October–November 2005). IAHS publication 311* (pp. 32-45). Oxfordshire: International Association of Hydrological Sciences.

Appendix

Future changes on low precipitation patterns projected by the super-high-resolution MRI-AGCM3.1S and CMIP3 AOGCMs

Background and objectives of this chapter

Freshwater availability for human use will be an increasing concern in the coming decades with ongoing population growth, economic development and climate change. The Intergovernmental Panel on Climate Change (IPCC) states that arid and semi-arid areas are particularly exposed to the impacts of climate change on freshwater (IPCC, 2007a), and also there is medium confidence that droughts will intensify in the 21st century in some seasons and areas such as southern Europe and the Mediterranean region, central Europe, central North America, Central America and Mexico, northeast Brazil, and southern Africa, due to reduced precipitation and/or increased evapotranspiration (IPCC, 2012).

The need for climate change adaptation has been widely recognized and various adaptations have already been instigated, especially since the establishment of the Adaptation Fund put forward by the Bali Action Plan of COP13 (UNFCCC, 2007). It is obvious that formulation of any adaptation policies regarding freshwater management under climate change requires as much information as possible on future climate conditions.

Global climate change projections are available in data sets assembled by the

Coupled Modeling Intercomparison Project (CMIP3) which contain the simulated results of a number of Atmospheric Ocean coupled General Circulation Models (AOGCMs) run under various scenarios (IPCC, 2007b). Using the CMIP3 data sets, various assessments and comparison studies are available at a global scale on hydro-meteorological extremes and their uncertainty levels, such as by Wang (2005), Neelin et al. (2006), Nohara et al. (2006), Tebaldi et al. (2006), Vaze et al. (2010), and Orlowsky and Seneviratne (2012). Most of these studies focus on precipitation, consecutive dry days (CDD), soil moisture, runoff or other climate variables based on either an annual average basis or a fixed season basis (e.g., boreal summer from June to August and boreal winter from December to February). It is important to focus on the frequency and intensity of extreme events rather than the mean climate, since extreme events are likely to affect society to a greater extent (e.g., Katz & Brown, 1992; Alexander et al., 2006). Such extremes would not necessarily occur in any fixed seasons or periods that might be expected from an anthropogenic perspective. However, a few studies have focused on changes in drought using unfixed observation windows in time frame or by considering the randomness of occurrence of dry spells in months or seasons (e.g. Sheffield & Wood, 2008). Hence this paper looks into the frequency and intensity of season free low precipitation patterns and future changes in the patterns under climate change using GCM outputs.

Although droughts usually extends over a wide area, the resolution of GCM places considerable limitations on the practical use of the outputs for climate change adaptation policies, especially on the fringes of arid zones. The spatial grid scales of most GCMs are about 100 to 400km. Such low resolution necessarily overshadows the extreme phenomena by spatially averaging, and becomes a serious limitation for

practical application. Therefore, a high spatial resolution model is much awaited to serve climate change analysis of extreme weather events and their adaptation studies. In this respect, it is a great scientific stride that a super-high-resolution Atmospheric General Circulation Model (MRI-AGCM3.1S) with a horizontal grid size of about 20 km has been developed by the Japan Meteorological Agency and Meteorological Research Institute (Kitoh et al., 2009). Analyses of the projected data sets are underway, of which this paper contributes regarding drought aspects.

The focus of this chapter is not drought itself but low precipitation. The cause of meteorological drought, which precedes other types of drought by eventual freshwater shortage in ecological system and human activities, may be not only decreases in accumulated precipitation for a certain period but also temporal and spatial shifts in precipitation activities. From the viewpoint of the hydrological cycle, accumulated precipitation is an important indicator because lack of precipitation for a certain period dries up land surfaces, lowers soil moisture, and reduces groundwater recharge, river discharge and reservoir storage (Tallaksen & van Lanen, 2004). The seasonal shift in the low precipitation period adversely affects water dependent activities such as rain-fed and irrigated agriculture as they are scheduled on an average annual water availability pattern.

A number of drought indices using precipitation and other climate variables have been proposed and applied to quantifying droughts, such as the Standardized Precipitation Index (SPI; Mckee et al., 1993) and the Palmer Drought Severity Index (PDSI; Palmer, 1965). Although each of them has advantages and disadvantages (e.g., Keyantash & Dracup, 2002), drought indices are applied for analyses of projected changes in drought using multi-model ensemble of GCMs (e.g., Burke & Brown, 2008).

However, Dai (2011) indicates that drought indices that consider precipitation only, without accounting changes in atmospheric demand for moisture due to increased radiative heating and surface warming, may not work well when they applied to model-projected 21st century climates with large warming. Besides, he says that even for the indices that consider the whole surface water budget, such as the PDSI, the interpretation of their values for the future climate may need to be revised because these drought indices have been defined and calibrated for the current climate. Values under future climates with large warming trends will be greatly out of the range for the current climate. Thus there is still difficulty applying drought indices to project future droughts.

Nevertheless, considering the importance of precipitation as the primary driver of drought and regarding the difficulty of assessing moisture as granted, this study assesses projected future changes in low precipitation patterns on global land areas using occurrence probability and observation windows in unfixed seasons. The precipitation data sets to be analyzed are those of MRI-AGCM3.1S and CMIP3 AOGCMs. First, the capability of the models reproducing low precipitation patterns is examined by comparing the model outputs with observations. By this way the merit of MRI-AGCM3.1S over other GCMs in low precipitation pattern realization is objectively assessed. Then, this study investigates how low precipitation patterns are projected in the future climates by MRI-AGCM3.1S and identifies the degree of agreement or uncertainty levels of the future pattern from ensemble analyses on consistency among different model results.

The chapter is organized as follows: DATA describes precipitation data to be used, both that simulated by GCMs and observed data. METHODOLOGY discusses the methodology employed to assess low precipitation patterns, including the probabilistic

treatment. In RESULT AND DISCUSSION, validation results of GCMs with the observed precipitation data are presented and the merit of MRI-AGCM3.1S is highlighted. Further, assessment of future changes of low precipitation patterns is presented and discussed. Finally, conclusion of this study is presented in CONCLUSION.

Data

MRI-AGCM3.1S

The focus of this paper is the precipitation data set derived by MRI-AGCM3.1S. It is an outcome of the Innovative Program of Climate Change Projection for the 21st Century (Kakushin21), MEXT (Kitoh et al., 2009). The model conducts simulations with a horizontal resolution of about 20 km (TL959 linear Gaussian grid in 1920×960 grid cells) and 60 layers in the vertical axis. MRI-AGCM3.1S has the data for the present period, from 1979 to 2003 (25 years), and the future period, from 2075 to 2099 (25 years) under the A1B scenario (A future world of very rapid economic growth, low population growth and rapid introduction of new and more efficient technology) of Special Report on Emissions Scenarios (SRES; Nakićenović et al., 2000). For the present climate simulation, the observed monthly sea surface temperature (SST) and sea-ice concentration during the 25 years are set as a boundary condition. For the future climate simulation, the boundary SST data is prepared by superposing; (a) the trend in the multi-model ensemble of SST within the future period projected by the CMIP3 multi-model data set, (b) future change in multi-model ensemble of SST between the present and the future periods, and (c) the detrended observed SST anomalies for the

period 1979 to 2003. Future sea-ice distribution is obtained in a similar fashion (Kitoh et al., 2009).

CMIP3 AOGCMs

For comparison and ensemble analyses with the MRI-AGCM3.1S simulations, the CMIP3 AOGCM precipitation data sets accessible in June 2010 were used. They are the 16 AOGCM data sets out of 23 models. We selected precipitation data derived by 15 AOGCMs from 1981 to 2000 (20 years) for the present climate using the 20C3M experiment, which used greenhouse gases increasing as observed through the 20th century and data from 2081 to 2100 (20 years) for the future climate under the SRES A1B scenario. Precipitation data derived by 8 AOGCMs using the AMIP experiment, which runs with prescribed SST for the 20th century, was also used for validation of the MRI-AGCM3.1S because the AMIP experiment was conducted using the same experiment design as the MRI-AGCM3.1S for the present climate simulation. A list of the climate models and their precipitation data sets used in this study is shown in Table 1.

Table 1 List of GCMs and precipitation data sets

No	Model Designation	Model Type	Modeling Group	Country	Resolution	Period of Precipitation data set present AMIP	Period of Precipitation data set present 20C3M	Period of Precipitation data set future A1B
1	MRI-AGCM3.1S	AGCM	Meteorological Research Institute	Japan	TL959 (~0.2° x 0.2°) L60	1979-2003	-	2075–2099
2	CGCM3.1(T47)	AOGCM in CMIP3	Canadian Centre for Climate Modeling & Analysis	Canada	T47 (~2.8° x 2.8°) L31	-	1981-2000	2081-2100
3	CGCM3.1(T63)	AOGCM in CMIP3	Canadian Centre for Climate Modeling & Analysis	Canada	T63 (~1.9° x 1.9°) L31	-	1981-2000	2081-2100
4	CNRM-CM3	AOGCM in CMIP3	Météo-France / Centre National de Recherches Météorologiques	France	T63 (~1.9° x 1.9°) L45	1979-2000	1981-2000	2081-2100
5	CSIRO-Mk3.0	AOGCM in CMIP3	CSIRO Atmospheric Research	Australia	T63 (~1.9° x 1.9°) L18	-	1981-2000	2081-2100
6	CSIRO-Mk3.5	AOGCM in CMIP3	CSIRO Atmospheric Research	Australia	T63 (~1.9° x 1.9°) L18	-	1981-2000	2081-2100
7	GFDL-CM2.0	AOGCM in CMIP3	US Dept. of Commerce / NOAA / Geophysical Fluid Dynamics Laboratory	USA	2.0° x 2.5° L24	-	1981-2000	2081-2100
8	GFDL-CM2.1	AOGCM in CMIP3	US Dept. of Commerce / NOAA / Geophysical Fluid Dynamics Laboratory	USA	2.0° x 2.5° L24	-	1981-2000	2081-2100
9	GISS-AOM	AOGCM in CMIP3	NASA / Goddard Institute for Space Studies	USA	3° x 4° L12	-	1981-2000	2081-2100
10	GISS-ER	AOGCM in CMIP3	NASA / Goddard Institute for Space Studies	USA	4° x 5° L13	1979-2002	-	-
11	INM-CM3.0	AOGCM in CMIP3	Institute for Numerical Mathematics	Russia	4° x 5° L21	1979-2003	1981-2000	2081-2100
12	IPSL-CM4	AOGCM in CMIP3	Institut Pierre Simon Laplace	France	2.5° x 3.75° L19	1979-2002	1981-2000	2081-2100
13	MIROC3.2(hires)	AOGCM in CMIP3	Center for Climate System Research (The University of Tokyo), National Institute for Environmental Studies, and Frontier Research Center for Global Change (JAMSTEC)	Japan	T106 (~1.1° x 1.1°) L56	1979-2002	1981-2000	2081-2100
14	MIROC3.2(medres)	AOGCM in CMIP3	Center for Climate System Research (The University of Tokyo), National Institute for Environmental Studies, and Frontier Research Center for Global Change (JAMSTEC)	Japan	T42 (~2.8° x 2.8°) L20	1979-2002	1981-2000	2081-2100
15	ECHO-G	AOGCM in CMIP3	Meteorological Institute of the University of Bonn (MIUB), Meteorological Research Institute of KMA (METRI), and Model and Data group (M&D)	Germany & Korea	T30 (~3.9° x 3.9°) L19	-	1981-2000	2081-2100
16	ECHAM5/MPI-OM	AOGCM in CMIP3	Max Planck Institute for Meteorology	Germany	T63 (~1.9° x 1.9°) L31	1978-1999	1981-2000	2081-2100
17	MRI-CGCM2.3.2	AOGCM in CMIP3	Meteorological Research Institute	Japan	T42 (~2.8° x 2.8°) L30	1979-2000	1981-2000	2081-2100

VASClimO observed data

The ability of 17 GCMs (MRI-AGCM3.1S and 16 AOGCMs using either the AMIP or the 20C3M experiment, or both) for reproducing the low precipitation phenomena in the present period was examined by comparison with the Variability Analysis of Surface Climate Observations 50-Year Data Set (VASClimO; Beck et al., 2005). This global data set is a monthly gridded ground-gauged precipitation time series for the period from 1951 to 2000 (50 years) based on quality-controlled and homogenized time-series from 9,343 stations, excluding Greenland and Antarctica. In order to minimize the risk of generating temporal heterogeneity in the gridded data due to varying ground-gauged station densities, the stations which measure more than 90% data during the analyzed period are used for interpolation to a regular 0.5°×0.5° latitude and longitude grid (Beck et al., 2005). Here we used VASClimO with 1° resolution produced by area-weighted averaging the four corner points of a 0.5° grid cell because precipitation data sets derived by MRI-AGCM3.1S were spatially averaged over 1° grid for fair comparison with other low resolution AOGCMs, as mentioned in Treatment of different grid sizes in METHODOLOGY.

Methodology

Measure of low precipitation

In this study, the low precipitation pattern refers to the temporal and spatial distribution of the annual minimum of accumulated precipitation over a given time interval on global land area. This is a modified version of the methodology using annual minima series of moving averages studied by Kikkawa and Takeuchi (1975) and

Takeuchi (1986). The annual minimum of accumulated precipitation at year i in the time interval τ, $f(i,\tau)$ is defined as:

$$f(i,\tau) = \min_{1 \le j \le 12} \left[\sum_{t=j-\tau+1}^{j} x_{i,t} \right] \qquad (1)$$

where j denotes a month and $x_{i,t}$ denotes monthly precipitation in year i at t month. When t becomes a negative value, t and i are replaced by $t+12$ and $i-1$, respectively. The first year of the original data set (more years in case τ is greater than 12-month) does not appear in the annual minima series.

Time interval of low precipitation

The intervals τ for assessing low precipitation were selected as 1-, 3-, 6- and 12-month in this study. The monthly time scale is considered appropriate for monitoring the effects of a drought in situations related to agriculture and water supply (Panu & Sharma, 2002). In addition to 1- and 12-month as the basic time intervals, the intervals of 3- and 6-month were paid special attention as they correspond to the total growing period of major grains produced around the world. According to Brouwer and Heibloem (1986), total growing period of three major grains, such as wheat, maize and rice, is in the range of 80 to 180 days, which roughly corresponds to 3- to 6-month. For other lengths, any particular findings were presented wherever necessary.

Assessment of probability levels

This study assessed low precipitation $f(i,\tau)$ by quantiles of six probability levels 0.01, 0.02, 0.05, 0.1, 0.2 and 0.5, which correspond to 100-, 50-, 20-, 10-, 5- and 2-year return periods, respectively.

The quantiles of $f(i,\tau)$ were estimated by fitting two parameter Weibull distributions to the sample data, $f(i,\tau), i = 1,...,N$, where N is the number of years of data sets, using the L-moment method at each grid point over land around the globe. We applied the Weibull distribution because probability distributions for low precipitation may be approximated best by the Weibull distribution (Kikkawa & Takeuchi, 1975). The Probability Plot Correlation Coefficient (PPCC) was used as a goodness-of-fit test to check whether the annual minima of accumulated precipitation were well approximated by the Weibull distribution. PPCCs using Gringorten's plotting position were examined by the critical points at 95% confidence level obtained by use of an empirical sampling procedure (Vogel, 1989).

Assessment of occurrence season of low precipitation

The low precipitation occurrence season was assessed from the centroid of the frequency distribution of the ending months with annual minima of low precipitation $f(i,\tau)$ over 1-, 3-, 6- and 12-month time intervals. Those ending months were evaluated at each grid point over land around the globe.

Assessment of model performance

The performance of 17 GCMs was assessed with respect to their capability of

reproducing low precipitation patterns. Both low precipitation quantiles and the occurrence season were estimated from the 17 model outputs for the present period and compared with those estimated from the VASClimO observed data. In order to clarify the performance of MRI-AGCM3.1S, multi-model ensemble means (un-weighted simple arithmetic means) of the low precipitation patterns from the CMIP3 AOGCMs were also calculated. For the ensemble analyses, each model simulation result was spatially interpolated from its original grid to a common $2° \times 2°$ grid which is a representative scale across the set of models.

Aagreement over a global distribution of the low precipitation patterns between the observed values and the model simulations was examined by eye on plotted maps, and a point-by-point coefficient of determination R^2 calculated for the low precipitation quantiles. The VASClimO observed data was spatially converted to the original grid of each model or the 2° grid of the ensemble mean to calculate R^2.

Assessment of future change in low precipitation patterns by model consistency

Projected future change in low precipitation quantiles was measured by the relative change in percent between the 20C3M for the present climate and the A1B scenario for the future climate. Special attention was paid to 0.1 probability low precipitation quantiles. The selection of 0.1 probability as a representative probability for drought follows some previous studies such as Sheffield and Wood (2007). Projected future shifts in low precipitation occurrence season was shown using the number of month shifted, which was calculated simply by the ending month of the low precipitation occurrence season for the A1B scenario minus that for the 20C3M.

Future changes in the low precipitation patterns were estimated from MRI-AGCM3.1S first and then multi-model ensemble means (un-weighted simple arithmetic means) of the future changes from 16 GCMs, consisting of MRI-AGCM3.1S and 15 AOGCMs, were also estimated in a common $2°\times2°$ grid to evaluate the uncertainty of the future climate projections. The un-weighted simple arithmetic mean was applied here since a robust approach to assigning weights to individual model projections of climate change has not yet been identified (IPCC, 2010). IPCC (2007b, 2012) shows future changes in the multi-model mean of precipitation, CDD and soil moisture anomalies (SMA) with consistency among the models. In this study, we applied the model consistency to show a degree of uncertainty; high model consistency means that 15 or all models out of 16 models agree with the sign change, whereas low model consistency means that less than 11 models out of 16 models agree with the sign change.

Treatment of different grid sizes

Since MRI-AGCM3.1S has high horizontal resolution of roughly 20 km, simulated precipitation data at one particular grid by MRI-AGCM3.1S may not represent a large-scale climate condition around the grid. To compare the model performances fairly with other low horizontal resolution AOGCMs, precipitation data sets derived by MRI-AGCM3.1S were spatially averaged over an $1°\times1°$ grid before assessment of model performance and future change.

Result and discussion

Goodness-of-fit test for the Weibull distribution hypothesis

The PPCC test was conducted as a goodness-of-fit test to examine the Weibull distribution hypothesis for annual minima of accumulated precipitation over 1-, 3-, 6- and 12-month intervals for all 17 models for the present and the future simulations. Figure 1 shows global maps of PPCCs estimated from the present simulation by MRI-AGCM3.1S as an example of results from the 17 models. The critical point of 95% confidence level is approximately 0.94 when the sample size is 24 (Vogel, 1989). Blue grids indicate those accepted by the Weibull distribution hypothesis, where their PPCCs exceed the critical point. White grids indicate no PPCCs because the sample data of annual minima contain zero values. PPCCs in 1- (Figure 1(a)), 3- (Figure 1(b)) and 12-month time intervals (Figure 1(d)) are high in almost all regions and exceed the critical point of 95% confidence level in 93%, 84% and 80% of the total grids over land around the globe, respectively. On the other hand, PPCCs in 6-month time interval (Figure 1(c)) are relatively low in Canada, eastern Russia, Mongolia and China and exceed the critical point in 65% of the total land grids. The same results are also seen under the other models. PPCCs of the 17 model simulations for the present and the future period in 1-, 3- and 12-month intervals exceed the critical point in the range from 76% to 95% of the total land grids, whereas the PPCCs in 6-month intervals exceed the critical point in the range from 65% to 82% of the total land grids. Although the PPCCs in the 6-month interval are relatively low compared to other time intervals, at least 65% of total land grids showed acceptance under the Weibull distribution hypothesis. These results indicate that the Weibull distribution hypothesis using L-moment method can be applied

to annual minima of monthly accumulated precipitation for the given time intervals over land around the globe.
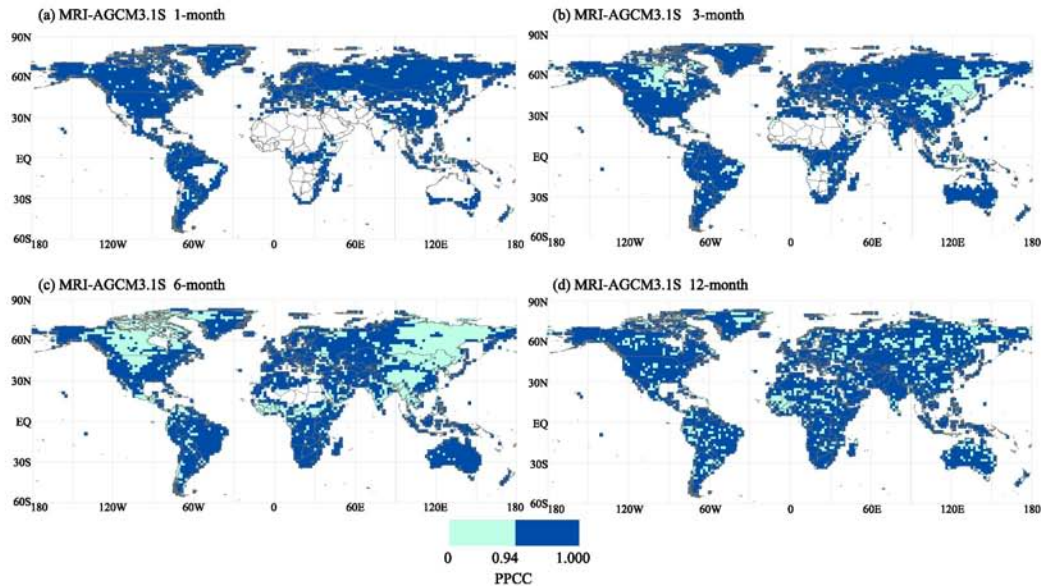
Figure 1 Probability Plot Correlation Coefficients for the Weibull distribution hypothesis of annual minima of monthly accumulated precipitation over the four time intervals estimated from the present simulation by MRI-AGCM3.1S

Assessment of GCM performance

First, low precipitation quantiles in six probability levels for the present climate estimated by MRI-AGCM3.1S, 8 CMIP3 AOGCMs on the AMIP experiment and 15 CMIP3 AOGCMs on the 20C3M experiment were examined with the VASClimO observed data. Figure 2 shows global maps of, as an example, 0.1 probability low precipitation quantile in 3-month time intervals derived by observations and the simulations by MRI-AGCM3.1S, 8 CMIP3 AOGCMs using the AMIP experiment and the multi-model ensemble mean of the 8 AOGCMs. From comparison by eye with the observations (Figure 2(a)), it can be seen that MRI-AGCM3.1S (Figure 2(b))

reproduces the global distribution of the low precipitation quantiles best in most regions. In other model results, some obvious mismatches are identifiable, such as in South America for GISS-ER (Figure 2(d)) and IPSL-CM4 (Figure 2(f)) and at dry region in western China for GISS-ER (Figure 2(d)), INM-CM3.0 (Figure 2(e)), IPSL-CM4 (Figure 2(f)), MIROC3.2 (hires) (Figure 2(g)) and MIROC3.2 (medres) (Figure 2(h)).

For numerical assessment of model reproducibility of low precipitation quantiles, coefficients of determination of low precipitation quantiles in six probability levels over 1-, 3-, 6-, and 12-month intervals were calculated between observations and simulations by MRI-AGCM3.1S, 8 AOGCMs using the AMIP experiment, 15 AOGCMs using the 20C3M experiment and two multi-model ensemble means estimated from the AMIP and the 20C3M experiments (Figure 3). Since estimates of lower probability (higher return period) quantiles contain high uncertainty due to extrapolating; those of lower probability such as 0.01 have lower coefficients for all models in all time intervals. Comparison between model simulations shows that MRI-AGCM3.1S has the highest coefficient of determination among all results across the six levels of probabilities for the four time intervals, which even include the multi-model ensemble means.

Second, model estimations for low precipitation occurrence seasons were also compared with observations. Figure 4 shows global distributions of the ending months of low precipitation occurrence season over 3-month time intervals estimated by observations and the simulations by MRI-AGCM3.1S, 8 AOGCMs using the AMIP experiment and the multi-model ensemble mean of the 8 AOGCMs, as an example. In comparison with the observed data (Figure 4(a)), MRI-AGCM3.1S (Figure 4(b)) shows relatively realistic reproduction of the occurrence seasons in most regions. In particular, good agreement is seen in the United States, South America, middle and southern

Africa and monsoon Asia, whereas differences like 2 to 4 months are seen over the Iberian Peninsula. In contrast, obvious discrepancies with observation are seen in central Asia for GISS-ER (Figure 4(d)), in Europe for CNRM-CM3 (Figure 4(c)), INM-CM3.0 (Figure 4(e)), IPSL-CM4 (Figure 4(f)) and ECHAM5/MPI-OM (Figure 4(i)).

These comparisons with observations illustrate that MRI-AGCM3.1S reproduces more realistic low precipitation patterns over global land areas for the present period than other models. Among many potential reasons that might have improved reproducibility of low precipitation phenomena, the main reason might be the high horizontal resolution of the MRI-AGCM3.1S that made it possible to simulate topographical effects that generate precipitation.
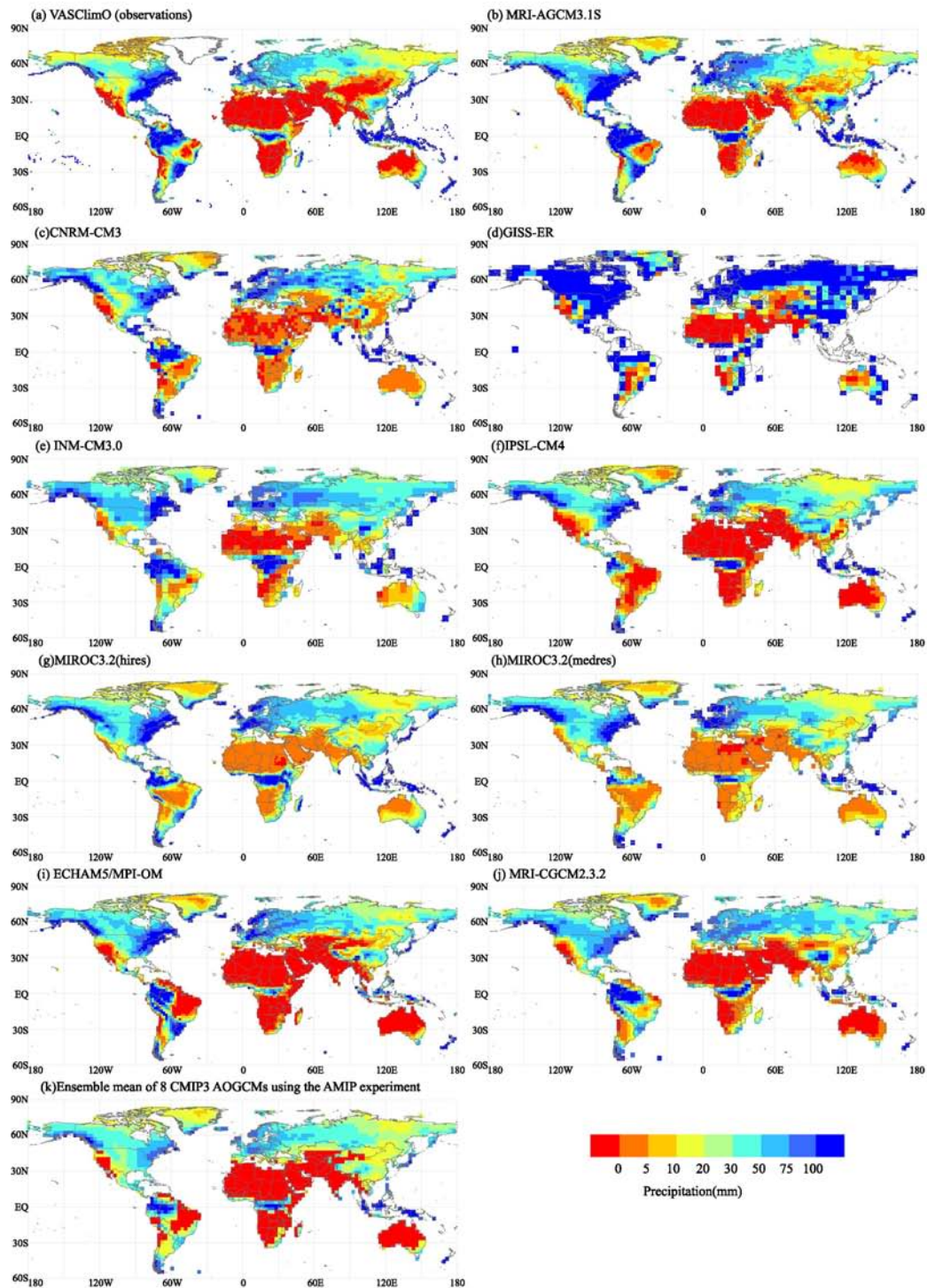
Figure 2 Reproducibility of 0.1 probability low precipitation quantiles in 3-month time intervals estimated by MRI-AGCM3.1S, eight CMIP3 AOGCMs using the AMIP experiment and the multi-model ensemble mean of eight CMIP3 AOGCMs (comparison with observations).
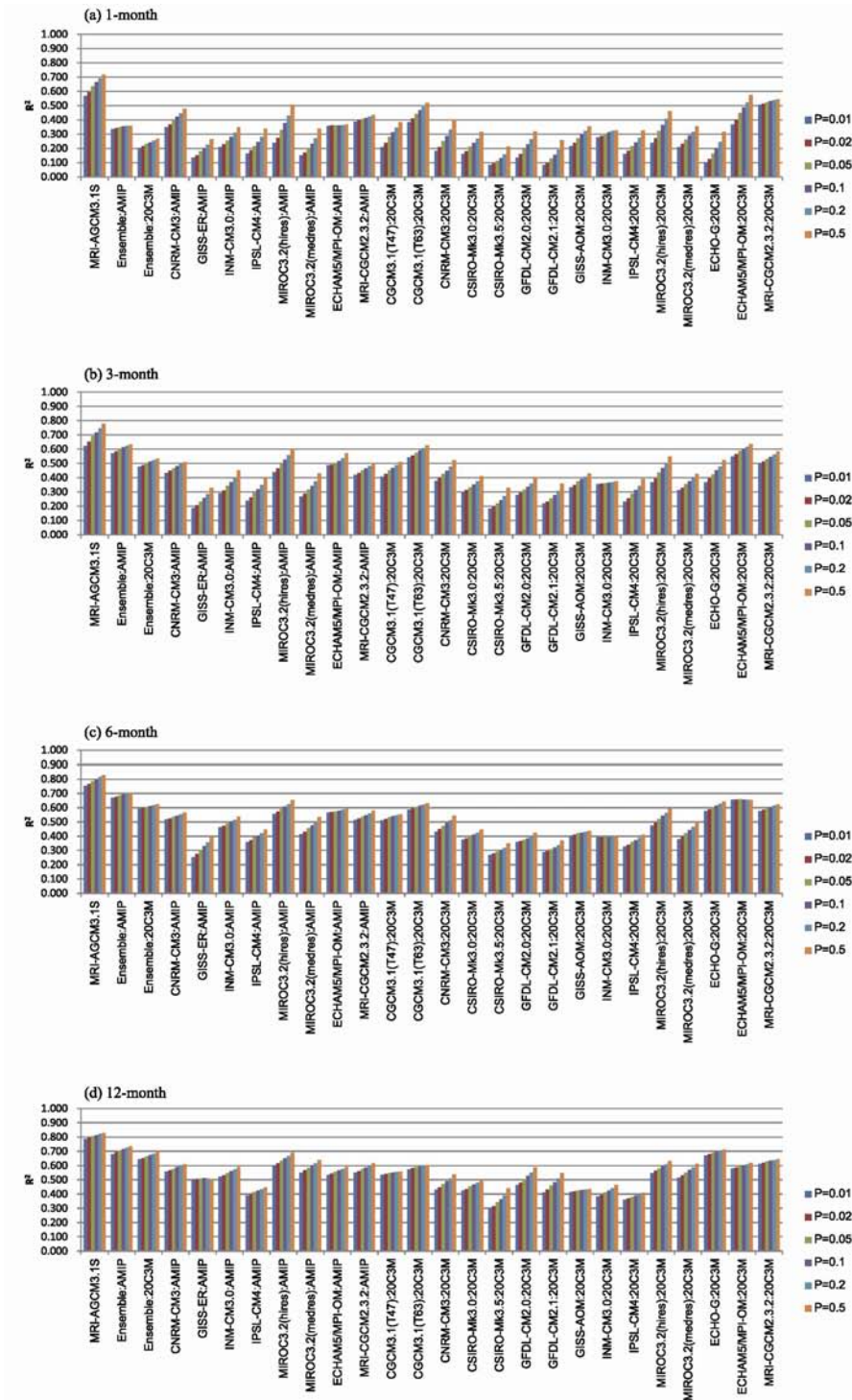
Figure 3 Coefficient of determination on low precipitation quantiles in six probability levels over four time intervals calculated between observations and simulations by MRI-AGCM3.1S, eight CMIP3 AOGCMs using the AMIP experiment, 15 CMIP3 AOGCMs using the 20C3M experiment and two multi-model ensemble means from the AMIP and the 20C3M experiments.

118

Figure 4 Reproducibility of the ending month of low precipitation occurrence season in 3-month time intervals estimated by MRI-AGCM3.1S, eight CMIP3 AOGCMs using the AMIP experiment and the multi-model ensemble mean of eight CMIP3 AOGCMs (comparison with observations).

Assessment of future change in low precipitation patterns by model consistency
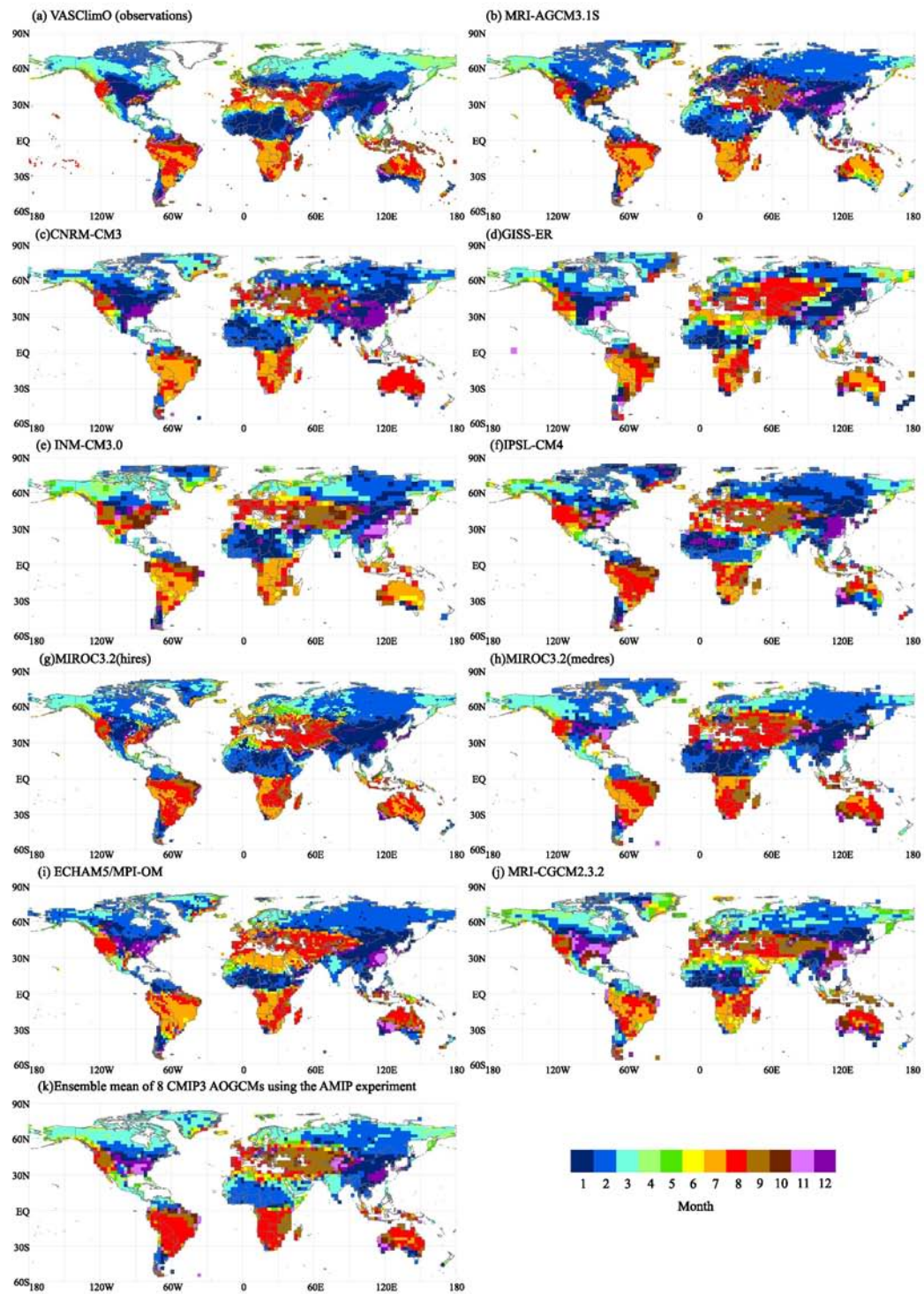
Figure 5 shows two sets of global maps of projected future changes in 0.1 probability low precipitation quantiles in 3- and 6- month time intervals estimated by MRI-AGCM3.1S and the multi-model ensemble mean calculated by 16 GCMs which consist of MRI-AGCM3.1S and 15 CMIP3 AOGCMs. The 3- and 6- month time intervals were selected here as they correspond to the total growing period of major grains produced in the world as mentioned in METHODOLOGY. From Figure 5, MRI-AGCM3.1S projects that the low precipitation quantiles in Mexico, southern Brazil, southern Argentina, Mediterranean area and southern Africa would decrease by 10 to 50 % compared to the present level, whereas low precipitation would increase more than 50 % in higher latitude and eastern African equatorial areas (Figure 5(a) and (b)). These regions coincide with that of the multi-model ensemble mean with high model consistency, 15 or all models out of 16 models agree with the sign of the change (black outlined grids in Figure 5(c) and (d)).

Figure 6 shows two sets of global maps of projected future shifts in the ending month of low precipitation occurrence season over 3- and 6- month time intervals estimated by MRI-AGCM3.1S and the multi-model ensemble mean of 16 GCMs. MRI-AGCM3.1S projects that the occurrence season would shift to more than 2 months earlier in East Europe (Figure 6(a) and (b)), where the low precipitation quantiles are projected to decrease as shown in Figure 5. In contrast, the multi-model ensemble projections show low model consistency in most regions, less than 11 models out of 16 agree on the sign of future shift of low precipitation occurrence season (masked out regions with white in Figure 6(c) and (d)).

The intensification of drought severity in those five regions, Mexico, southern

Brazil, southern Argentina, Mediterranean area and southern Africa, are in fact pointed out by IPCC (2007a) based on the analyses of multi-model mean changes in annual precipitation constructed by 21 model simulations for the SRES A1B scenario for the period 2080 to 2099 relative to 1980 to 1999, and also by IPCC (2012) based on multi-model analyses of changes in two indices, CDD and SMA, under the SRES A2 scenario for the period 2081 to 2100 relative to 1980 to 1999 constructed by 17 (CDD) and 15 (SMA) GCMs contributing to the CMIP3. This study adds support to the conclusion that the possible impacts of climate change in the five regions would include changes, in the sense of occurrence probability, in seasonal low precipitation over 3- and 6-month time intervals. This could lead to lower yields or crop damage in an agriculture sector, increased risk of water and food shortage for human health and water shortage for industry. However, low model consistency in the results of projected future shift of low precipitation occurrence season shows that current GCMs still have difficulty in simulating seasonal precipitation variations, and therefore it is difficult to identify future water shortage season with high model consistency. Dai (2006) compares precipitation characteristics in 18 AOGCMs and shows that many of the major precipitation biases, such as intraseasonal variations, still exist in current AOGCMs and further improvements in these areas will likely require higher model resolution and improved model physics. Considerable improvements in GCMs are still necessary in order to obtain more reliable projections of seasonal drought shift, which is essential for developing practical climate change adaptation policies. In this respect, MRI-AGCM3.1S is expected to reduce the precipitation bias owing to its high resolution, which was proved by the observation of best model reproducibility among the GCMs compared in this study.
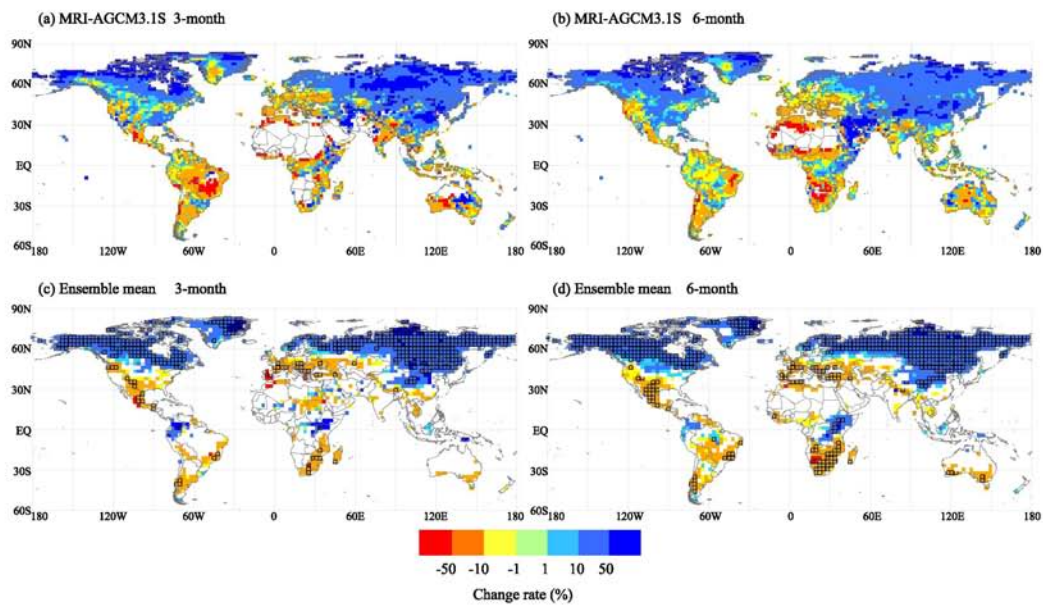
Figure 5 Projected future change of 0.1 probability low precipitation quantiles in 3- and 6-month time intervals estimated by MRI-AGCM3.1S and the multi-model ensemble mean of 16 GCMs. In the ensemble results, black outlined land grids indicate high model consistency that 15 or all models out of 16 models agree on the sign of the change and masked out land grids with white indicate low model consistency that less than 11 models out of 16 models agree on the sign of the change.
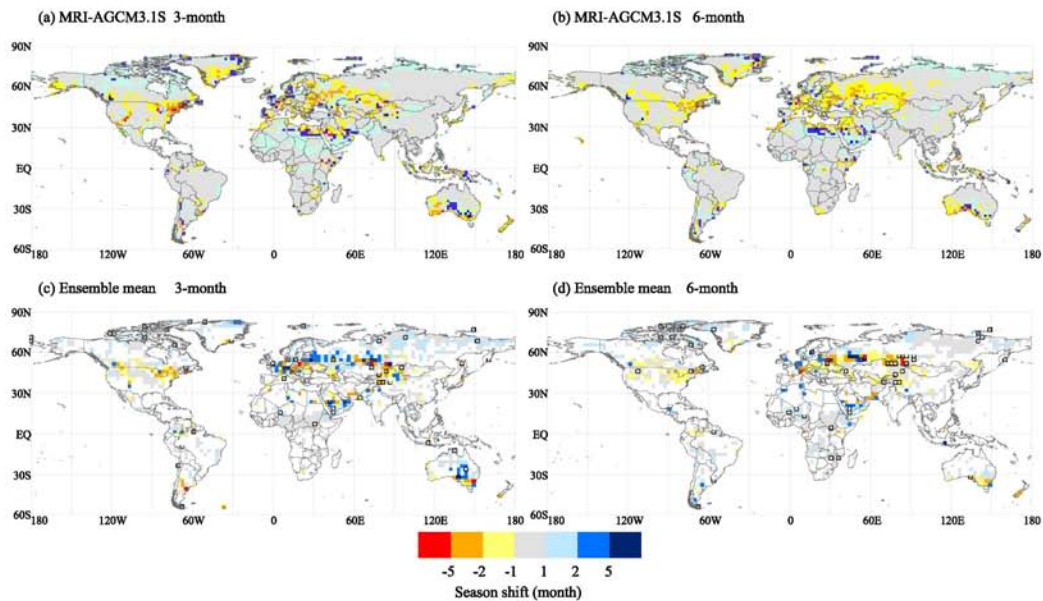
Figure 6 Projected future shift of the ending month of low precipitation occurrence season in 3- and 6-month time intervals estimated by MRI-AGCM3.1S and multi-model ensemble mean of 16 GCMs. In the ensemble results, black outlined land grids indicate high model consistency that 15 or all models out of 16 models agree on the sign of the change, and masked out land grids with white indicate low model consistency that less than 11 models out of 16 models agree on the sign of the change.

Conclusion

This study analyzed precipitation data from the super-high-resolution MRI-AGCM3.1S and 15 CMIP3 AOGCMs and their ensemble mean to assess future changes in low precipitation patterns over the global land area under the SRES A1B scenario. As for the low precipitation patterns, we assessed low precipitation quantiles in six probability levels approximated by the Weibull distribution using annual minima of monthly precipitation accumulations over 1-, 3-, 6- and 12-month time intervals. Also, low precipitation occurrence seasons were assessed from the centroid of the frequency

distribution of the ending months with annual minima of low precipitation over the four time intervals. First, the ability of models for reproducing low precipitation quantiles and occurrence seasons for the present period was examined by comparison with the VASClimO observed data. Second, future changes in low precipitation patterns projected by MRI-AGCM3.1S and multi-model ensemble mean calculated over 16 GCMs, consisting of MRI-AGCM3.1S and 15 CMIP3 AOGCMs, were assessed on the basis of uncertainty level by measuring the degree of consistency among the model results. Main findings are as follows:

A comparison of low precipitation patterns for the present period between observations and model simulations shows that MRI-AGCM3.1S reproduces current low precipitation patterns relatively realistically. MRI-AGCM3.1S shows, among all models, the highest coefficient of determination for the low precipitation quantiles and the best agreement with observations for global distribution of current low precipitation quantiles and occurrence seasons.

MRI-AGCM3.1S projects that at the end of 21st century 0.1 probability low precipitation quantiles for 3- and 6-month time intervals would decrease by 10 to 50 % compared to the present level in Mexico, southern Brazil, southern Argentina, Mediterranean area and southern Africa. These regions coincide with the regions with high model consistency estimated by the multi-model ensemble mean of 16 GCMs.

MRI-AGCM3.1S projects that low precipitation occurrence seasons would shift to more than 2 months earlier in Eastern Europe, where their low precipitation quantiles are projected to decrease. However, the multi-model ensemble mean by 16 GCMs shows low model consistency in future shifts in occurrence seasons. Specially, future projections of the seasonal shifts in low precipitation are essential for developing

124

practical climate change adaptation policies, but current projections still have high uncertainty as suggested by the present analysis.

Throughout the analyses of future changes in low precipitation patterns, the emphasis was put on model consistency. It should be noted that, although it is impossible to verify that projections with high model consistency documented here have higher probability of being realized in the future than those with the low model consistency, the consistency indicated by 15 or all models out of 16 models implies that the results is currently the best available knowledge on future low precipitation.

Reference

Alexander, L. V., Zhang, X., Peterson, T. C., Caesar, J., Gleason, B., Klein Tank, A. M. G., Haylock, M., Collins, D., Trewin, B., Rahimzadeh, F., Tagipour, A., Kumar, K. R., Revadekar, J., Griffiths, G., Vincent, L., Stephenson, D. B., Burn, J., Aguilar, E., Brunet, M., Taylor, M., New, M., Zhai, P., Rusticucci, M., & Vazquez-Aguirre, J. L. (2006). Global observed changes in daily climate extremes of temperature and precipitation. Journal of Geophysical Research, 111, D05109. doi: 10.1029/2005JD006290

Beck, C., Grieser, J., & Rudolf, B. (2005). A new monthly precipitation climatology for the global land areas for the period 1951 to 2000. In *Climate Status Report, 2004. German Meteorological Service* (pp. 181–190). Offenbach: German Weather Service.

Brouwer, C., & Heibloem, M. (1986). *Irrigation Water Management: Irrigation Water Needs, Irrigation water management Training manual no. 3.* Retrieved October 19, 2010, from http://www.fao.org/docrep/s2022e/s2022e00.HTM

Burke, E. J., & Brown, S. J. (2008). Evaluating uncertainties in the projection of future drought. *Journal of Hydrometeorology, 9*(2), 292–299.

Dai, A. (2006). Precipitation Characteristics in Eighteen Coupled Climate Models. *Journal of Climate 19,* 4605–4630. doi: 10.1175/JCLI3884.1

Dai, A. (2011). Drought under global warming: a review. *Wiley Interdisciplinary*

Reviews: *Climate Change 2,* 45–65. doi: 10.1002/wcc.81

IPCC. (2007a). *Climate Change 2007: Impacts, Adaptation and Vulnerability. Contribution of Working Group II to the Fourth Assessment Report of the Intergovernmental Panel on Climate Change.* Cambridge: Cambridge University Press.

IPCC. (2007b). *Climate Change 2007: The Physical Science Basis. Contribution of Working Group I to the Fourth Assessment Report of the Intergovernmental Panel on Climate Change.* Cambridge: Cambridge University Press.

IPCC. (2010). *Meeting Report of the Intergovernmental Panel on Climate Change Expert Meeting on Assessing and Combining Multi Model Climate Projections IPCC Working Group I Technical Support Unit.* Bern: University of Bern.

IPCC. (2012). *Managing the Risks of Extreme Events and Disasters to Advance Climate Change Adaptation. A Special Report of Working Groups I and II of the Intergovernmental Panel on Climate Change.* Cambridge: Cambridge University Press.

Katz, R. W., & Brown, B. G. (1992). Extreme events in a changing climate: Variability is more important than averages. *Climatic Change 21*, 289–302. doi: 10.1007/BF00139728

Kikkawa, H., & Takeuchi, K. (1975). Characteristics of drought duration curve and its application. *Proc. JSCE, 234,* 61-71.

Kitoh, A., Ose, T., Kurihara, K., Kusunoki, S., & Sugi, M. (2009). Projection of changes in future weather extremes using super-high-resolution global and regional atmospheric models in the KAKUSHIN Program: Results of preliminary experiments. *Hydrological Research Letters*, *3*, 49–53. doi: 10.3178/HRL.3.49

McKee, T. B., Doesken, N. J., & Kleist, J. (1993). The relationship of drought frequency and duration to time scales. In *Preprints, 8th Conference on Applied Climatology, January 17–22 Anaheim, CA* (pp. 179–184). Retrieved October 30, 2010, from http://ccc.atmos.colostate.edu/relationshipofdroughtfrequency.pdf

Nakićenović, N., Davidson, O., Davis, G., Grübler, A., Kram, T., Rovere, E. L. L., Metz, B., Morita, T., Pepper, W., Pitcher, H., Sankovski, A., Shukla, P., Swart, R., Watson, R., & Dadi, Z. (2000). *Emissions scenarios—summary for policymakers. Intergovernmental Panel on Climate Change.* Retrieved October 29, 2010, from http://www.ipcc.ch/ipccreports/sres/emission/index.php?idp=1

Neelin, J. D., Münnich, M., Su, H., Meyerson, J. E., Holloway, C. E. (2006). Tropical drying trends in global warming models and observations. *Proceedings of the*

National Academy of Sciences, 103, 6110–6115.

Nohara, D., Kitoh, A., Hosaka, M., & Oki, T. (2006). Impact of climate change on river discharge projected by multimodel ensemble. *Journal of Hydrometeorology 7,* 1076-1089. doi: 10.1175/JHM531.1

Orlowsky, B., & Seneviratne, S. I. (2012). Global changes in extremes events: Regional and seasonal dimension. *Climatic Change, 110*(3-4), 669-696. doi: 10.1007/s10584-011-0122-9

Palmer, W. C. (1965). *Meteorological Drought. Research Paper, No.45*. Retrieved October 29, 2010, from http://www.ncdc.noaa.gov/temp-and-precip/drought/docs/palmer.pdf

Panu, U. S., & Sharma, T. C. (2002). Challenges in drought research: some perspectives and future directions. *Journal of Hydrological Science, 47*, 19–30.

Sheffield, J., & Wood, E. F. (2007). Characteristics of global and regional drought, 1950–2000: analysis of soil moisture data from off-line simulation of the terrestrial hydrologic cycle. *Journal of Geophysical Research, 112,* D17115. doi: 10.1029/2006JD008288

Sheffield, J., & Wood, E. F. (2008). Projected changes in drought occurrence under future global warming from multi-model, multi-scenario, IPCC AR4 simulations. *Climate Dynamics, 31,* 79–105. doi: 10.1007/s00382-007-0340-z

Takeuchi, K. (1988). Hydrological persistence characteristics of floods and droughts - Interregional comparisons-. *Journal of Hydrology, 102,* 49-67. doi: 10.1016/0022-1694(88)90091-1

Tallaksen, L. M., & van Lanen, H. A. J. (2004). *Hydrological Drought: Processes and Estimation Methods for Streamflow and Groundwater. Developments in Water Science 48*. Amsterdam: Elsevier.

Tebaldi, C., Hayhoe, K., Arblaster, J. M., Meehl, G. A. (2006). Going to the extremes. An intercomparison of model-simulated historical and future changes in extreme events. *Climatic Change, 79*(3-4), 185-211. doi: 10.1007/s10584-006-9051-4

UNFCCC. (2007). *Report of the Conference of the Parties on its thirteenth session, held in Bali from 3 to 15 December 2007*. Retrieved October 6, 2011, from http://unfccc.int/resource/docs/2007/cop13/eng/06a01.pdf

Vaze, J., Teng, J., Chiew, F. H. S. (2011). Assessment of GCM simulations of annual and seasonal rainfall and daily rainfall distribution across south-east Australia. *Hydrological Processes, 25*, 1486–1497. doi: 10.1002/hyp.7916

Vogel, R. M., & Kroll, C. N. (1989). Low Flow Frequency Analysis Using Probability Plot Correlation Coefficients. *Journal of Water Resource Planning and*

Management, 115(3), 338-357. doi: 10.1061/(ASCE)0733-9496(1989)115:3(338)

Wang, G. (2005). Agricultural drought in a future climate: Results from 15 global climate models participating in the IPCC 4th Assessment. *Climate Dynamics, 25,* 739–753.